**Fakultät für Medizin**

**Institut für Mikrobiologie, Immunologie und Hygiene**

# Isolation and functional characterization of antigen-specific TCRs from the healthy donor repertoire

**Shwetha Lakshmipathi**

Vollständiger Abdruck der von der Fakultät für Medizin der Technischen Universität München zur Erlangung des akademischen Grades eines

**Doctor of Philosophy (Ph.D.)**

genehmigten Dissertation.

**Vorsitzende/r: Prof. Dr. Jürgen Ruland**

**Betreuer/in: Prof. Dr. Dirk Busch**

**Prüfer der Dissertation:** 1. **Prof. Dr. Angela Krackhardt**

2. **Prof. Dr. Ulrike Protzer**

Die Dissertation wurde am 27.09.2017 bei der Fakultät für Medizin der Technischen Universität München eingereicht und durch die Fakultät für Medizin am 27.12.2017 angenommen.

# Table of Contents

# Index of Figures

# Index of tables

## Summary

Adoptive cell therapy (ACT), by transfer of naturally occurring or genetically engineered T cells modified to express T cell receptors (TCRs) of interest, is known to be a promising approach for treatment of some cancers and infections. Despite success in the field, one of the current challenges is the identification of large repertoires of suitable TCRs for treatment of diseases in patients, who are usually characterized by diverse and highly variable HLA molecules with different relevant target epitopes.

Since in diseased patients the TCR repertoire might undergo evolutionary changes that make the identification of protective TCRs difficult or even impossible, the TCR repertoires of healthy individuals selectively matching with HLA molecules presenting epitopes of interest, get more into the focus of current research. Especially for foreign or novel mutation-derived epitopes, a healthy donor should have a broad polyclonal repertoire of antigen-specific TCRs within the naive T cell compartment and might be a rich source for the search of a wide range of TCR specificities and avidities. However, exact compositions of naïve repertoires towards different epitopes/antigens have not been explored in depth. Furthermore, epitope-specific populations within the naïve T cell compartment are extremely small in size. The aim of this thesis work was the development of a technology platform that allows to identify and isolate these rare antigen-specific T cells for virus- and tumor-specific epitopes from healthy donor repertoires.

Several groups of antigens like viral proteins, overexpressed tumor antigens or mutation-derived neo-antigens were chosen as targets. In order to visualize rare T cells recognizing epitopes derived from these antigens within a healthy donor repertoire, we decided to use MHC class I multimer staining technologies, which are characterized by a high degree of staining specificity as well as sensitivity. The extremely low target cell frequencies make direct visualization and sorting of antigen-specific T cells difficult. Therefore, we explored different pre-enrichment methods - MACS based and a novel flow based speed enrichment (SE) technique (established and validated together with the MIH institute flow core) - to improve target cell identification. Since MHC multimer double staining can further improve specificity, we also implemented this strategy into the workflow for high-purity cell sorting.

We found that with SE it is indeed possible to visualize rare T cell population of interest with lower loss of positive events as compared to MACS. Combining MHC multimer double staining with SE enrichment allowed us to isolate antigen-specific T cells which occur at a very low frequency in the healthy donor repertoire. These cells were single cell sorted, and single cell RACE PCR was performed to identify individual αβ TCR pairs, which were then re-expressed in both Jurkat T cells and healthy donor PBMCs using non-viral gene transfer systems. Antigen-specificity of recombinantly expressed TCRs was finally tested by MHC multimer staining.

The overall aim of this project work was to isolate epitope-specific T cells from healthy donors, transduce their cognate TCRs into target T cells and validate their functionality and specificity. As a proof of concept, we achieved the goal with successful TCR extraction and sequencing for FluMP (Influenza Virus), YFV (Yellow Fever Virus), WT1 (Wilm's Tumor), Her2Neu and NYESO1, and indeed some of these identified TCRs could rebind to the peptide MHC complex post transduction by multimer staining. In conclusion, we have demonstrated that it is possible to develop a TCR identification workflow enabling us to isolate a broad spectrum of TCRs for various epitopes from the healthy donor repertoire. In the future, this may represent a promising approach to identify TCRs for adoptive T cell therapy, especially when TCR identification in diseased patients is either technically challenging or thought to be biased by evolutionary changes of the TCR repertoire during disease.

# Abbreviation

| | |
|---|---|
| ACT | Adoptive cell therapy |
| BSA | Bovine serum albumin |
| CARs | Chimeric antigen receptors |
| CD | Cluster of differentiation |
| CDR3 | complementary determining region 3 |
| Cfu | Colony forming units |
| CMV | Cytomegalovirus |
| CTA | Cancer testis antigen |
| CTLA4 | cytotoxic T lymphocyte antigen 4 |
| DMEM | Dulbecco's modified essential medium |
| DMSO | Dimethyl Sulfoxide |
| Erk | Extracellular-signal-regulated kinases |
| Et-OH | Ethanol |
| FACS | Fluorescence-activated cell sorting |
| FCS | Fetal calf serum |
| Fig | Figure |
| FPLC | Fast protein liquid chromatograph |
| GA | Gibson Assembly |
| GVHD | graft-versus-host- disease |
| HLA | human leukocyte antigen complex |
| HSCT | hematopoietic stem cell transplantation |
| IFNγ | Interferon gamma |
| IL-15 | Interleukin-15 |
| IL-2 | Interleukin-2 |
| IL-7 | Interleukin-7 |
| ITR | inverted terminal repeats |
| LAG3 | lymphocyte activation gene 3 protein |
| LB | Lysogeny broth |
| FluMP | Influenza virus Flu |
| YFV | Yellow fever virus |
| WT1 | Wilms tumor |
| NY-ESO-1 | New York esophageal squamous cell |

| | |
|---|---|
| PRAME | Preferentially expressed antigen in melanoma |
| MART1 | Melanoma antigen recognized by T cells |
| PR1 | Proteinase 1 |
| HA1 | Minor histocompatibility antigen 1 |
| MFI | Mean fluorescence intensity |
| MHC | Major histocompatibility complex |
| mTCR | Murine constant region of transgenic TCR |
| P2A | Porcine teschovirus 2A |
| PBMCs | Peripheral blood mononuclear cells |
| PD1 | programmed cell death protein 1 |
| pHLA | Peptide loaded human leukocyte antigen |
| RPMI | Roswell Park Memorial Institute |
| RT | Reverse transcriptase |
| SB | Sleeping Beauty |
| TAAs | Tumor associated antigens |
| TAP | transporter proteins for antigenic peptide |
| $T_{CM}$ | T cell central memory phenotype |
| TCR | T cell receptor |
| $T_{EM}$ | T cell effector memory phenotype |
| TILs | Tumor infiltrating lymphocytes |
| $T_N$ | naïve T cell phenotype |
| TNFα | Tumor necrosis factor α |
| TRAB | TCR β-chain variable region |
| TRAJ | TCR α-chain J-Segment |
| TRAV | TCR α-chain variable region |
| α | Alpha |
| β | Beta |
| γ | Gamma |

# 1 Introduction

The human immune system constitutes two main lines of defense mechanisms to protect the host from infectious diseases and combat against different pathogens, as well as to control/eliminate cancer cells. These defense mechanisms are classified as humoral or antibody-mediated immunity and cellular or T cell-mediated immunity. The mode of action in humoral responses is mediated by antibodies that are produced by B cells. Antibodies can directly bind to specific antigens to form antigen-antibody complexes, which can for example facilitate phagocytosis and subsequently antigen elimination. T cells recognize with their surface-expressed T cell receptor (TCR) antigen-derived peptides that are presented on MHC complexes to launch for example specific killing processes or the production of effector cytokines (1). The entire process of T cell-mediated antigen recognition and target cell lysis requires many additional associated interactions, which include co-receptors CD4 or CD8 and costimulatory molecules. During T cell development in the thymus, a diversified and highly polymorphic T cell repertoire is generated by random rearrangement of T cell receptor alpha and beta chains. Subsequently, T cells undergo a series of selection processes, especially to eliminate cell carrying receptors which recognize self-antigens and could lead to autoimmune disorders, leaving behind a broad repertoire of naïve T cells out of which with a high probability immunologically active epitope-specific T cells can be recruited and clonally expanded when encountering infections or malignant cells (2).

## 1.1 Thymic selection and shaping of T cell repertoire

The thymus plays an important role in generating and shaping the T cell receptor repertoire of an individual. Every individual is equipped with a unique as well as highly diverse TCR repertoire to potentially combat any invading pathogen and non-self-antigen. While a highly diverse TCR repertoire enables the immune system to fight non-self-antigens, it also has the potential risk to generate autoreactive T cells. To overcome this hurdle, T cells undergo several steps of screening and selection within the thymus as well as in the periphery. T cell antigen recognition depends on conversion of antigens into MHC bound peptides. MHC class I molecules (MHC I) usually present peptides to $CD8^+$ T cells, whereas MHC class II molecules (MHC II) mainly present peptides to $CD4^+$ T helper cells. Since every cell protein, independent of foreign or self, can enter the antigen processing pathway, antigen-presenting cells (APCs) in the thymus express a large array of self-proteins to facilitate tolerance to self-antigens. Developing T cells that react against self-antigens with high affinity are deleted by a process called ‘negative selection’. An essential component of this process is the

display of self-antigens, including antigens whose expression is usually restricted to specific tissues, by specialized thymic epithelial cells to developing T cells within the thymus (3) .
T cells with TCR of low affinity for self-peptide-MHC complexes receive survival signals and are positively selected; subsequently these cells emigrate the thymus into the 'naïve' T cell pool. T cells with TCRs that lack any reactivity to self-peptide-MHC complexes cannot provide MHC-restriction and are therefore useless; the cells die within the thymus by 'neglect' (no survival signal). T cells with TCR of high affinity for self-peptide-MHC complexes can die ('negative selection', deletion by overstimulation induced cell death) or enter counter-regulatory differentiation pathways (e.g. clonal diversion into the regulatory T cell ($T_{reg}$) lineage). Clonal deletion and clonal diversion are the major 'central tolerance' processes in the thymus that eliminate or control self-reactive T cells. Although these processes are thought to be highly efficient, they are not 100% complete and unable to prevent self-reactivity in all circumstances. Therefore, additional peripheral tolerance processes exist wherein self-reactive T cells become functionally unresponsive (anergy) or are deleted after encountering self-antigens outside the thymus. Recent advances in mechanistic studies of central and peripheral T-cell tolerance are promoting the development of therapeutic strategies to treat autoimmune diseases, cancer and improve transplantation outcome (4).
Circulating naive T cells represent the peripheral repertoire of TCR reactivities after passing through the selection and screening processes within the thymus. Prevalence of T cells specific for different epitopes in the peripheral repertoire is dependent on the mechanism of somatic recombination of the V(D)J gene segments which in turn controls the generation of appropriate TCR-α/β chains during T cell development as shown in the figure 1-2. TCR αβ diversification within the naive T cell pool results in approximately $2 \times 10^7$ different TCRs per individual in humans (5), which is significantly lower than the upper limit of potentially possible TCR diversification ($1 \times 10^{13}$ different TCRs) (6). Therefore, an individual's TCR repertoire is only a small selection from an enormous reserve, explaining why even genetically identical individuals differ in their TCR repertoires and that no two individuals have same TCR repertoire (7). Nevertheless, in response to defined epitopes, within the epitope-specific T cell population some TCRs can be found that are identical on the protein amino acid sequence level across different individuals (public clonotypes) (8, 9). Overall, the precursor frequencies of defined 'foreign epitope'-specific T cell populations within the peripheral naïve T cell pool are believed to be extremely low and depending on the epitope they might differ in polyclonality as well as their avidity spectrum (10).

## 1.2 CD8+ T cells and cellular Immunity

T cells determine the clinical outcome of various diseases, including infections, cancer, and autoimmune diseases. CD8+ T cells play a crucial role in adaptive immunity, as they can directly recognize and eliminate infected cells or tumor cells (11). In response to pathogen-associated stress or danger signals, dendritic cells (DCs) mature into potent antigen presenting cells (APC), which includes upregulation of MHC and expression of costimulatory receptors. Probably only such mature antigen presenting cells (APCs) are capable to provide all required co-stimulatory signals to differentiate a naïve T cell into T cells that can exert effector function (like effector cytokine production or target cell killing). This process is called 'T cell priming'.

Naïve T cells constantly circulate throughout the bloodstream and lymphoid organs in order to increase chances to encounter APCs expressing their specific epitope. In the case a naïve CD8+ T cell encounters its cognate pMHC expressed on activated DCs, this results in the formation of a so-called 'immunological synapse'. These synapses are formed to maintain a longer-lasting interaction of T cells and DCs, which are further stabilized by recruitment of adhesion molecules to the interface.

During primary antigen responses, epitope-specific naïve CD8+ T cells are activated (primed) and further undergo clonal expansion and differentiation into effector and memory CD8+ T cells.

## 1.3 Anatomy of T cell activation - T cell Receptor - MHC Interactions

CD8+ T cells can recognize intracellularly processed and MHC-I presented peptides, which might for example be derived from intracellular pathogens (like viruses or intracellular bacteria) or altered/mutated/overexpressed proteins in cancer cells. In humans, there are 3 classical MHC-I genes within the HLA complex- HLA-A, -B, and -C (3). Binding of epitope expressing MHC molecules (pMHC) to TCRs from CD8+ T cells together with co-stimulatory factors trigger the downstream signaling cascade leading to activation, expansion and differentiation of T cells, as well as to cytolysis of the target cells presenting the epitope (3, 12, 13).

### 1.3.1 TCR structure

The T cell receptor is a highly polymorphic heterodimeric complex comprising TCR-α and TCR-β chains. The noncovalent pMHC-TCR binding is the crucial primary event that initiates CD8+ T cell activation. However, additional factors like costimulatory signals are required for

T cells 'priming' as well as to enhance the discriminating ability of a T cell (13). The overall TCR structure (as shown in figure 1-1) resembles some components of the immunoglobulin B cell receptor or antibodies. Both TCR α and β polypeptide chains consist of different parts. The extracellular domain is the largest part and it includes a variable region (V) and a constant region (C) followed by a short hinge region-like domain, which contains a cysteine to link the two chains by a disulfide bond. There is a transmembrane region through which the chains are anchored on the cell. Positively charged amino acids in the transmembrane region allow the interaction with invariant chains of the CD3 complex, which is always co-expressed on the cell surface with the TCR and mediates intracellular signaling after T cell activation.

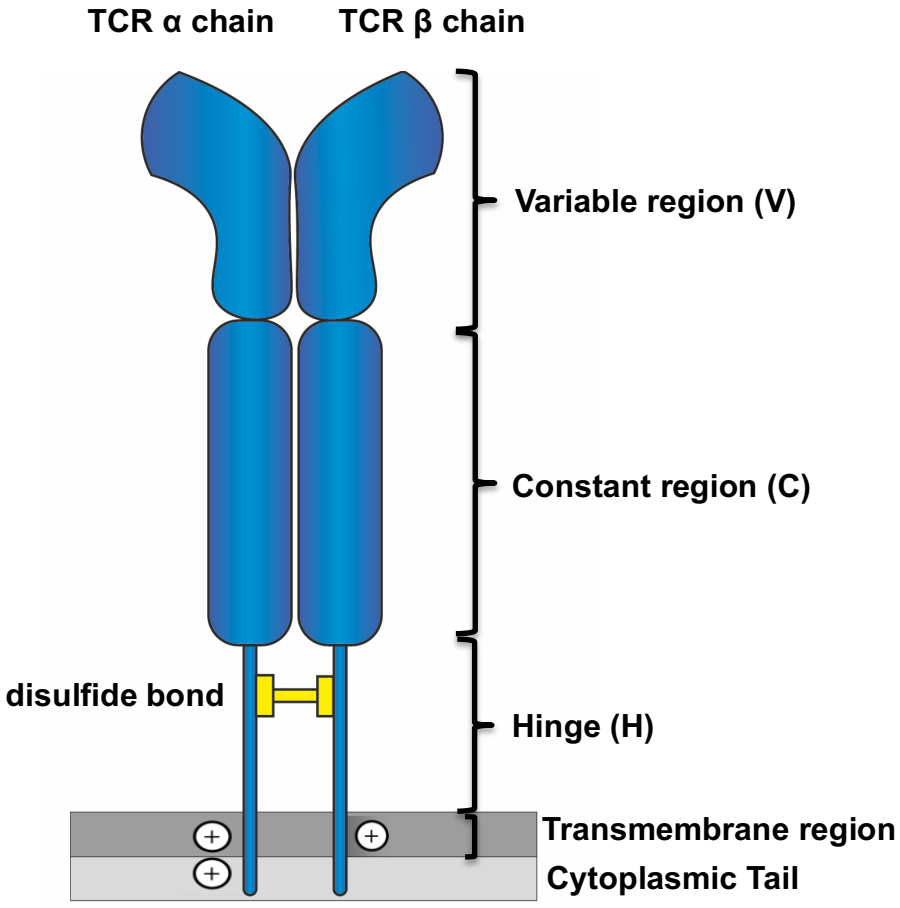


**Figure 1-1. T cell receptor structure (TCR)** Each TCR contains α and β chain both chains present a variable and a constant region. The variable region contains the complementary determining regions (CDRs) and mediates the interaction with the ligand; a constant region (C), a hinge region like domain to associate both chains with a disulfide bond, as well as a transmembrane region and a short cytoplasmatic tail. Positively

charged (+) amino acids in the transmembrane region allow the association with the CD3 complex.

### 1.3.2 T cell Receptor (TCR) repertoire shaping

Due to manifoldness and unpredictability of antigens/epitopes an individual might get exposed to during his/her lifetime, the adaptive immune system has to provide a highly diverse pool of naïve T cell repertoires. Each naïve T cell usually expresses only one TCR (approximately 1 x $10^5$ surface expressed copies), and T cell precursor frequencies of T cells expressing the same TCR or the same epitope-specificity are extremely low.

The TCR is a heterodimer composed of an α- and a β-chain (or less frequent γδ-chains), both chains contain a variable and a constant region. The variable, antigen binding region is encoded by several gene segments: variable (V), diversity (D) and junctional (J) segments in case of a β-chain, and V and J segments in a α-chain (fig. 1-2).

Somatic recombination (rearrangement) of (V) (D) (J) occurs in the thymus during T cell development resulting in functional and highly diverse TCR repertoire. TCR gene rearrangement is a defined system for random combination of different gene segments as structural components of the B and T cell receptor. The main reason for the high diversity in TCRs is due to the availability of different segments for α- and β-chains. The human TCR loci are comprised of 42 Vβ, 2 Dβ,12 Jβ, 43 Vα, 58 Jα gene segments (14)

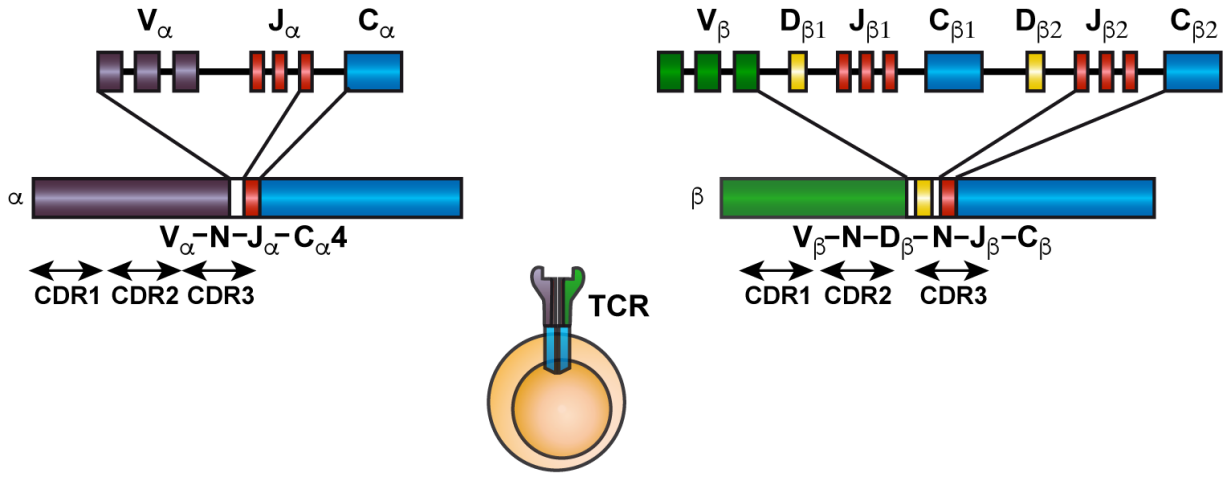


**Figure 1-2. Generation of functional TCR-αβ chains** Recombination of variable (V), joining (J) and diversity (D) segment to a constant region (C) results in the formation of TCR β chain (shown on the right). The α-chain (shown on the left) assembly happens with V and J segment as well as the constant region (modified from Nikolich-Zugich, Slifka, and Messaoudi 2004). Recombinatorial diversity is further enhanced by addition and deletion of nucleotides (N) at the junctions between the segments but is reduced by thymic selection

### 1.3.3 T cell Receptor - MHC Interactions and T cell activation

The pMHC ligand interaction with the TCR is mediated by the three-hypervariable complementary determining regions (CDRs) on the V region. CDR1 and CDR2 are encoded by variable genes in the germline (47 TRAV genes for the α and 57 TRBV genes for β). Junctional modifications lead to the formation of the CDR3 region. CDR3 is therefore characterized by the highest variability among individual TCRs (15, 16) .

TCR engagement (signal 1) leads to phosphorylation of the CD3 co-receptor, ZAP70 and downstream Src kinases and induces a signaling cascade that results in T cell proliferation and differentiation (17). The CD28 costimulatory molecule of the Immunoglobulin (Ig) receptor family is expressed on the T cell surface and binds to its ligand CD80/86 on mature DCs (signal 2). Further intracellular kinases and adaptor proteins are recruited to the triggered TCR, thereby amplifying the TCR signals (18). T cell survival and effector functions can be further augmented by engaging other costimulatory molecules of the tumor-necrosis factor (TNF) receptor family, such as OX40 (CD134) and 4-1BB (CD137) (19). Inflammatory cytokines, e.g. interleukin (IL)-12 and type I interferons (IFNs) are also involved in supporting T cell expansion and function, therefore considered to be ‘signal 3’ in T cell activation (20). Subsequently, activated/primed T cells clonally expand and adopt different phenotypes and functional profiles (T cell subset diversification). Some daughter cells down (or up-)-regulate crucial organ-restricting molecules, like the expression of CD62L and CCR7, for which downregulation or surface shedding enables $CD8^+$ T cells to exit lymphatic organs.

Activated T cells circulate through the periphery and some subsets – especially with effector phenotypes - are capable of migrating preferentially to inflamed tissue where they exhibit effector function upon antigen-encounter (21). Cytotoxic $CD8^+$ T cells are capable of killing target cells by cell-cell contact dependent pathways (e.g. engagement of the TNF receptor family member Fas (CD95) or through release of toxic granules). Preformed cytolytic molecules are delivered to the contact area between T cell and target cell by directed exocytosis. Pore-forming proteins, such as perforin, cause membrane lesions and the serine proteases granzyme A and B induce caspase-linked apoptosis. Programmed cell death is also triggered by the binding of Fas ligand (FasL) on activated CD8+ T cells to its receptor Fas on the target cell. Secretion of pro-inflammatory cytokines. like IFN-γ and TNF-α ,plays a critical role in recruiting and activating innate immune cells and supporting antigen recognition. Further non-cytolytic functions of $CD8^+$ T cells contribute to the inflammatory response (22).

## 1.4 Application of T cells - Adoptive cell therapy - ACT

Adoptive cell therapy (ACT) with T cells has become a powerful therapeutic tool, which has proven its curative potential in several studies targeting chronic infections as well as cancer (23, 24). Recent developments in immunotherapy have shown ACT to be an emerging and promising branch of cellular therapy. This success is a result of availability of modern genetic tool boxes, which enable engineering of T cells to display desired antigen-specific receptors with enhanced functionalities (24, 25).

With recent technical advances, it is further possible to identify and isolate T cells and extract their TCR sequences with wide range of applicability, for example for adoptive transfer of TCR - engineered T cells for treatment of infections or cancer, or for the modulation of aberrant T cell reactivity associated with autoimmune disease (11, 26).

Therapeutic benefit upon clinical application of TCR gene-modified T cell transfer has been shown in melanoma patients (27). Especially in melanoma patients, also application of unmodified autologous TILs showed some activity going along with prolonged survival (28). Another clinical trial for melanoma treatment was based on adoptive transfer of genetically engineered MART-1-specific T cells, here TCRs were derived from melanoma patient who responded initially to TIL therapy (29). However, broader applicability of this therapeutic approach is still highly challenging even with the availability of more efficient methods of antigen-specific T cell isolation, complete TCR sequence extraction and autologous T cell engineering. This is mainly due to the fact that TCR with a relatively high avidity are required for effective therapeutic responses upon ACT, and often (especially for tumor reactivities or during chronic infection or within the naïve T cell pool) high avidity T cells are very rare in frequency and it is extremely difficult to identify such receptors for subsequent T cell engineering approaches.

## 1.5 Sources of antigen-specific T cells for ACT

There are several sources for the identification of suitable TCRs to produce genetically engineered T cells. Broadly we can classify sources into three categories

1) Patient-derived T cells - TILs (Tumor infiltrating lymphocytes)
2) Healthy donor derived material.
3) Vaccinated HLA transgenic mice.

TCR gene therapy sources from patient-derived material comprise peripheral blood, resected tumor biopsies and draining lymph nodes (28). An advantage of TCRs derived from responding patients is that such TCR clones often have enhanced frequencies, which

facilitates detection and isolation of these populations (29, 30). A possible disadvantage might be that most tumor-specific T cell populations in patients might carry relatively low-affinity TCRs, because T cells with high affinity TCRs can get deleted during chronic antigen exposure. In the case of overexpressed 'self' tumor antigens, most high avidity TCRs are most likely already eliminated by central tolerance in patients.

Immunization of HLA and human TCR locus transgenic mice with tumor antigens, which are self-antigens for the patient, could circumvent the problem of central tolerance, if the mouse doesn't express sequence identical self-epitopes. Generation of a mouse line in which the complete (unarranged) human TCR loci were introduced while the murine TCR loci were inactivated has been successfully reported. Crossing this mouse model on HLA-transgenic backgrounds allows to isolate complete human TCRs from a non-tolerant repertoire directed against those human peptide antigens that differ between mice and humans. Whether such "human" TCRs selected on a murine self-peptide repertoire are not promiscuous or immunogenic upon adoptive transfer into humans still has to be demonstrated.

### 1.5.1 Healthy donor as a source for antigen-specific T cell receptors

A healthy donor who has not been exposed to a (non-self) target antigen/epitope should contain a broad polyclonal repertoire of epitope-specific TCRs within the naïve T cell compartment, including high-avidity epitope-specific TCRs. These cells are in circulation but have not encountered their cognate antigens (11, 31). Major challenge is here to get access to these extremely rare cell population.

Many methods of detection and isolation of epitope-specific $CD8^+$ T cells have limitations in terms of application towards detection of naïve T cells because they involve functionality testing (e.g. cytokine secretion assay) and naïve T cells are usually not capable to respond after short-term stimulation with effector cytokine production. pMHCI multimer staining can overcome this problem, as this method does not rely on effector function. However, the precursor frequency of epitope-specific T cells within the naïve T cell pool is so low that the detection limit of conventional pMHCI multimer staining makes it difficult to screen for epitope-specific T cells. Most of the data available on the precursor frequencies are based on significant bias involving external stimulation of antigen-specific cells and variability of assays used e.g. serial dilution, micro titer assays etc. (5, 10).

Major challenge in the field is, therefore, the isolation of extremely rare cells with target epitope specificity from a large amount of starting cell material. FACS - fluorescent activated cell sorting - for isolation of different cell types is an established method in the field of

immunology. Although there are several established FACS-based methods used for identification and isolation of cells whose target frequency is low, traditional cell sorting techniques still pose challenges with respect to time taken for screening a large volume donor PBMCs and isolate rare T cells with desired specificities. Other groups have shown that MHC multimer-based bead enrichment system can get access to extremely low frequency T cells specific for a given pMHC-peptide complex (down to $10^{-6}$) (32). However, these methods still have to deal with a quite low efficacy, which lowers the chances to identify high avidity TCRs within a polyclonal repertoire. These issues highlight the need for establishment of a workflow which can expedite the entire process of isolating rare epitope specific cells from a healthy donor source with high efficacy (11, 31).

## 1.6 T Cell Epitopes as Targets for Immunotherapy

The success of adoptive cell therapy to a large extent depends on the choice of target antigen (33). The choice of antigens is one of the biggest factors in deciding the success or failure TCR gene therapy. Unfortunately, there is lack of truly tumor-specific antigens shared across tumor types, and recent clinical studies have shown in some cases lethal effects of receptor-engineered T cells due to on-target recognition of normal tissues.

Optimal target antigens should be exquisitely expressed by tumor cells and not by healthy tissues, and thus should not evoke an immune response against healthy non-tumor tissues. Neo-epitopes derived from mutated proteins only in tumor cells might fulfill these criteria. Especially neo-epitopes from mutations in genes which are functionally important for tumor growth or progression, so called ‘oncogenic drivers’, might be attractive targets for ACT, since loss of their expression might reduce tumor cell fitness or survival, reducing the likelihood of tumor escape from epitope-specific ACT. Ideal therapeutic targets should be present with relatively high frequency in common cancers to treat larger groups of patients (34).

In general, tumor associated antigens (TAAs) discussed as targets for ACT can be divided into four groups: over-expressed antigens (differentiation antigens, cancer testis antigens (CTAs), others) and neo-antigens. Most tumor associated antigens are self-proteins (although often not detectable in adult tissues), and T cells bearing high-affinity TCRs specific for such antigens are commonly deleted in the thymus. The family of Cancer Testis Antigens (CTA's) is frequently expressed by the developing embryo but are not expressed in significant quantities in the normal adult other than in the testis and placenta (35). Differentiation antigens are expressed during different time points of tissue development, but their expression is not limited to tumor cells. Other over-expressed antigens are

predominantly, but not selectively, expressed by tumor cells. Neo-antigens are exclusively expressed by tumor cells without a counterpart in healthy tissues. (33) (36). For all TAAs is has to be further considered that not all tumor cells might express the same TAAs (mosaic), which can significantly affect the success of therapy. Although it has been shown at least in some experimental models that T cells targeting cross-presented epitopes on tumor stroma cells can cause extensive tumor tissues damage leading to tumor cell regression, including tumor cells that are not expressing the relevant TAA.

## 1.7 Evaluating choice and source of target antigens

The choice of obtaining T cells from the naïve repertoire of an unprimed individual could be favored to the isolation of T cells from TILs for several reasons. For examples, studies have shown that there is a reduction in TCR repertoire diversity in melanoma metastases (similar to changes observed in some chronic viral infections), since the tumor resident TILs are constantly stimulated by antigens and exposed to a tumor suppressive microenvironment. This could go along with silencing and/or subsequent deletion of high-avidity T cells directed against TAAs (37, 38). It is suggested that structural avidity (the binding strength of a TCR to cognate epitope/MHC molecules in combination with co-receptor binding of TCRs) and functional avidity (quality of cytokine production after stimulation or lysis of peptide-pulsed target cells) represent parameters that can be used to predict which remaining T cells (and which TCRs) are capable to exert a protective/therapeutic immune response, especially upon ACT (39).

Despite some clinical success, adoptive cell therapy with transgenic T cells directed against different kinds of TAAs has also caused serious off-site and off-target toxicities. Several clinical trials have demonstrated significant off-tumor toxicities (40). Treatment-related toxicities were observed in clinical trials with TCRs against antigens overexpressed in tumors but also expressed on normal tissues. These toxicities included serious but treatable inflammation of various tissues. A TCR gene-therapy trial with patients receiving TCR gene-modified T cells targeting the melanocyte differentiation antigens MART-1 and gp100 experienced vitiligo and eye or ear toxicity. This on-target, but off-site toxicity was induced by recognition of these antigens on melanocytes in the ear, epidermis and immunoprivileged sites as the eye (41). Even treatment-associated patient deaths due to neurological and cardiac toxicity became evident. Infusion of MAGE-A3 TCR engineered T cells into cancer patients resulted in the death of 2 out of 9 treated patients due to the recognition of its cognate epitope expressed in a subset of neurons in the human brain (40). In another study

with gene-engineered T cells, also targeting MAGE-A3, two patients suffered from cardiac toxicity and subsequently died of cardiac arrest. This effect was probably caused by off-target recognition of the entirely unrelated muscle protein titin, which is expressed in pulsating heart muscle cells. In the latter case, the TCR was affinity enhanced by site-directed mutagenesis in the TCR complementarity-determining region (CDR) (42). It was shown that this can improve protective immunity through elevated avidity, but can also increase promiscuity of the TCR to other epitope targets (43) (44) (45).

A strong correlation between TCR avidity and immunogenicity has been reported *in vivo* as well as *in vitro* (46). Based on these findings, it was hypothesized that chronic antigen exposure by viral infections or cancer cells will eventually lead to the functional exhaustion and subsequent deletion of high avidity T cells and the recruitment and expansion of low avidity T cells (47). Several inhibitory receptors like T cell immunoglobulin and mucin domain-containing protein 3 (TIM3), lymphocyte activation gene 3 protein (LAG3), cytotoxic T lymphocyte antigen 4 (CTLA4) and programmed cell death protein 1 (PD1) have been implicated in initiating T cell exhaustion (48).

About 20% of all the identified tumor antigens are encoded by genes that are overexpressed in cancer cells as compared to normal cells. Regardless the limitations discussed above regarding central tolerance towards self-antigens and tissue restricted expression, some candidates, e.g. antigens expressed by genes WT1, HER-2/neu and PRAME, which are all critical for proliferation and overexpressed in tumor cells, are believed to be expressed selectively in tumor tissues and considered to be safe with respect to off-tumor toxicities (33). Importantly, these genes are overexpressed in tumor cells of many histological types. As an example, the gene HER-2/neu is overexpressed in many types of carcinomas and T cells recognizing HER-2/neu peptides were derived from tumor-infiltrating lymphocytes (TILs) of ovarian carcinomas (33, 49-51), without evidence of off-tumor reactivities/toxicities.

A major obstacle of tumor-associated self-antigens is that only a minority (if at all) of TCRs directed against them - derived from the patient or a healthy donor matching in the restricting HLA element - have a low avidity due to negative selection in the thymus. This prevents the identification of high-avidity TCRs capable of recognizing low antigen-HLA levels, normally expressed on tumor cells (52). Although improved objective response rates with avidity enhanced TCRs - accomplished by genetic modification - has been described, this strategy has also shown some fatal adverse events (40, 42).

## 1.8 T Cell epitopes of interest

We chose for our studies epitopes, which are restricted by HLA-A201, the most common caucasian HLA molecule. The epitopes of interest are listed below (Table 1-1) together with the peptide sequences.

| Epitope of interest | Sequence |
|---|---|
| $WT1_{126-134}$ | RMFPNAPYL |
| $Her2Neu_{369-377}$ | KIFGSLAFL |
| $PRAME_{300-309}$ | ALYVDSLFFL |
| $NY\ ESO1_{157-165}$ | SLLMWITQV |
| $PR1_{169-177}$ | VLQELNVTV |
| $HA1_{137-145}$ | VLHDDLLEA |
| $pp65_{495-503}$ | NLVPMVATV |
| $Flu\ MP_{58-66}$ | GILGFVFTL |
| $YFV_{214-222}$ | LLWNGPMAV |

**Table 1-1 : Epitopes of choice with their respective sequences.**

As previously discussed in (section 1.7), the selection of different epitopes was based on the availability of T cells directed against them in the periphery of healthy donors.

**Tumor specific epitopes**

**WT1**

The Wilms tumor gene 1 (WT1) is a transcription factor encoded by a gene that is overexpressed in some leukemia and various solid tumors (33). WT1 is a transcription factor with C-terminal zinc finger domains and is involved in many pathways regulating cellular growth and metabolism. During embryogenesis, the expression of WT1 is essential for kidney development but is also present in other organs. After birth, however, WT1 is only expressed at a very low level and is restricted to certain kidney cells and hematopoietic stem cells (53). Several WT1 peptides have been identified as T cell antigens. The WT1 antigens are among the few that so far have been identified as antigen-targets for leukemic patients. Tumor regressions following WT1 vaccination have been reported.

**HER-2/neu**

The gene HER-2/neu is overexpressed in many types of carcinomas and T cells recognizing HER-2/neu peptides were derived from tumor-infiltrating lymphocytes (TILs) of ovarian carcinomas, metastatic effusions of breast cancer patients, or TILs from lung cancer patients (54, 55).

**PRAME**

PRAME is the preferentially expressed antigen on melanomas (PRAME) and of potential interest because it is highly expressed in many different cancers, including acute and chronic myeloid and lymphoid leukemia as well as lung carcinomas. The gene for PRAME is expressed in some normal tissues such as testis, endometrium, adrenals or ovary, at levels that are about 100-fold lower than in tumors, and it is overexpressed in tumors whereas normal tissues have low PRAME expression (40, 56). High-avidity TCRs specific for TAA that are shared between various tumors would be attractive tools for TCR gene therapeutic strategies (57).

**NYESO1**

The family of Cancer Testis Antigens (CTA's) is especially regarded as a promising target antigens in sarcomas. These antigens are frequently expressed in developing embryos, however they are also expressed in testis and placenta but not in significant quantities (35, 57). Solid tumor malignancies such as melanoma have been treated by targeting CTAs in early phase immunotherapy trials (28). Published results from NCI Surgery Branch showed their treatment of 6 synovial sarcoma patients using T cells with a transduced T-cell receptor targeting NY-ESO-1 (28, 51, 58).

**PR1**

PR1, a human-lymphocyte-antigen (HLA) -A2 -restricted peptide derived from proteinase 3. PR1 was used to elicit CTLs from normal individuals. It has been previously shown that HLAA2.1-restricted self-peptide PR1 (aa 169–177) derived from proteinase 3 could be used to elicit CTL lines from healthy donors. These PR1-specific CTLs lysed myeloid leukemia cells in patients with CML. The amount of leukemia lysis and colony inhibition was proportional to proteinase-3 overexpression in leukemia cells compared with HLA-matched normal marrow cells. Based on these results and because proteinase 3 is aberrantly expressed in many cases of myeloid leukemia, proteinase 3 may serve as a leukemia-associated target antigen for immunotherapy. Lymphocytes with PR1-specificity may,

therefore, be useful in adoptive immunotherapy strategies to treat patients with myeloid leukemia if the lymphocytes could be easily isolated and expanded.

### Viral epitopes

### A2pp65

Cytomegalovirus (CMV) is a double stranded DNA virus, which belongs to the herpesviridae family and causes a lifelong chronic infection. The virus is widely spread (60-90 %) (59). In healthy individuals, the viral protein pp65 is one of the main targets of T cell-mediated responses. pp65 is a lower matrix phosphoprotein with the molecular mass of 65 kDa. Isolated TCRs from healthy carriers show high preferences to single viral epitopes and low TCR diversity (51). In immunocompromised patients, the CMV infection cannot be controlled, it becomes a severe threat. A transfer of donor-derived CMV-specific T cells has shown to reconstitute the cytotoxic T cell reaction against CMV and controls the disease in affected patients (60).

As other viral epitopes of interest we chose were influenza FluMP - influenza matrix protein and YFV - Yellow fever virus epitope (61, 62).

# 2. Thesis objectives

The goal of my thesis work was to set up a workflow for isolating rare epitope-specific naïve T cells and extract T cell receptors (TCRs) using time efficient and cost effective methods for identification of functional TCRs, which can be used for future clinical application.

The detailed aims of this thesis were:

1) To provide a proof of concept that extremely rare epitope-specific T cells can be enriched by available selection technologies from large donor cell samples.
2) To provide a proof of concept that TCRs can be isolated from enriched epitope-specific naïve T cell populations.
3) To provide a proof of concept that identified TCRs can be re-expressed using transposon based sleeping Beauty (SB) non-viral gene transfer system.

# 3 Materials and Methods

## 3.1 Materials

### 3.1.1 Chemicals and reagents

| Reagent | Supplier |
|---|---|
| 1-bromo-3-chloropropane | Sigma-Aldrich |
| 2-mercaptoethanol | Gibco BRL |
| 2-propanol | Roth |
| 5x Herculase II Rxn buffer | Agilent |
| Agar | Remel |
| Ampicillin | Sigma-Aldrich |
| Betain | Sigma-Aldrich |
| Biocoll Separation Solution | Biochrom AG, Berlin, Germany |
| Bovine serum albumin (BSA) | Sigma-Aldrich |
| Carbenicillin | Roth |
| CaCl2 | Merck |
| D (+)- Glucose anhydrous, ≥99.5 % | Roth |
| D-biotin | Sigma-Aldrich |
| Dimethylsulfoxide (DMSO) | Sigma-Aldrich |
| DMEM | GE Healthcare |
| DNA-ladder | Fermentas |
| dNTPs | Roche |
| Ethanol | Klinikum rechts der Isar, München, Germany |
| Fetal calf serum (FCS) | GE Healthcare |
| Gentamicin | Roth |
| Gibson Assembly Master Mix (2x concentrate) | New England Biolabs |
| Glycerol | Sigma-Aldrich |
| Guanidine-HCl | Calbiochem |
| HEPES | Gibco BRL |

| | |
|---|---|
| Interleukin-2 (IL-2) | Peprotech, Novartis |
| Interleukin-7 (IL-7) | Peprotech |
| Interleukin-15 (IL-15) | Peprotech |
| KCl | Merck |
| LB-ampicillin selective plates (100µg/ml) | Sigma-Aldrich |
| L-arginine-HCl | Sigma-Aldrich |
| Leupeptin | Sigma-Aldrich |
| MgCl2 | Roth |
| NaCl | Roth |
| Na2HPO4 | Roth |
| NaH2PO4 | Merck |
| Neomycin | Sigma-Aldrich |
| NH4Cl | Sigma-Aldrich |
| Nuclease-free water | Promega |
| Paraformaldehyde (PFA) | Sigma-Aldrich |
| Penicillin/Streptomycin | Roth |
| Pepstatin | Sigma-Aldrich |
| Phosphate buffered saline (PBS) | Biochrom |
| Polyethylene glycol 4000 (PEG) | Merck |
| Propidium iodide (PI) | Sigma-Aldrich |
| Puromycin | Sigma-Aldrich |
| Retronectin | Takara Bio Europe |
| Roti-Safe Gel Stain | Roth |
| RPMI 1640 | GE Healthcare, Gibco BRL |
| SOC medium | New England Biolabs |
| Sodium-EDTA (Na-EDTA) | Roth |
| Sodium pyruvate | PAA |
| Sodium succinate | Sigma-Aldrich |
| Strept-actin-PE | IBA |
| Strept-actin-APC | IBA |
| Streptavidin-PE | Biolegend |
| Streptavidin APC | Biolegend |
| Streptavidin BV421 | Biolegend |
| TAE-buffer | Thermo Scientific |

| | |
|---|---|
| Tris-hydrochloride (Tris-HCl) | Roth |
| Trypan Blue solution | Sigma-Aldrich |
| Trypsin/EDTA (0.05%/ 0.02%) | GE Healthcare |
| Yeast extract | Roth |

### 3.1.2 Media and buffers

| Buffer | Composition |
|---|---|
| Complete freezing media (CFM) | 90% FCS |
| | 10% DMSO |
| Cell-culture media (T cell) | 1x RPMI 1640 |
| | 10% (w/v) Human Serum |
| | 0.025% (w/v) L-Glutamine |
| | 0.1% (w/v) HEPES |
| | 0.001% (w/v) Gentamycin |
| | 0.002% (w/v) Penicillin |
| DMEM complete | 0.002% (w/v) Streptomycin |
| | 1x DMEM |
| | 10% (w/v) FCS |
| Electroporation buffer 1SM | 5 mM KCl |
| | 15 mM MgCl2 |
| | 120 mM Na2HPO4/NaH2PO4 pH 7.2 |
| | 25 mM Sodium Succinate |
| | 25 mM Manitol |
| Erythrocyte lysing solution (ACT) | 153 mM NH4Cl |
| | 17 mM Tris-HCl |
| FACS buffer | 1x PBS |
| | 0.5% (w/v) BSA |
| | pH 7.45 |
| LB-ampicillin | 10 g/l bacto-tryptone |
| | 5 g/l yeast extract |
| | 20 g/l agar |
| | 10 g/l ampicillin |
| | pH 7.0 |

| | |
|---|---|
| RPMIcomplete | 1x RPMI 1640 |
| | 10% (w/v) FCS |
| | 5% (w/v) SC+ |
| Transfection buffer | 1.6 g NaCl |
| | 74 mg KCl |
| | 50 mg Na2HPO4 |
| | 1 g HEPES |
| | 100 ml H2O |
| | pH 6.76 |

### 3.1.3 Antibodies

| Antibody | Clone | Supplier |
|---|---|---|
| FITC mouse anti-human HLA-A2 | | BD-Bioscience, Heidelberg, Germany |
| Human CD3 AmCyan | SK7 | BD-Bioscience, Heidelberg, Germany |
| Human CD3 BV650 | OKT3 | Biolegend, London, UK |
| Human CD3 FITC | UCHT1 | Beckman Coulter, Fullerton, USA |
| Human CD3 PE | UCHT1 | Beckman Coulter, Fullerton, USA |
| Human CD3 stimulating antibody | OKT3 | Beckman Coulter, Fullerton, USA |
| Human CD4 FITC | 13B8.2 | Beckman Coulter, Fullerton, USA |
| Human CD8 APC | RPA-T8 | BD Pharmingen, Heidelberg, Germany |
| Human CD8 Pacific Blue | B9.11 | Beckman Coulter, Fullerton, USA |
| Human αCD8a-PECy7 | SK1 | Beckton Dickinson, Heidelberg, Germany |
| Human αCD8a-PerCP | SK1 | Beckton Dickinson, Heidelberg, Germany |
| αCD28 stimulating antibody | L293 | Beckman Coulter, Fullerton, USA |
| αCD107a-PE | eBioH4A3 | eBioscience, San Diego, USA |
| αIFNγ-FITC | 4S.B3 | eBioscience, San Diego, USA |

| | | |
|---|---|---|
| α-mouse TCR beta (β) chain-APC | H57-597 | Biolegend, London, UK |
| αTNFα-PECy7 | MAb11 | eBioscience, San Diego, USA |

### 3.1.4 Kits

| Reagent | Supplier |
|---|---|
| CloneJET PCR Cloning Kit | Thermo Fisher Scientific |
| Gibson Assembly Kit | New England Biolabs |
| PureLink™ HiPure Plasmid Filter Maxiprep Kit | Invitrogen |
| PureYield™ Plasmid Midiprep System | Promega |
| PureYield™ Plasmid Miniprep System | Promega |
| Wizard® SV Gel and PCR Clean-Up System | Promega |
| CMV-IgG-ELA Test PKS | Medac, Hamburg, Germany |
| Qiaquick Spin Column | Qiagen, Hilden, Germany |

### 3.1.5 Equipment

| Equipment | Model | Provider |
|---|---|---|
| Cell sorters | FACS Aria III | Becton Dickinson (BD Bioscience) |
| | MoFlo™ Legacy | Beckman Coulter, Fullerton, California, US |
| | MoFlo™ XDP | Beckman Coulter, Fullerton, California, US |
| Centrifuge | Biofuge fresco | Heraeus, Hanau, Germany |
| | Multifuge 3 S-R | Heraeus, Hanau, Germany |
| | Sorvall® RC 26 Plus | Thermo Fisher |

| | | |
|---|---|---|
| | Varifuge 3.0RS | Heraeus, Hanau, Germany |
| | Biofuge stratos | Heraeus, Hanau, Germany |
| Electrophoresis chambers | 40-0911 | PEQLAB |
| | 40-1214 | PEQLAB |
| | 40-2314 | PEQLAB |
| Electrophoresis power supply | E455 | Consort |
| Electroporation cuvettes | Ingenio Cuvettes | Mirus Bio LLC |
| Electroporator | Nucleofector™ II/2b | Lonza |
| Flow Cytometers | Cyan™ Lx Flow cytometer | Beckman Coulter, Fullerton, California, US |
| | Cyan™ ADP Lx9 Color Analyzer | Beckman Coulter, Fullerton, California, US |
| Microscopes | Axiovert S100 | Zeiss |
| | Zeiss LSM 510 | Carl Zeiss |
| Spectrophotometer | NanoDrop ND-1000 | Nano Drop, Baltimore |
| Heat block | Thermomixer Compact | Eppendorf |
| Laminar flow hood | Hera Safe | Heraeus |
| Thermocycler | T 3000 Thermocycler | Biometra |
| | T Gradient | Biometra |
| UV-sensitive camera | Eagle Eye | Bio-Rad |
| UV-microscope | Olympus CKX41 | Olympus |
| Incubator | Cytoperm 2 | Heraeus, Hanau, Germany |
| | Minitron | Infors, Bottmingen, Switzerland |
| | BE 500 | Memmert, Schwabach, Germany |
| BioSafety Cabinets | HERAsafe | Heraeus, Hanau, Germany |
| Hemocytometer | Neubauer | Schubert, Munich, Germany |
| Water Bath | LAUDA ecoline 019 | Lauda, Königshofen, Germany |

| | | |
|---|---|---|
| Photometer | Bio Photometer | Eppendorf |
| pH-meter | MultiCal® pH 526 | WTW, Weilheim, Germany |
| Weighing Scale | CP 124 S | Sartorius, Göttingen, Germany |

### 3.1.6 Cells and Cell lines

| Cell line | Provider |
|---|---|
| T2 | ATCC: CRL-1992 |
| E. coli Stbl3 | Institute of Virology,TU Munich (Prof. Ulrike Protzer) |
| Jurkat cells (J76) | Max-Delbrück-Center for Molecular Medicine (Prof. Wolfgang Uckert) |
| B-LCLs | Institute of Hematology Klinikum Rechts der Isar, Munich (Dr. Angela Krackhardt) |

Jurkat 76 cells were grown at 37°C, 95 % humidity, 5 % CO2 in 1640 RPMI medium supplemented with 10 % fetal calf serum and 100 U/ml penicillin, 100 U/ml streptomycin and gentamycin.

### 3.1.7 Primers and Oligos

| Names | 5'-3' sequence |
|---|---|
| pJET fwd | GACTCACTATAGGGAGAGCGGC |
| pJET rev | AGAACATCGATTTTCCATGGCAG |
| pT2 seq fwd | AAGAGCCCACAACCCCTCACT |
| pT2 seq rev | GGTTTGTCCAAACTCATCAAT |

### 3.1.8 Enzymes

| Enzymes | Supplier |
|---|---|
| DreamTaq DNA Polymerase | Thermo Fisher Scientific |

| | |
|---|---|
| Herculase ® II Fusion DNA Polymerase | Agilent |
| T4 ligase | Thermo Fisher Scientific |
| Affinity Script, Reverse Transcriptase | Agilent |
| Superscript II, Reverse Transcriptase | Invitrogen |

### 3.1.9 Peptides

| HLA-type | Peptide | Sequence | Supplier |
|---|---|---|---|
| A*02:01 | Flu $MP_{58-66}$ | GILGFVFTL | IBA, Göttingen, Germany |
| A*02:01 | $YFV_{214-222}$ | LLWNGPMAV | IBA, Göttingen, Germany |
| A*02:01 | $pp65_{495-503}$ | NLVPMVATV | IBA, Göttingen, Germany |
| A*02:01 | $WT1_{126-134}$ | RMFPNAPYL | IBA, Göttingen, Germany |
| A*02:01 | $Her2Neu_{369-377}$ | KIFGSLAFL | IBA, Göttingen, Germany |
| A*02:01 | $PRAME_{300-309}$ | ALYVDSLFFL | IBA, Göttingen, Germany |
| A*02:01 | NY $ESO_{1157-165}$ | SLLMWITQV | IBA, Göttingen, Germany |
| A*02:01 | $PR1_{169-177}$ | VLQELNVTV | IBA, Göttingen, Germany |
| A*02:01 | $HA1_{137-145}$ | VLHDDLLEA | IBA, Göttingen, Germany |
| A*02:01 | UV-cleavable peptide | KILGFVF**J**V | Ton Schumacher, NKI, Amsterdam, Netherlands |

### 3.1.10 pMHC-Multimers

| pMHC | Peptide Sequence |
|---|---|
| HLA-A2 / hβ2m/ Flu $MP_{58-66}$ | GILGFVFTL |
| HLA-A2 / hβ2m/$YFV_{214-222}$ | LLWNGPMAV |
| HLA-A2 / hβ2m/ $pp65_{495-503}$ | NLVPMVATV |
| HLA-A2 / hβ2m/ $WT1_{126-134}$ | RMFPNAPYL |
| HLA-A2 / hβ2m/ $Her2Neu_{369-377}$ | KIFGSLAFL |
| HLA-A2 / hβ2m/ $PRAME_{300-309}$ | ALYVDSLFL |

| | |
|---|---|
| HLA-A2 / hβ2m/ NY $ESO_{1157-165}$ | SLLMWITQV |
| HLA-A2 / hβ2m/ $PR1_{169-177}$ | VLQELNVTV |
| HLA-A2 / hβ2m/ $HA1_{137-145}$ | VLHDDLLEA |
| HLA-A2 / hβ2m/ UV-cleavable peptide | KILGFVF**J**V |

UV-cleavable peptide was provided by Ton Schumacher, NKI, Amsterdam, Netherlands.

### 3.1.11 Software

| Software | Provider |
|---|---|
| Adobe Illustrator | Adobe Systems, San Jose, USA |
| EndNote Program | Microsoft, Redmond, USA |
| FlowJo | Treestar, Ashland, USA |
| | BD Biosciences, Heidelberg, Germany |
| Prism | Graph Pad Software, La Jolla, USA |
| imgt.org | IMGT/V-QUEST |
| BLAST | NCBI |
| ensembl.org | EMBL-EBI |
| Microsoft Office | Microsoft 2017, Redmond, USA |
| Summit V4.5 | Beckman Coulter, Fullerton, California, US |

## 3.2 Methods

### 3.2.1 Donor material preparation

#### 3.2.1.1 FACS-screening of healthy donor buffy coats for HLA-A2 expression

Blood from healthy donors was tested for HLA-A2. 20µl of buffy coat or whole blood was stained with 1µl of a HLA-A2-FITC antibody and was further incubated for 10 min at room temperature in the dark. The sample was then lysed by addition of 180µl Lyse/Fix buffer (BD) and incubated for 15 min at room temperature in the dark. After washing the sample twice with FACS-buffer it was analyzed by flow cytometry.

#### 3.2.1.2 Screening for CMV-IgG using ELISA

For proof of principle experiments, PBMCs from Cytomegalovirus(CMV) negative donors were needed. In order to screen whether a donor is positive or negative for CMV, the blood plasma was tested for CMV-specific antibodies (IgG). The CMV-IgG-ELA Test PKS (medac GmbH) was performed according to the manufactures recommendations. The samples were photometrically analyzed at 450 nm using the Sunrise$^{TM}$ microplate absorbance reader (Tecan Group Ltd.). Donors with values above 1.24 AU/ml were considered seropositive.

#### 3.2.2.3 Ficoll Density Gradient Separation of PBMCs

PBMCs were extracted from whole blood collected from healthy donors or from buffy coats of healthy individuals at the blood bank (German Heart Centre Munich). The blood was pre-diluted 1:1 with 1x PBS (sterile-filtered) and transferred to a layer of Ficoll (Biocoll Separation Solution). Ficoll gradients were centrifuged for 20 min at 2500 rpm (20°C) without brakes. The PBMC layer was collected and washed twice with PBS. The cell pellet was resuspended in 1ml FACS buffer. PBMCs were counted and adjusted to a cell concentration of $2x10^8$ for further enrichment processes.

### 3.2.2 Multimer generation and staining of cells of interest

Conventional MHC-I multimers for the detection of Ag-specific $CD8^+$ T cells were routinely produced in our laboratory according to well established protocols (63). All pMHC monomers loaded with specific peptides were refolded by Anna Hochholzer (AG Busch). pMHC multimers for all the epitopes of interest were generated according to the established standard protocol (Busch et al., 1998).

We used 2 different types of MHC multimerization method for staining cells of interest:

1. Conventional multimerization

2. UV cleavable multimerisation

#### 3.2.2.1 Generation of peptide-MHC multimer complex through conventional method

pMHC multimers, loaded with a specific-peptide, can be used to identify and also purify antigen-specific T cells. For multimerization, monomeric peptide loaded MHC molecules were incubated with the streptavidin backbone for 40 min at room temperature in the dark. Optimal concentrations of each streptavidin backbone, conjugated to different fluorochromes (PE, APC, BV421), were previously titrated in relation to a pMHC concentration of 0.04 mg/ml. After multimerization the sample was stained in a ratio of 1:5 for 30 min on ice in the dark and washed twice with FACS buffer.

#### 3.2.2.2 Generation of peptide-MHC multimer complex through UV-mediated peptide exchange

All pMHC-multimers for human MHC-I allele HLA-A2 were generated using UV-mediated peptide exchange (64). The protocol was slightly modified to perform UV-peptide exchange in a 96-well polypropylene V-bottom plate. For the respective peptide of interest, stocks were diluted to a final concentration of 400µg/ml with 1x PBS. The refolded UV-sensitive HLA-A2 monomers were diluted to a final concentration of 200µg/ml with 1x PBS. Then, 60 µl of respective peptide of interest and 60 µl of HLA-A2 monomers were combined and exposed to UV light at a distance of 2-5 cm for 1h. The plate was centrifuged at 3300 g for 5 min at 20°C and 50 µl each supernatant was transferred to a fresh 96-well plate for following tetramer formation. Each of the pMHC monomers was multimerized with fluorochrome-Streptavidin conjugates coupled to the fluorophores Allophycocyanine (APC) (Biolegend), Brilliant Violet BV421 (Biolegend), or Phycoerythrin (PE) (Biolegend), for 30 min in the dark on ice. In order to saturate residual free binding sites on the Streptavidin conjugates, D-biotin was added to a final concentration of 25 µM, followed by incubation for 20 min in the dark on ice. Plates with multimers of interest were stored in the refrigerator (4°C) for future experiments.

50 µl of each of the previously generated pMHC-Multimer conjugated to PE were added to 2.5ml FACS/EDTA. $2x10^8$ PBMCs were transferred to a new tube, washed once with FACS buffer and resuspended in the Multimer-mix. This mixture was incubated at 4°C for 30min and later washed 2.5 times with FACS buffer. The cells were filtered and stored at 4°C in FACS-EDTA for further processing (enrichment).

## 3.2.3 Enrichment of antigen-specific T cells

### 3.2.3.1 Magnetic cell separation - MACS based enrichment

Magnetic activated cell sorting (MACS) enrichment of multimer-positive target cells was performed with Miltenyi anti-PE nanobeads on Miltenyi MS-columns according to the manufacturer's instructions. Multimer-PE-labeled cells were coincubated with anti-PE-antibody-labeled paramagnetic beads for 15min in the refrigerator (4°C). The cell suspension was washed once. The MACS column was placed on the magnet of MACS separator and equilibrated with FACS buffer. Then, the cell suspension was transferred to the MACS column. The principle behind the method being magnetically labeled cells will be retained within the column whereas the unlabeled cells pass through and are collected as the negative fraction. The retained cells were eluted to be the enriched positive cell fraction by removal of the column from the magnetic field and washing off the column by pushing the plunger to elute the cells of interest into a fresh tube.

### 3.2.3.2 Flow based cell sorting - speed enrichment (SE)

For isolating cell populations with a very small frequency in human PBMCs, like antigen-specific T cells, a pre-enrichment called speed enrichment (SE) was performed. The enrichment was performed on the MoFlo$^{TM}$ XDP with a 70 µm nozzle with the help of the flow core team (Mathias Schiemann, Imanuel Andra, Hanna Ulrich) who optimized the machine settings for the process of speed enrichment. The concept of speed enrichment was developed in the lab in collaboration with the flow core team and we were able to show an application of the method. The multimer-labelled samples were filtered (30 µm) and taken up in a concentration of about $2x10^8$ cells/ml. If the gating strategy (as discussed in the results section) included a live/dead discrimination, PI (final concentration 1 µg/ml) was added right before the sort. The maximal pressure difference between the sheath and the sample pressure was adjusted to 2 psi. Based on the fluorochrome defining the cell population, the trigger was set to the respective fluorescence channel. Changing the trigger from normal FSC (forward scatter) to a fluorescence channel (PE) and further adjusting the threshold to reduce the event rate are key components of SE; enrichment with this setting blinds the machine to any particle under the threshold. Also, such events will not be detected, only the PE-multimer-labelled positive events (T cells) were then visualized and sorted into a 24 well plate containing 1 µg/ml Okt3 antibody,100 U/ml IL-2, B-LCLs irradiated with 50 Gy and human PBMCs irradiated with 35 Gy. Cells were kept at 37°C, 95% relative humidity and 5% $CO_2$ in a total volume of 2 ml RPMI+, 10 % human serum, Streptomycin, Penicillin, Gentamycin.

#### 3.2.3.3 *In vitro* short term expansion of enriched antigen-specific T cells

After speed enrichment, the enriched T cells were transferred into a 24 well cell culture plates containing 1 mg/ml Okt3 antibody (Orthoclone), 1 mg/ml anti CD28 (BD 340975), B-LCLs irradiated with 50 Gy and human PBMCs irradiated with 35 Gy at a ratio of 1:5 ($25x10^5$, $5x10^5$) for 8-12 days. On day 1 after transfer into the culture plates, 100 U/ml IL-2 and 5ng/ml IL-7 and IL-15 were added. On day 4 and day 11 cells were completely washed off to get rid of any stimulating antibodies, on day 8-9 half media change was done and if the cells were 80-100% confluent they were split. After Day 8 the cells were passaged and the culture plates were kept at 37°C, 95% rel. humidity and 5% $CO_2$ in a total volume of 2 ml CTL medium/ well. Once the cells were expanded to sufficient numbers they were further double multimer stained with epitope specific multimers and sorted.

#### 3.2.3.4 FACS analysis and sorting of *in vitro* expanded antigen-specific cells

In order to sort cells for single cell PCR from *in vitro* expanded cells, we labeled the cells with HLA-A2 multimers coupled to two different fluorophores (PE,BV421) in separate stainings for all the different epitopes. Cells were first incubated with the appropriate pMHC multimers for 20 min, in the dark on ice. Then the cells were stained for the surface molecules CD3 and CD8 for 30 min, in the dark on ice. Discrimination between viable (live) and non-viable (dead) cells was carried out using propidium iodide (PI). Cells were washed 1.5 times with FACS buffer. Samples were analyzed using a CyanLx 9 color flow cytometer (Beckman Coulter). The obtained data were analyzed using the FlowJo v9.5.2 software. After day 10, cells were single cell sorted from the samples which had cells stained positively for both multimers. Single-cells were spotted using the Cyclone system MoFlo legacy (Beckman Coulter) cell sorter to pre-defined slide positions. Between day 12-14 cells were either used for further experiments or frozen in complete freezing medium (CFM) and stored in liquid nitrogen.

### 3.2.4 Single cell PCR and TCR sequencing

#### 3.2.4.1 Reverse Transcription and single cell PCR for TCR extraction

Reverse Transcription and PCR of TCR chains from single cells was performed as described in the published protocol (51). Also, as highlighted in the protocol to prevent cross contamination during the single cell PCR process “all the RNA processing steps were performed by a person who was precluded from all areas where the PCR product

preparation and further processing took place. Cross-contamination by personal was avoided by “spatial separation“ (51). Reverse transcription was performed for 20min at 51°C followed by 30min at 70°C. Primer exonuclease I digest, was performed for 30min at 37°C. For oligo-dG tailing, complete reaction was transferred to a 96 well plate. Oligo-dG tailing was performed for 45min at 37°C. After anchor PCR, the product was separated in two reactions for PCR amplification of α- and β- chain. Reaction conditions for nested PCR were the same as for anchor PCR except for primers.

**PCR program**

| | | |
|---|---|---|
| Initial denaturation | 94°C | 3min |
| Cycles | 24 | |
| Denaturation | 94°C | 15s |
| Annealing | 60°C | 30s |
| Elongation | 72°C | 45s |
| Final Extension | 72°C | 5min |
| | 16°C | Pause |

Due to extremely high sensitivity of the technique and risk involved by contaminations, all single cell PCRs were kindly performed by Isabelle Scheidwitz.

#### 3.2.4.2 DNA Isolation using Agarose Gel electrophoresis

PCR amplified DNA fragments were electrophoretically separated using a 1% agarose gel supplemented with Roti-Safe DNA dye (Roth).1.5g agarose was mixed with 1x TAE–buffer and boiled until the solution became clear. After cooling Roti-Safe GelStain (100 ul/l) was added. The solution was transferred to a gel chamber (Biorad) and allowed to polymerize for 20-30 min. PCR samples were supplemented 1:1 with a 2x Glycerol DNA loading dye. For size reference 7.5µl of a 1 kb DNA ladder (GeneRuler, Fermentas) was used. The gel run was performed at 130 V for 45 min. DNA bands were visualized by UV-light and gels were photographed with a UV sensitive camera (Eagle Eye, Biorad).

#### 3.2.4.3 Purification of DNA by gel extraction

DNA fragments of the desired size (500bp) were excised from the agarose gel with a sharp scalpel. The DNA was extracted from the gel slice using the Wizard SV Gel and PCR Clean-Up System, according to the manufacturer’s instructions. DNA concentration and purity of the DNA fragments were assessed using a NanoDrop ND-1000 (PeqLab) spectrophotometer. The adsorbance ratio at 260/280 nm and 260/230 nm was used to

assess the purity of the DNA samples and exclude potential contaminations with proteins, RNA or denaturated DNA.

#### 3.2.4.4 Transformation and sequencing of PCR product from single cell PCR

Single cell PCR products were prepared for sequencing by standard blunt end cloning using the CloneJet-kit according to the manufacturer's instructions. Aliquots of competent E. coli Stbl3 were thawed on ice for 5 min. 10 µl of plasmid solution was mixed with 50 µl competent bacteria and placed on ice for 5 min. Subsequently, cells were heat shocked at 42°C for 60 sec in a heating block. The transformation mix was placed back on ice for another 30 min. At the end, the bacteria solution was plated on LB-selective agar and incubated at 37°C for at least 16 h. The colonies appeared on the following day.

**Blunt-end ligation**

Reaction mixtures for blunt end ligations were prepared as follows:

| | |
|---|---|
| Linear vector DNA | 20-100 ng |
| Insert DNA | 3:1 to 5:1 molar ratio over vector |
| 10x T4 DNA Ligase buffer | 2 µl |
| 50% PEG 4000 solution | 2 µl |
| T4 DNA Ligase | 5 U |
| H2O, nuclease-free | to 20 µl |

Ligation occurred at RT within 30 min.

To screen for full-length assemblies, colony PCR was performed on the colonies. A colony was picked with a 10 µl pipette tip and swirled in 20 µl of the PCR reaction mixture. Subsequently, the very same pipette tip was used for inoculation of 2 ml LB-ampicillin growth medium. Colony PCR was performed

**Colony PCR**

All Colony PCRs were performed with DreamTaq DNA polymerase (Thermo Fisher Scientific). The reaction mixture was prepared as follows:

| | |
|---|---|
| 10x Dreamtaq buffer | 2µl |
| Forward primer [10 µM] | 0.5 µl |
| Reverse primer [10 µM] | 0.5 µl |

| | |
|---|---|
| dNTPs [100 mM] | 0.2 µl |
| DreamTaq DNA polymerase | 0.2 µl |
| H2O, nuclease-free | to 20µl |

After PCR, samples were Sanger sequenced at GATC Biotech AG, Konstanz. The obtained sequences were then analyzed for TCR integrity and correctness.

The LB culture media inoculated with colony was incubated at 37°C until the medium was cloudy. The PCR was conducted according to the following conditions in a thermocycler:

| | | |
|---|---|---|
| Initial denaturation | 95°C | 2min |
| Cycles | 35 | |
| Denaturation | 95°C | 30 sec |
| Annealing | 55°C | 30 sec |
| Elongation | 72°C | 30 sec |
| Final Extension | 72°C | 3min |

From colonies with the right TCR fragment size, plasmids were extracted using the Pure Yield Mini column extraction kit. Selected plasmids were sent for Sanger sequencing to GATC Biotech AG, Konstanz.

## 3.2.5 TCR sequencing and sleeping beauty mediated gene transfer

### 3.2.5.1 Transposon construction for gene transfer

TCR sequences obtained from sanger sequencing were then tested by analyzing them on IMGT/QUEST international ImMunoGeneTics information system (IMGT; http://www.imgt.org) and BLAST (Basic Local Alignment Search Tool, www.ncbi.nlm.nih.gov/BLAST/). The published sequences were matched to identify the start codon which represents the beginning of the TCR chain. Comparing the obtained sequence with the published cDNA sequences (www.ensembl.org) for human constant regions of each chain and the end of J region was identified. β and α chains were connected via the self-cleaving porcine teschovirus 2A sequence (P2A; listed in Appendix). At the 5' and 3' end of the construct, homology sequences to the pT2 vector (listed in Appendix) were added. TCR sequences for alpha (α) and beta (β) were assembled together *in silico* along with the P2A element and murine constant region to have them all as a single cassette. The general assembly scheme is as depicted in the figure below.


**Figure 3.2.5.1 Scheme for *in silico* TCR cassette assembly**

This *in silico* assembled and verified sequence cassette was then sent to a commercial provider (GeneArt) for synthesis of the complete TCR cassette as a single gene string. (Complete sequences of TCR cassettes are listed in the Appendix).

### 3.2.5.2 Gibson assembly of pT2-TCR construct

The expression cassette containing the chimeric α- and β-TCR sequences separated by a self-cleaving P2A linker peptide sequence was cloned into a SB (Sleeping beauty) pT2 transposon backbone using Gibson Assembly. TCR cassette and pT2 backbone, both containing the same 5'- and 3'-homology regions, were ligated via Gibson Assembly. Adding equimolar amounts (0.02-0.5pmol) of linear TCR-cassette and pT2 backbone into a PCR vial, to this 5 µl of Gibson assembly mastermix was added as per the Gibson assembly transformation protocol. The contents were then mixed by pipetting and after a quick spin the samples were sealed. The sealed samples were then set on a PCR cycler for 20 minutes and 50°C.The resulting TCR encoded transposon (Schematic representation of pT2-TCR transposon as shown in the figure below) in combination with SB100X transposase coded on a second plasmid, were used for gene transfer (electroporation) in order to transduce primary human PBMCs with engineered TCRs.

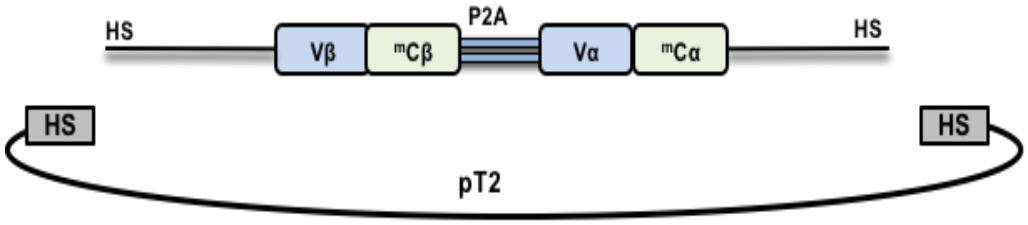


**Figure 3.2.5.2 Gibson assembled pT2-TCR transposon**

### 3.2.5.3 Transformation and plasmid preparation

PCR was followed by transformation and colony PCR. The PCR product (pT2-TCR construct) was mixed with 50 µl *E. coli* Stbl3 cells, this mixture was then heat shocked for 30 seconds in a 42°C waterbath. *E.coli* were allowed to recover in 250 µl SOC medium at 37°C, at 500rpm for 1h. The transformations were plated on pre-warmed LB-ampicillin selection plates and incubated over night at 37°C. Finally, successful TCR integration was

confirmed by colony PCR, using the primers “pT2 fwd” and “pT2 rev”. Properly linked pT2-TCR vectors were purified from the bacterial culture via PureYield™ Plasmid miniprep System. Base by base integrity of the original TCR cassette was confirmed by Sanger sequencing (Eurofins).

#### 3.2.5.4 Electroporation using the sleeping beauty mediated gene transfer system

PBMCs from healthy donors were isolated by Ficoll density gradient centrifugation. PBMCs were transferred to 24-well non-tissue culture plates, which were coated with 10µg/ml OKT-3 and 10µg/ml anti-CD28 in 200 µl 1x PBS for 12h at 4°C, followed by a blocking step with FCS (sterile-filtered) for 3h at 4°C. PBMCs were incubated at 37°C, 24h later 50U/ml IL-2, 5ng/ml IL-7 and 5ng/ml IL-15 were added and samples were incubated at 37°C overnight. Then, PBMCs were harvested, washed twice with RPMI and counted. Subsequently $1x10^7$ PBMCs or $1x10^6$ jurkat cells (J76) for each reaction were transferred to a 96 well tissue culture plate. Cells were washed 1.5 times with 1x PBS (sterile-filtered), cells were then resuspended into a mix of 0.5µg SB100X and 4µg pT2-respective transposon prepared and pipetted just before electroporation in 100 µl self-made electroporation buffer “1SM” specific for Sleeping Beauty-mediated gene transfer with human T cells adapted from Chicaybam et al (65). This mixture is then transferred into electroporation cuvettes and directly electroporated. The cells were electroporated with the program U-014 for human stimulated PBMCs and X-005 for jurkat cells. Since, the electroporation mix is toxic to the cells, electroporated cells were directly diluted with pre-warmed complete media (RPMI containing 25 U/ml IL-2 ) and later taken into culture at 37°C and 5% $CO_2$.Electroporated cells were and transferred into wells of a 12-well tissue culture plate, prewarmed with 1.5 ml CTL medium. After electroporation OKT-3 (anti-CD3), anti-CD28 were added to the culture media, cytokines (IL-2, -7 and -15) were added to the culture media on day 1 after electroporation. Cells were incubated in a humidified 37 °C/5 % CO2 incubator until analysis. Cells in culture were split if they were 80-90% confluent in a 1:1 ratio and concurrent half media change of CTL medium supplemented with IL-2, IL-7 and IL-15 at a final concentration of 50U/ml and 5ng/ml, respectively. Transduced PBMCs were tested for TCR expression on Day 1 and Day 7 by staining a small volume with anti-mTRBC antibody to check for surface expression of murine constant region indirectly confirming the surface expression of the TCR. On Day 8 purified TCR+/CD8+ T- cells were tested for multimer staining. The successfully transduced and tested cells were then used to perform functional assays.

Electroporation was performed using a Lonza Nucleofector™ II/2b.Electroporation of primary T cells was performed with the self-made buffer as described in the protocol by

Chicaybam et.al 2013 (65). Sleeping Beauty transposition was performed using SB100X transposase, featuring a 100-fold higher enzyme efficiency compared to the first-generation transposase (66). In order to allow a fast and easy readout and as a control, pT2-GFP transposon was used to transfer the green fluorescent protein encoding gene into the cells.

### 3.2.6 Functionality testing - Double multimer staining and ICS (Intracellular cytokine staining)

#### 3.2.6.1 Double multimer staining and FACS analysis

*In vitro* cultured electroporated cells were harvested and washed 1.5 times with FACS buffer. Staining was performed in 96-well plates with the corresponding MHC-multimers conjugated to 2 different fluorophores (PE, BV421) and incubated on ice. First multimer was added and the mixture was incubated for 30 minutes, after washing 1.5 times the cells were stained with the second multimer and were subsequently stained for surface molecules CD3, CD8 and murine TCR beta chain after 20 min. Discrimination between viable (live) and non-viable (dead) cells was carried out with the use of propidium iodide (PI) for last 5 minutes. The samples were washed three times in 200µl FACS buffer, resuspended in FACS and were analyzed by CyanLx9 color flow cytometer. The data were analyzed using FlowJo v9.5.2 software.

#### 3.2.6.2 Intracellular cytokine staining (ICS)

The transduced T cells were analyzed for antigen recognition and cytokine release assays. As effector cells peptide-pulsed T2 cells were used. The mutant human T2 cell line is deficient in transporter proteins for antigenic peptide (TAP) and is therefore unable to present endogenous antigens in the context of HLA-A2. However, HLA-A2 molecules are presented on the cell surface and can be loaded with exogenous peptides (67). T2 cells were pulsed with 1µM of respective peptides for 2h. PBMCs were then together with an anti-CD107 antibody stimulated with the peptide-loaded T2 cells at an effector/ stimulator cell ratio of 1:1 for 5h at 37°C, 5% CO2, 95% rel. humidity. For the last 4 hours of incubation GolgiStop was added at a ratio of 1:1000. Live/dead cell discrimination was performed with EMA at a final concentration of 2µg/ml. After adding phenotyping antibodies for cell surface receptors CD3 and CD8, cells were permeabilized with Cytofix/Cytoperm solution and washed twice with 1x PermWash buffer. Intracellular cytokine staining with performed with antibodies directed against TNFα and IFNγ. Samples were analyzed using a CyanLx flow cytometer (Beckman Coulter). The obtained data were analyzed using the FlowJo v9.5.2 software.

# 4. Results

The results section of this thesis is divided into four parts: the first few chapters are focused on the technical improvements for establishment of a functional workflow for isolation of T cells of interest, with the focus on enrichment methods used. The following chapter “Cloning and extraction of TCR sequences” details the cloning methods and extraction of sequences from the enriched T cells of interest. The next chapter focuses on the transgenic expression of TCRs of interest using sleeping beauty mediated gene transfer system. In the final chapter results from the functional evaluation of the TCRs of interest are summarized.

## 4.1 Establishment of a functional workflow for enrichment of epitope specific T cells

The frequency of circulating antigen-specific T cells of interest prior to antigen encounter in the peripheral blood is usually extremely low and this makes it challenging to detect these rare events and even more difficult to isolate these cells. One of the main objectives of my project was to establish a reliable workflow to isolate rare epitope-specific T cells. We used MHC multimer labeling to detect rare epitope-specific cells. For pre-enrichment, we explored purification of cells stained with phycoerythrin (PE)-conjugated MHC multimers via an anti-PE-paramagnetic bead-conjugated antibody. Subsequently, the enriched cells were stained with a second MHC multimer, since double multimer labeling has been described to reduce the rate of false positive cells. The double multimer positive cells were then sorted for single cell PCR and TCR sequence extraction. The workflow below gives an overview of different steps involved to achieve the project goal of isolation and functional characterization of epitope-specific T cells.

## Workflow for enrichment of epitope specific T cells

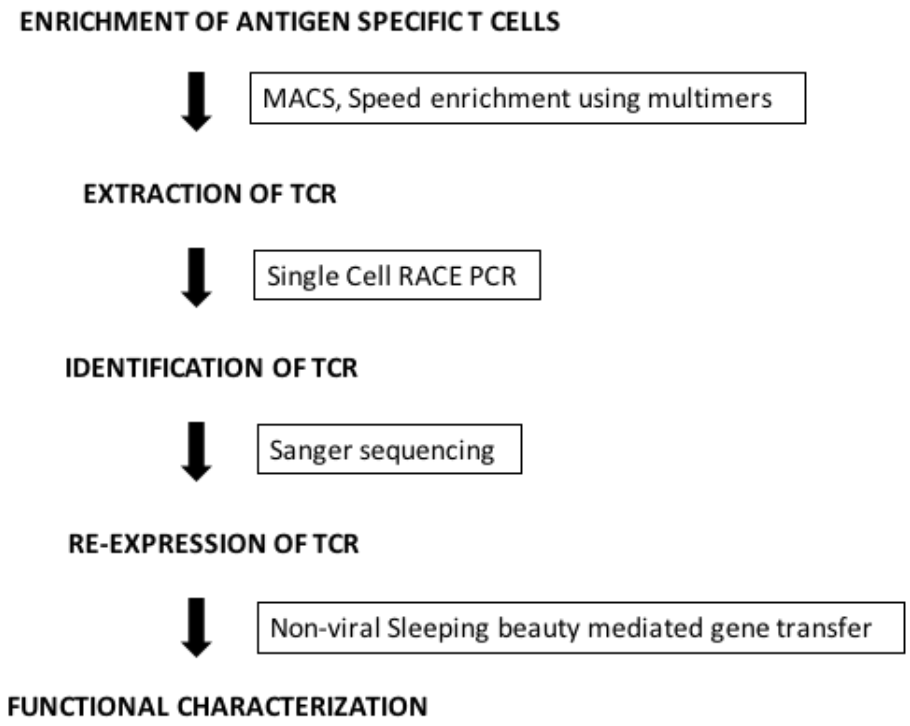


### 4.1.1 MACS enrichment and sorting of epitope specific T cells

Previously it has been shown that MHC multimer assisted magnetic enrichment increases detection of antigen-specific T cells by more than 100-fold (10). This procedure is based on a 3-step process used for separating cells where the cells are first labelled with a specific peptide-HLA multimer conjugated with PE (biotinylated fluorophore) for 30min at 4°C in the dark. $4x10^8$ - $6x10^8$ PBMCs were isolated by density gradient ficoll separation and were resuspended into two samples of $2x10^8$ cells in separate tubes, one sample referred to as purity sample was stained only with the backbone PE fluorophore (used as one of the controls for eliminating any unspecific binding and eliminate background). The other sample was labelled with epitope specific multimers. Peptide MHC class I multimers were generated freshly just before staining as described in the methods section.

Small volume of the sample was saved as pre-enriched sample (sample before enrichment). Samples were further incubated with magnetically labelled anti-PE microbeads for 15 minutes at 4°C then washed twice and resuspended in 1 mL of FACS buffer. The cell suspension was then added on a MS magnetic column as shown in the (**Fig. 4-1**). The enriched sample corresponds to the positive fraction of magnetically labelled cells retained in the column, the flow through or the negative depleted fraction with other unlabeled cells

and debris was collected into a separate falcon by gravity. After allowing the sample to flow through the column by gravity in the cold room (at 4°C), the column was then removed from the magnet and positive enriched fraction on the column was eluted by applying pressure using a plunger on the column into a fresh falcon tube. Pre-enriched sample, post-enriched sample and purity control samples (sample of PBMCs stained just with the backbone PE labelling), are all further labeled with a second peptide-HLA-A2 multimer conjugated with BV421, antibodies for other surface markers as defined in the flow cytometric panel (table 4-1) and acquisition was performed on a polychromatic flow cytometer.

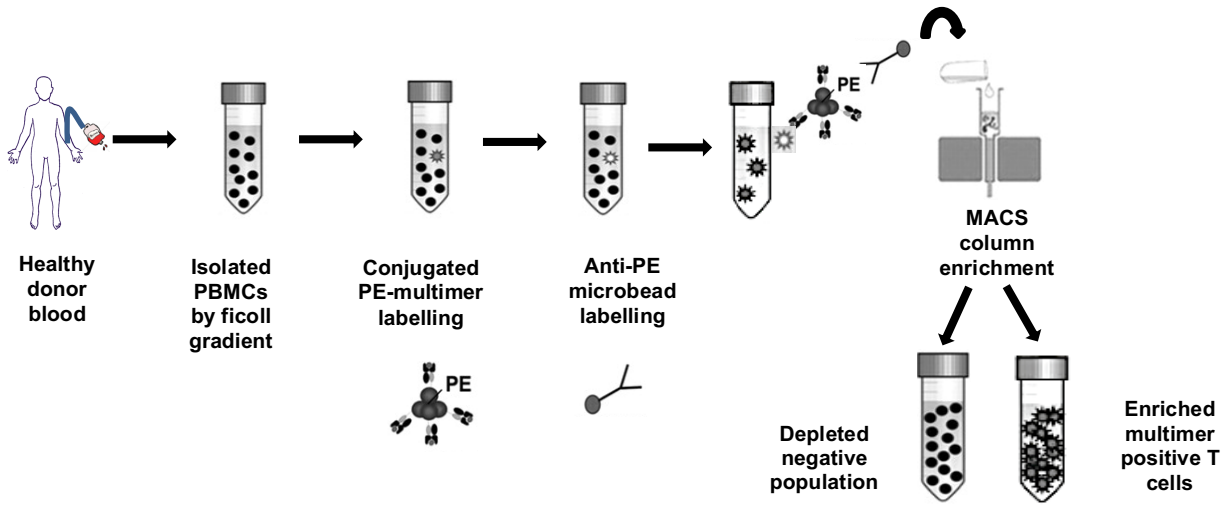


**Figure 4-1. MACS-based MHC multimer enrichment of epitope-specific T cells.** Multimer enrichment was performed on $2\times10^8$ freshly isolated A2+ donors with the help of ficoll density gradient later stained with PE-conjugated HLA multimers (sample before enrichment) followed by staining with magnetically labelled anti-PE microbeads and then loaded onto a MS column for magnetic separation. The enriched cells within the column were then eluted using a plunger and collected in a fresh tube for additional labeling with a staining panel and a second multimer for further characterization by flow cytometer (adapted from Alanio et al BLOOD, 2010).

### Staining panel for characterizing MACS enriched T cells

T cell characterization with a well differentiable staining panel was necessary in order to isolate and sort epitope-specific T cells for single cell analysis. To minimize false positive staining, we labelled enriched cells with a second pMHC-multimer conjugated to BV421. Additionally, we used control samples with back bone labelling (purity control) pre- and post-enrichment with the same panel to exclude any background staining and sort only pure double multimer positive cells. For further phenotypic characterization we used markers to differentiate B and T cells by CD19, CD3 and CD8 staining. Finally, staining for CCR7 and

CD45RA to further characterize the phenotype of the selected cells. Altogether, our staining panel comprises 8 different dyes (Table 4-1). The staining panel was primarily set up for Cyan-P6 FACS analyzer, but in order to use it for cell sorting on a MoFlo-legacy sorter, antibodies were further titrated and tested for compatibility on MoFlo. All the antibodies for the were titrated on MoFlo-legacy sorter. Representative histograms from titration are shown in the **fig. 4-1-1** and a table summarizing the right concentrations of flurophores is shown in the **table 4-1-1.**

| Specificity | Label | Detection |
|---|---|---|
| CD19 | PE- A610 | B cell |
| CD3 | BV650 | T cell |
| CD8 | PE - Cy5 | T cell |
| CD45RA | PE - Cy7 | Naïve T cell |
| CCR7 | FITC | Naïve T cell |
| pMHC-Multimer | PE | T cells of interest |
| pMHC-Multimer | BV421 | T cells of interest |

**Table 4-1: Staining panel for characterization and isolation of naïve antigen-specific T cells.**

**Staining panel for characterizing MACS enriched T cells**

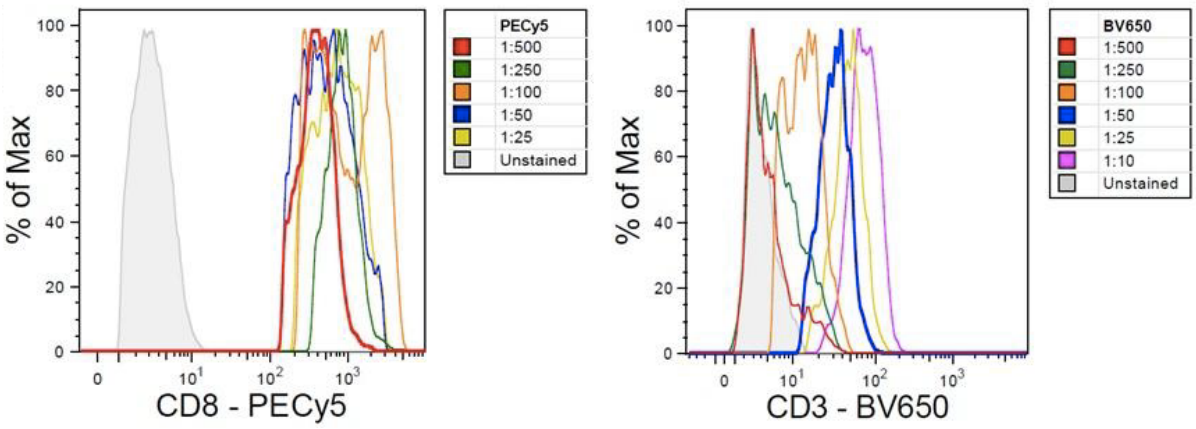


**Figure 4-1-1. Titration of fluorophores for staining panel**

Histogram showing titration data for CD8 PECy5 and CD3 BV650 performed on the MoFlo-legacy sorter.

| Specificity | Label | Titer |
|---|---|---|
| CD19 | PE- A610 | 1:50 |
| CD3 | BV650 | 1:50 |
| CD8 | PE - Cy5 | 1:500 |

| | | |
|---|---|---|
| CD45RA | PE - Cy7 | 1:50 |
| CCR7 | FITC | 1:10 |
| pMHC-Multimer | PE, BV421, APC | 1:5 |

**Table 4-1-1.** FACS staining panel for characterization of MHC multimer enriched T cells showing the right titrated concentration tested on MoFlo legacy.

### Gating strategy for sorting T cells of interest after MACS enrichment

We first gated on the lymphocyte population followed by singlets gate. Live-dead discrimination was achieved with the help of PI (Propidium iodide) staining and all dead cells were gated out as shown in the gating scheme (**Fig. 4-2 A**). In order to reduce the number of pMHC-multimer false positive cells the next step was to deplete B cells and other sticky cells. All non-specific cell populations were labelled with antibodies conjugated to a dye in the same channel as live/dead dye referred to as “dump channel”. B cells were stained with a fluorophore CD19-AE-A610 which is also detected in the dump channel. The next step in gating was to isolate multimer specific cells with a gate on double multimer positive population. Final gating was for characterizing multimer positive cells where naïve T cells were defined by $CCR7^{+}$ and $CD45RA^{+}$.

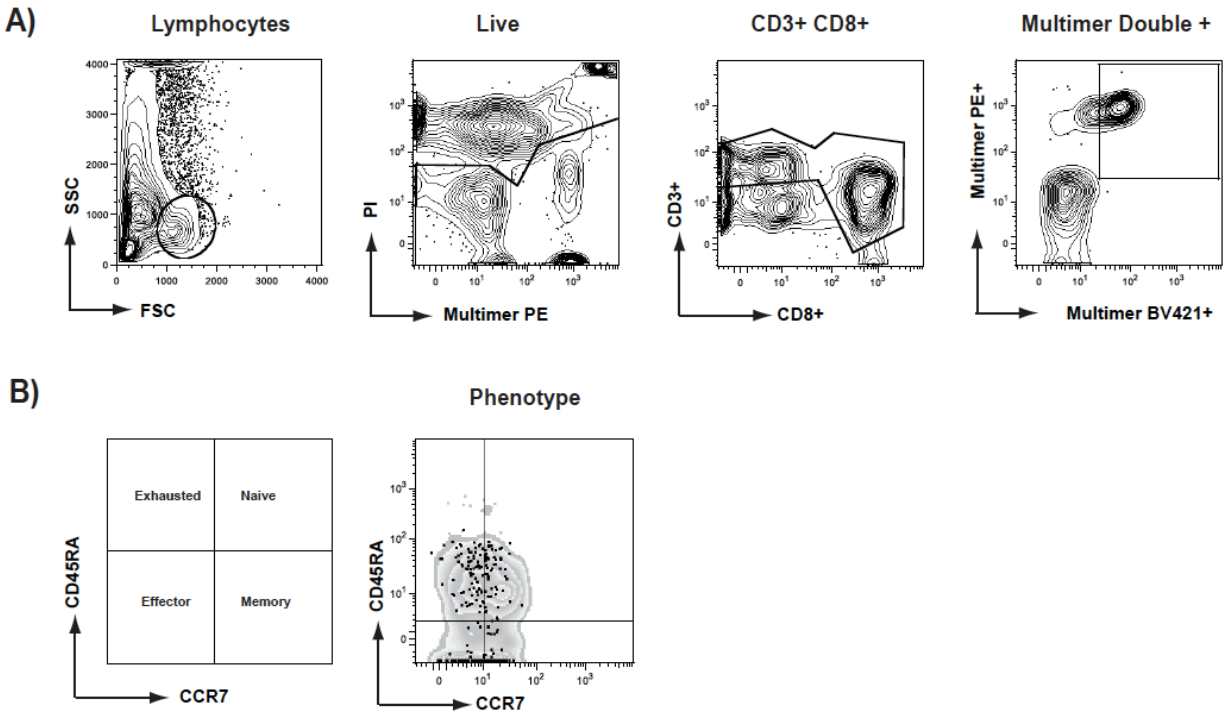

**Figure 4-2 : Representative FACS plots and gating scheme for multimer-enriched population post MACS enrichment.** Multimer enrichment was performed on 2 × $10^8$ freshly isolated PBMCs from A2+ donors with the help of ficoll density gradient . PBMCs were stained with PE-conjugated HLA-A2 multimers and enriched using MACS. MACS enriched cells were further analyzed by staining with FACS panel (as described in Table 4-1) (A) We gated on lymphocytes and further eliminated sticky cells and clumps by setting a strict singlets gate. Dead cells were stained by PI and PI (dump) vs PE was set in order to record only multimer-PE positive events. From the live cells CD3-CD8 double positive gate was set followed by double pMHC multimer positive gate. (B) Pregated on double multimer positives for discrimination of naïve and memory T cells enriched cells were further analyzed based on the expression of CD45RA and CCR7. Phenotype classification: Naïve T cells are $CCR7^+CD45RA^+$, memory T cells are $CCR7^+CD45RA^-$, effector T cells are $CCR7^-$ $CD45RA^-$ and T cells $CCR7^-CD45RA^+$. Black dots indicate the phenotype of the multimer positive cells and grey shades indicate $CD3^-CD8^+$ cells .

### MACS-based enrichment of viral epitope-specific T cells of interest

In the early stages of the project we tried to isolate A2pp65 (CMV- Cytomegalovirus) from a CMV negative donor as a proof of concept for the isolation of rare epitope-specific T cells of interest from the naïve T cell repertoire.

Several experiments with different donors were performed to test and validate compatibility of the complete panel to isolate naïve T cells specific for A2pp65 from healthy CMV negative donors (shown in the **Fig. 4-2-1**). Although we were able to detect T cells binding to A2pp65 multimers, the number of cells was extremely low and not sufficient for sorting and subsequent single cell PCR. Due to the extremely low cell numbers of A2pp65-specific T cells (10) we chose to target other viral specific T cells e.g. FluMP (Influenza virus) and YFV (yellow fever virus).

T cells of interest were labelled by pMHC multimers and isolated with the help of enrichment techniques. As a first step in the workflow, multimer labelling and MACS enrichment was performed on 2x$10^8$ freshly isolated PBMCs. Later these FluMP-PE multimer labelled cells were subjected to MACS enrichment.

## 4.1.1 MACS enrichment

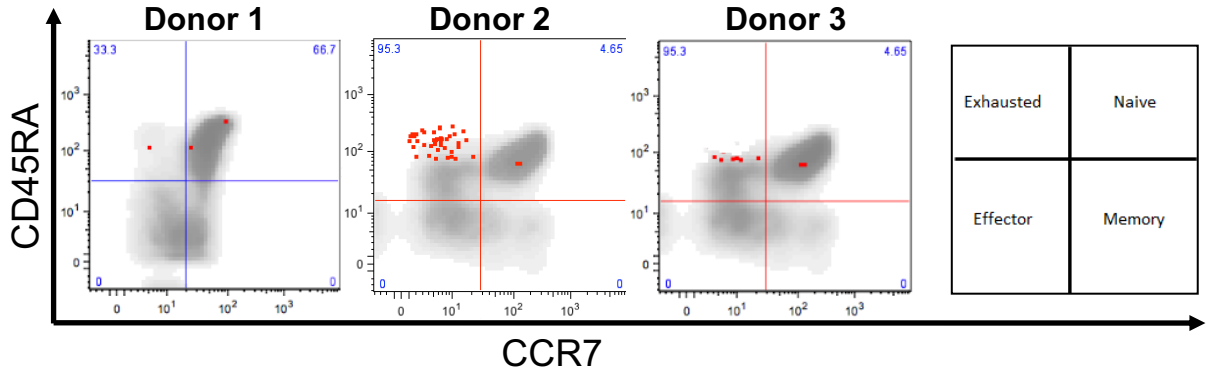


**Figure 4-2-1. MACS based multimer enrichment of CMV-A2pp65 T cells** (A) Multimer enrichment was performed on 2 × $10^8$ freshly isolated PBMCs. PBMCs were isolated from $A2^+$ and CMV negative donors with the help of ficoll density gradient later stained with PE-conjugated HLA-A2 multimers and enriched using MACS (B) Gating strategy for detection of multimer positive events is shown in the gating scheme we gated strictly on the lymphocytes and further eliminated clumps by setting a strict singlets gate. Dead cells were stained by PI and PI(dump) vs PE was set in order to record only multimer-PE positive events. CD8 T cells specific for A2pp65 multimer within the enriched fraction are indicated, with minimal background staining in the CD8 CD3 T-cell population. (C) Data shown are representative of 3 independent experiments performed on $A2^+$ and CMV negative donors.

### MACS enrichment of FluMP-specific T cells

Healthy donor PBMCs were isolated using Ficoll, and MACS enrichment was performed after labelling the cells of interest. For enrichment of epitope-specific T cells, peptide-MHC multimers (PE,BV421) specific for FluMP were generated as described in the methods section. Since the staining of cognate T cells can be improved by using optimal amounts of pMHC multimer (68), the optimum titrated amount of pMHC multimer for T cell staining reactions was validated before using them for rare population staining.

PBMCs were stained with PE-conjugated MHC multimers and subsequently incubated with magnetically labelled anti-PE microbeads. Cell suspensions were loaded on a MS magnetic column as shown in the (**Fig. 4-1**). **The** enriched sample was labeled with a second peptide-HLA-A2 multimer conjugated with BV421 and antibodies for other surface markers as defined in the flow cytometric panel (**table 4-1**) and purity sort was performed on MoFlo-Legacy sorter. Double multimer positive FluMP specific cells were detected as shown in the **Fig. 4-3**.

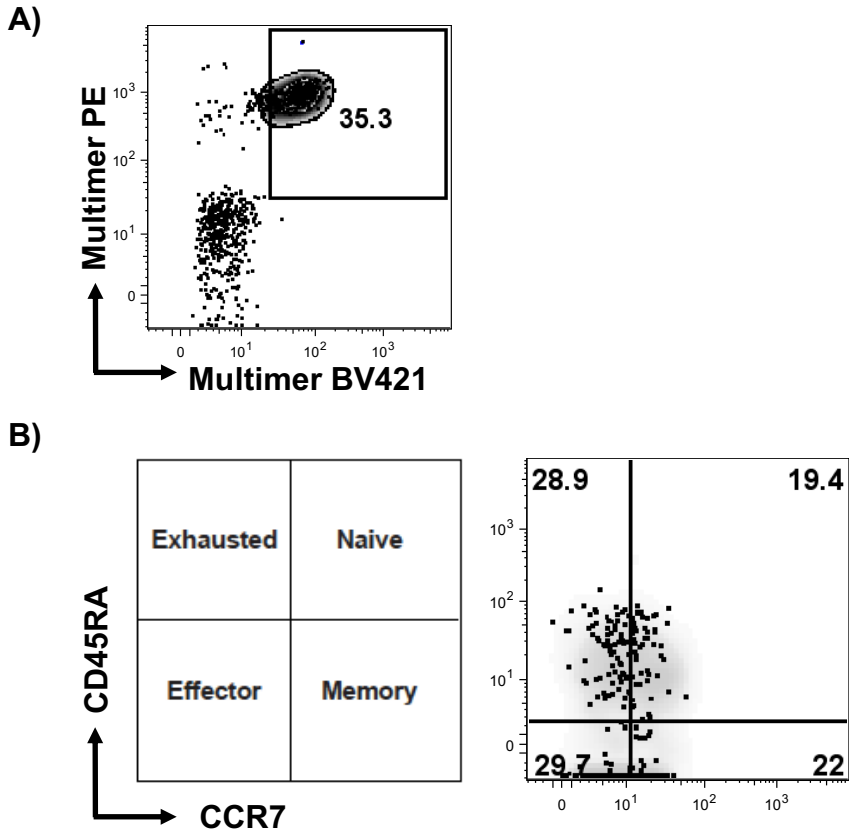


**Figure 4-3 : Detection of FluMP epitope-specific T cells by MHC multimer staining and enrichment using MACS** Multimer enrichment was performed on 2 × $10^8$ freshly isolated PBMCs from A2+ donors with the help of ficoll density gradient . PBMCs were stained with PE-conjugated HLA-A2 multimers and enriched using MACS (A) PBMCs from a healthy donor was stained with FluMP 58-66 HLA-A2-PE multimer, the cells were subsequently incubated with anti-PE magnetic beads and enriched using a magnetic column. MACS enriched FluMP specific T cells were labelled with second multimer FluMP-BV421. Enrichment was performed and the double multimer frequency is reported. Enriched cells were pre-gated on lymphocytes, live and $CD3^+$ and $CD8^+$ cells as shown in the gating scheme (Fig. 2). (B) Tetramer enriched population was further analyzed using anti-CD45RA, anti-CCR7 staining for further discrimination of naïve and memory T cells. FACS plots show the frequencies and phenotypes of FluMP specific cells where the dots shown in black represent the phenotype of multimer double positive cells and gray indicates the bulk CD8 T cells as a reference. Data shown is a representative of 3 different experiments.

### 4.1.2 Proof of concept for FACS-based enrichment (speed enrichment)

Speed enrichment (SE) was performed as described in the methods section (refer to 3.2.3.2). Both the sorters available in the core facility, MoFlo-legacy sorter and MoFlo-XDP, were tested for speed enrichment settings. The optical setup and the fluidic system for MoFlo-legacy sorter and MoFlo-XDP are similar in principle, but they differ in their electronics and therefore the two sorters were tested for compatibility with the speed

enrichment settings and staining panel. Due to extremely sensitive machine fluidic system, compatibility testing and optimization of machine settings was performed by our flow core team (AG Schiemann).

**Speed enrichment of FluMP-specific cells**

For conventional cell sorting, the trigger lays on the forward scatter (FSC), which gives an estimation of the particle size. By increasing the threshold, smaller particles like erythrocytes or debris can be pushed under the threshold. The trigger on newer cell sorters can also be set to the side scatter (SSC) or even fluorescence channels. If the trigger is set to a fluorescence channel, unstained cells or particles are detected due to their low intrinsic fluorescence. However, if a fluorochrome is used to label a specific cell, e.g. through conjugated antibodies, a discrimination between different cell populations is possible. By increasing the threshold for this fluorescence channel, cells with lower fluorescence intensities are not detected. In principle, SE can be used for all particles which can be characterized by one distinctive marker or scatter parameter. SE was used as a pre-enrichment step to reduce the total sort duration and minimal loss of the target cell population.

In the following, the general experimental setup for SE and changes to the settings will be explained (shown in **Fig. 4-4 A**). The machine was set up for the speed enrichment setting using controls (speed enrichment set-up control). After the set up was established with the control samples, the actual speed enrichment sample was run for a short time to visualize the population of interest. The recorded data from the sample was then used to set up the gates and the threshold was set. Once the threshold is set any event below the threshold will not be detected. Adjusting threshold on the MoFlo-Legacy was difficult as it had fixed values and on MoFlo-XDP we had the flexibility of adjusting thresholds for different fluorescent channels.

During conventional FACS analysis, the forward scatter (FSC) light from 488nm laser (correlating with the cell size) is used as the basic parameter to define whether or not a sample droplet would contain a cell. Any signal above this defined threshold intensity activates the other photomultiplier tube (PMT) detectors resulting in measurement of all the fluorescent signals. In order to allow a very high sample flow rate, the machine was set up to perform speed enrichment and the trigger was switched from the FSC to PE-signal which is now the activation trigger. Speed enrichment setting with the trigger on PE-signal enables detection of positive cells and permits the use of high pressure to run a sample faster as compared with the trigger on FSC in normal setting. As mentioned in the methods section,

machine settings like changing sample-sheath pressure for machine alignment and switching the trigger from FSC to a channel with the fluorophore of interest were optimized with the help of the flow core team.

We performed initial experiments on a MoFlo-Legacy sorter to isolate epitope-specific T cells from healthy donor PBMCs. $2x10^8$ cells were taken in a 15ml falcon tube and T cells of interest were labelled with MHC multimer-PE. Excess unbound MHC multimer reagent was removed by a wash step before transferring it onto the sorter for processing. Speed enrichment was performed with the trigger on PE. The speed enriched-positive population was sorted into a 5ml round bottom tube with 1ml FCS. Enriched cells were then labelled with the second pMHC multimer conjugated to BV421 and staining panel of surface markers as listed in the **table 4-1**. Gating strategy for speed enrichment is as shown in the **Fig. 4-4-1** Based on the phenotypic characterization of MHC multimer-specific cells we could classify them as naïve T cells. The naïve double multimer FluMP-specific cells were then sorted on slides for single cell PCR and TCR extraction (Isabell Schiedewitz and Georg Dössinger).

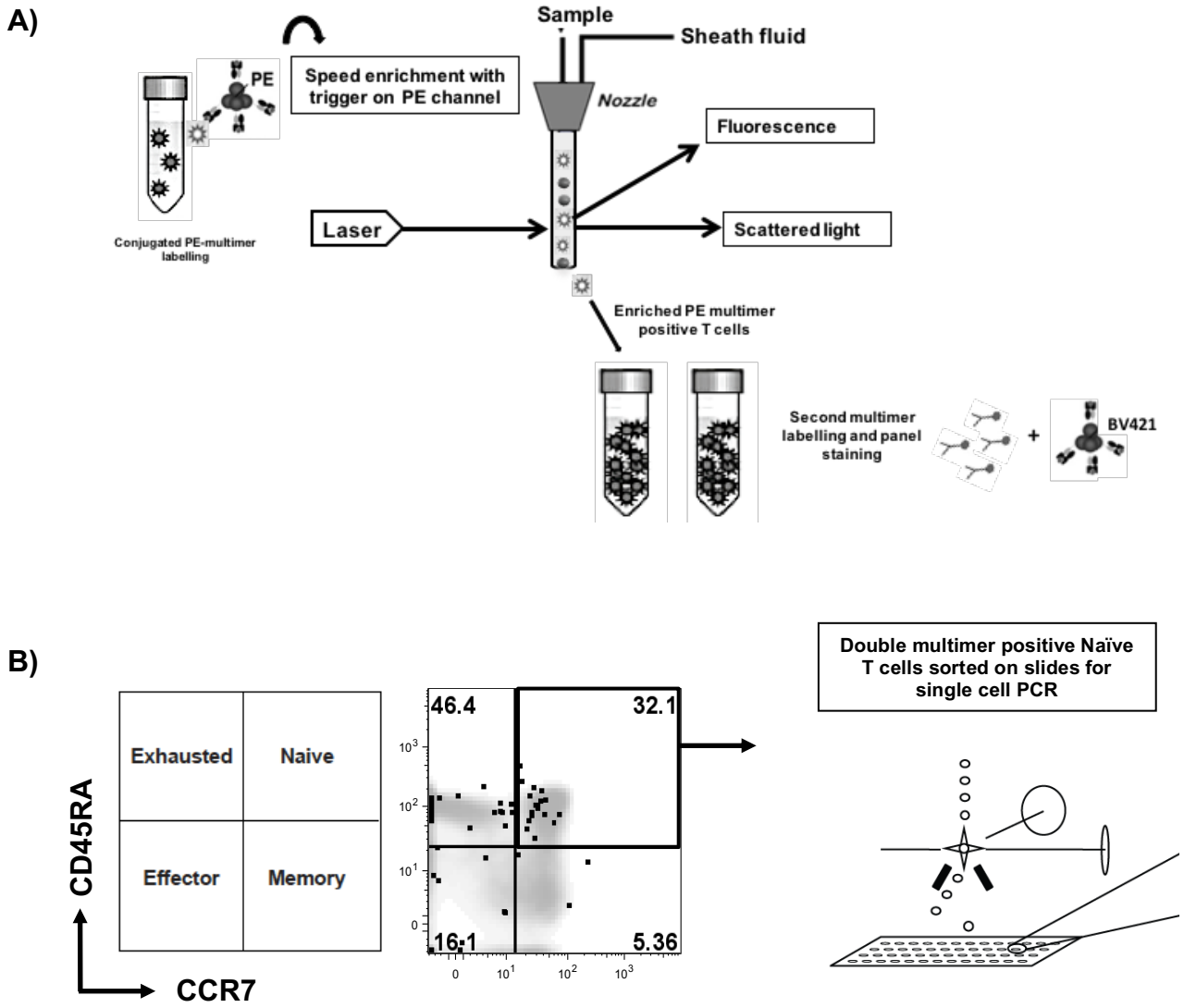


**Figure 4-4 : Multimer-based speed enrichment strategy for detection of FluMP epitope specific T cells** (A) PBMCs from a $A2^+$ healthy donor was stained with FluMP 58-66 HLA-A2-PE multimer. Speed enrichment was performed to isolate PE multimer positive population. Schematic representation of speed enrichment on the sorter shown with trigger on PE channel (adapted from schematic representation of jet-in-air sorter). Final enriched cells were pre-gated on lymphocytes, live and $CD3^+$,$CD8^+$ and double multimer positive cells as shown in the gating scheme in Fig. 4-2. (B) A representative staining obtained following FluMP speed enrichment is shown indicating the frequency of naïve multimer positive cells. Single cells were sorted on slides for single cell PCR (adapted from Dossinger et al. 2013).

### Speed enrichment gating strategy

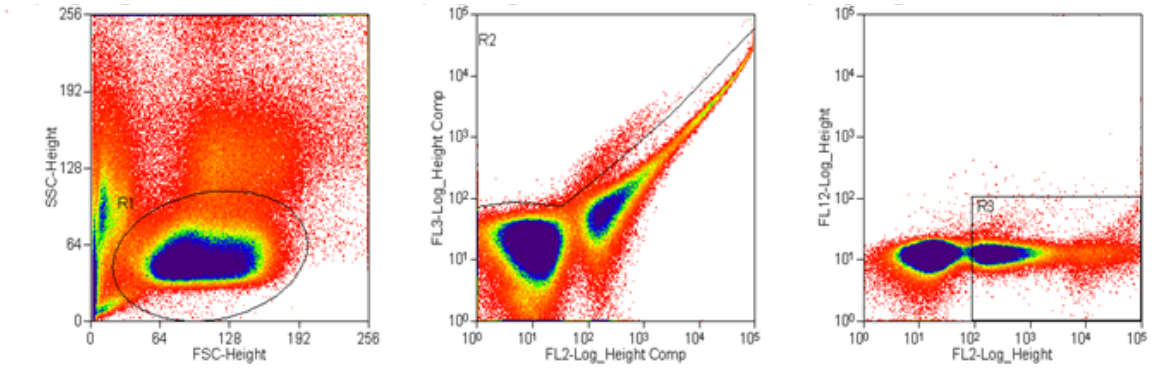


**Figure 4-4-1. Original SE settings with the trigger on PE** FACS plots showing speed enrichment gating on lymphocytes and after elimination of dead cells only PE positive cells within the gate R3 were sorted.

### Speed enrichment of YFV-specific cells

PBMCs from a healthy donor was stained with YFV-PE multimer, the labelled cells were then subjected to speed enrichment with the trigger on PE and, after enrichment, all the YFV-PE multimer specific cells were subsequently labelled with a second multimer YFV-BV421 (staining panel as listed in **Table 4-1**). We performed speed enrichment on samples from 2 different donors who were not vaccinated for yellow fever and were healthy at the time of sample collection. **Fig. 4-5** shows the final characterization of YFV specific cells, speed enriched and labelled cells with the staining panel.

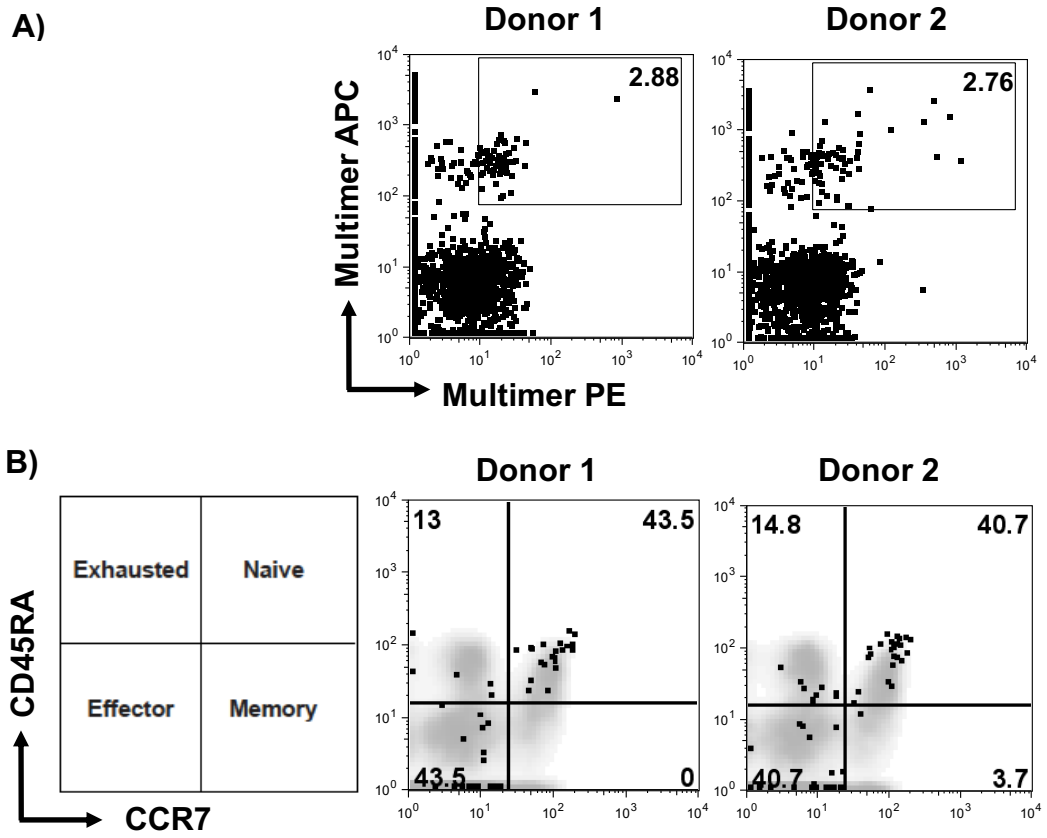


**Figure 4-5 : Detection of YFV epitope-specific T cells by speed enrichment** (A) The speed enriched and stained cells were pre-gated on lymphocytes, live and $CD3^+$ $CD8^+$ and the double multimer positive cells were then analyzed using anti-CD45RA, anti-CCR7 for further discrimination of naïve and memory T cells (as per the gating scheme Fig. 4-2). (B) FACS plots show the frequencies and phenotypes of YFV specific cells where the dots shown in black represent the phenotype of multimer double positive cells and gray indicates the bulk CD8 T cells. A representative staining obtained following YFV speed enrichment performed on 2 different donors is shown indicating the frequency of naïve multimer positive cells.

### 4.1.3 Comparison of MACS and Speed enrichment using spiked in cells

Although for some antigen-specificities MACS based enrichment worked, it proved to be very challenging for other epitopes. The novel enrichment method (SE - Speed enrichment) holds potential as a fast and precise enrichment method for isolating naïve antigen-specific T cells. In the following sections, we discuss the results of a direct comparison between the two enrichment methods used to detect epitope-specific T cells of interest.

#### Experimental set up for the comparison of MACS and speed enrichment

The experiment was set up to isolate FluMP-specific T cells from a healthy donor. PBMCs were isolated, and split into 2 samples with $2x10^8$ cells each in a 15ml falcon tube one for MACS and the other for speed enrichment. Cell pellets were then resuspended in 2 ml of

FACS buffer. These samples were then spiked in with a known number of cells specific for Her2Neu. For the “spike in” sample, we stained Her2Neu-specific cells derived from a cell line with multimers conjugated to PE and BV421. With help of the MoFlo sorter, a known number of double multimer positive Her2Neu-specific cells (1000 cells) were spiked into both the samples. The samples were further stained with MHC multimers specific for FluMP conjugated to PE and subjected to MACS and speed enrichment. MACS enrichment was performed as described in **Fig. 4-1** and speed enrichment was performed as described in **Fig. 4-4 A**. The enriched cells were then labelled with a second FluMP multimer conjugated to APC fluorophore. Therefore, the FluMP-specific T cells could be detected in the MHC multimer PE and APC double-positive gate and the “spiked in” cells could be detected with multimer PE and multimer BV421 double positive gate. After a wash step the samples were then analyzed on a flow cytometer for the retrieval of the spiked in cells in both the speed enriched and MACS sorted samples. The results from the comparison is described in the **Fig. 4-6 A B.**

FACS plots on the left indicate T cells specific for FluMP, which were successfully enriched using MACS enrichment and on the right FACS plots showing enriched cells from speed enrichment. **Fig. 4-6 A** shows the double MHC multimer-positive population of FluMP-specific cells before and after enrichment. The numbers on the right corner of the quadrant indicate the percentage of antigen-specific cells, 13.9% of the total $CD3^+CD8^+$ population were detected after MACS enrichment and 30.7% of the total $CD3^+CD8^+$ population were detected after speed enrichment. Comparing the percentages of antigen-specific cells enriched, we see that with speed enrichment we had a higher enrichment rate. In addition to this we also compared the “spiked in” cell numbers post enrichment. **Fig. 4-6 B** shows the number of “spiked in” cells post enrichment. Post MACS enrichment, out of 1000 cells spiked into the sample only 55 were detected as opposed to speed enrichment where 433 cells were detected.

Together with the results from the percentage of FluMP epitope specific cells detected post enrichment and the total number of spiked in Her2Neu-specific T cells retrieved after enrichment, we conclude that by using speed enrichment we achieved a much better enrichment rate and could minimize the loss of epitope-specific cells during enrichment.

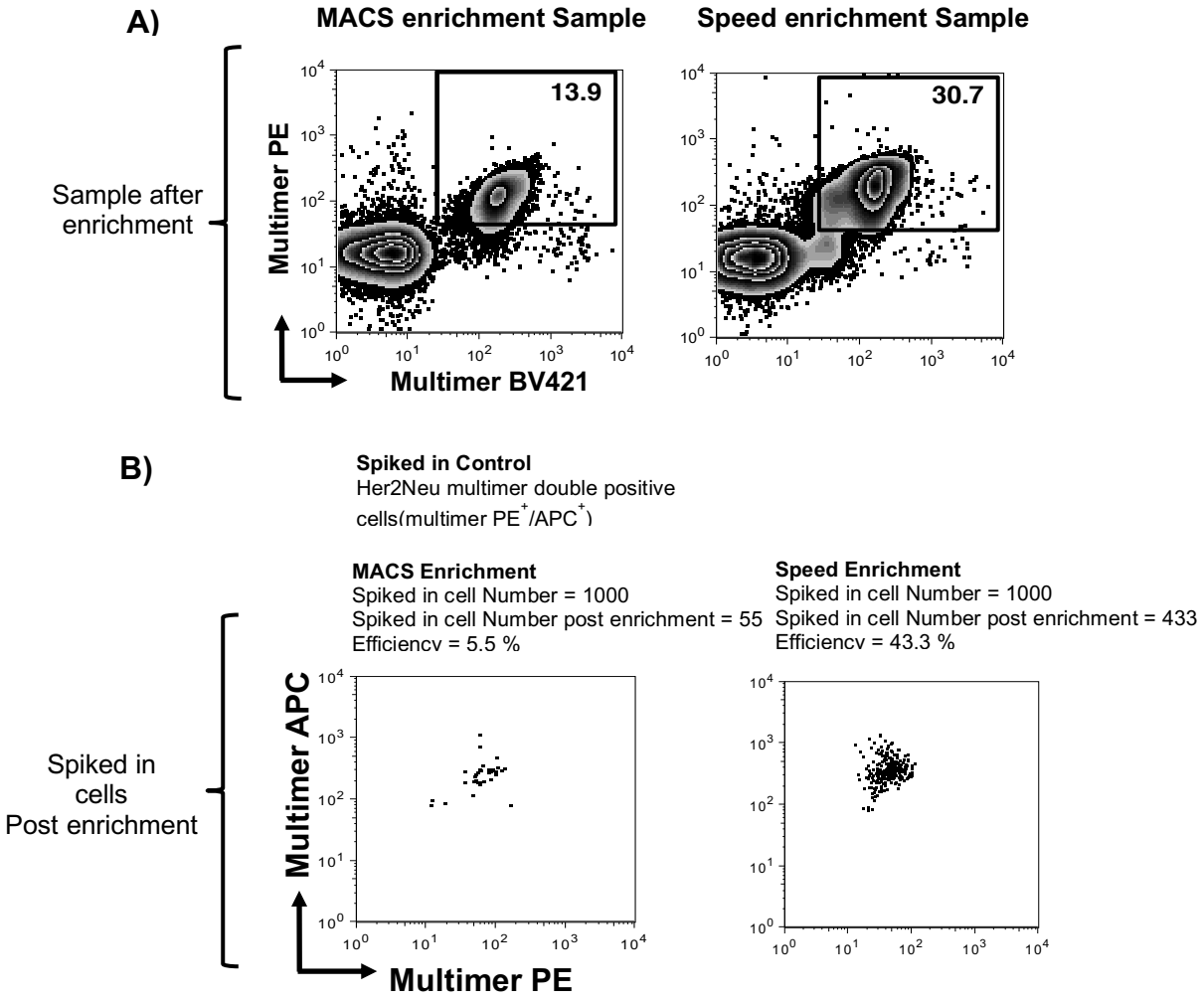


**Figure 4-6 : Comparison between enrichment methods MACS vs Speed Enrichment**

A2-FluMP positive cells enriched using MACS based and speed enrichment system with the same donor. Comparison of the two methods were based on the retrieval of the spiked in cells post enrichment. Her2Neu cells labelled with multimer conjugated to PE and BV421 was spiked in prior to MACS and speed enrichment (A) Final plots with gates defining antigen-specificity through multimer staining with comparison of samples enriched using MACS/speed enrichment. The FluMP double multimer positive cells were gated on lymphocytes, living, $CD19^-$, $CD3^+$ $CD8^+$. The FACS plots on the left shows FluMP double multimer positive cells after MACS enrichment and on the right FACS plots show FluMP double multimer staining after speed enrichment. (B) FACS plots of samples analyzed separately after the complete sorting and enrichment reflect the number of spiked in cells labelled with Her2Neu multimer PE and Her2neu multimer APC that could be detected post enrichment.

## 4.2 Cloning and sequencing of TCRs

After single cell PCR of the TCR ( performed by Isabell Schiedewitz) the PCR products were gel extracted and then cloned into a carrier plasmid for sequencing. The sequences of the TCR α / β chain PCR products were identified as described in the methods section (refer section 3.2.4). Healthy donors were screened for virus-specific epitopes like FluMP, YFV

and the MHC multimer-specific T cells of interest were sorted on a slide for single cell PCR and TCR extraction (**Fig. 4-4**, **Fig. 4-5**). The double MHC multimer-positive cells for different epitopes of interest from the parallel pull down and *in vitro* expansion (**Fig. 4-12**) were FACS-sorted onto PCR slides for single cell PCR and TCR amplification (**Fig. 4-4B**). This chapter summarizes the results of single cell PCR products and extraction of TCR α / β sequences of the double MHC multimer-positive cells from all the epitopes of interest and different donors.

### 4.2.1 Extraction of epitope-specific TCRs by single cell PCR and sanger sequencing for different epitopes.

**FluMP**

FluMP-specific T cells were MACS enriched and double MHC multimer-positive T cells were FACS sorted onto slides for single cell PCR as described in the results (**Fig. 4-4 B**). All control samples where no cells were sorted were negative and pairing of α- and β-chains occurred in the same combination (**Fig. 4-8 A**). A fraction of samples from single sorted cells contained full-length TCR α- and β-chains, as illustrated by green boxes. After Sanger-sequencing and analysis of TCR pairs TCR 7 α / 7 β pairing occurred two times (**Fig. 4-8 B**).

**A)**

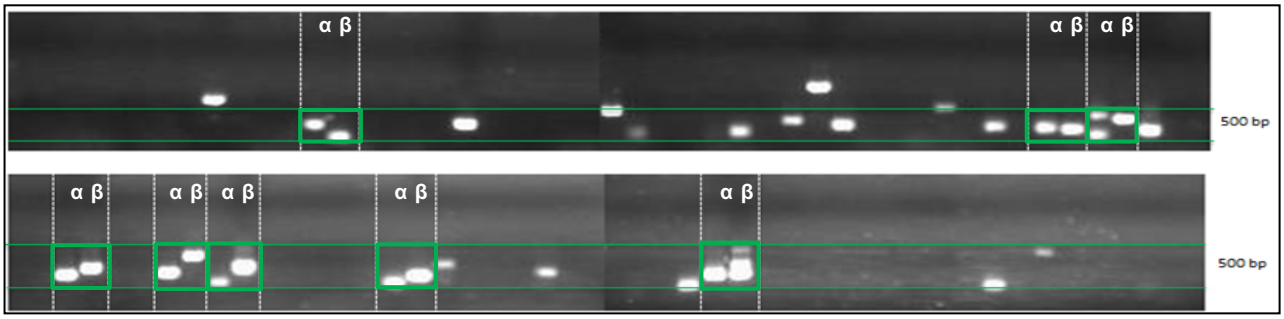


**B)**

| V-Segment | D-Segment | J-Segment | CDR3 Sequence | Label | Detected |
|---|---|---|---|---|---|
| TRAV12-1*01 F | - | TRAJ42*01 F | CVVNTLLRSQGNLIF | 7α | 2x |
| TRBV7-2*01 F | TRBD2*01 F | TRBJ2-3*01 F | CASSLVAGSITDTQYF | 7β | 2x |

**Figure 4-7 : Sequence analysis of single cell PCR products from enriched FluMP-specific TCRs.**

(A) Single PCR products were subjected to agarose gel electrophoresis. The results from the electrophoresis on the gel photography shows the white bands α- and β-chain adjacent to each other. White lines separate matched α- and β-chain products derived from same single cell and green boxes indicate TCR α- and β-chains with the expected size. The two white bands at the 500bp band indicate TCR chains with the expected size. (B) The table shows V-, D-, J-segment type and amino acid sequences of TCR CDR3 regions from sanger-sequenced FluMP-multimer positive T cells.

### YFV

YFV-specific T cells were speed enriched and YFV double MHC multimer-positive cells with a naïve phenotype were FACS sorted onto slides for single cell PCR as described in the results (**Fig. 4-5**). TCR α- and β-chains from the single cell sorted population with full-length, are illustrated by green boxes. After Sanger-sequencing and analysis of TCR pairs TCR 2α / 2β pairing occurred two times (**Fig. 4-9 B**) and TCR 26 α / 26 β, 38 α / 38 β and 40 α / 40 β were detected once respectively.

**A)**

**Donor 1**

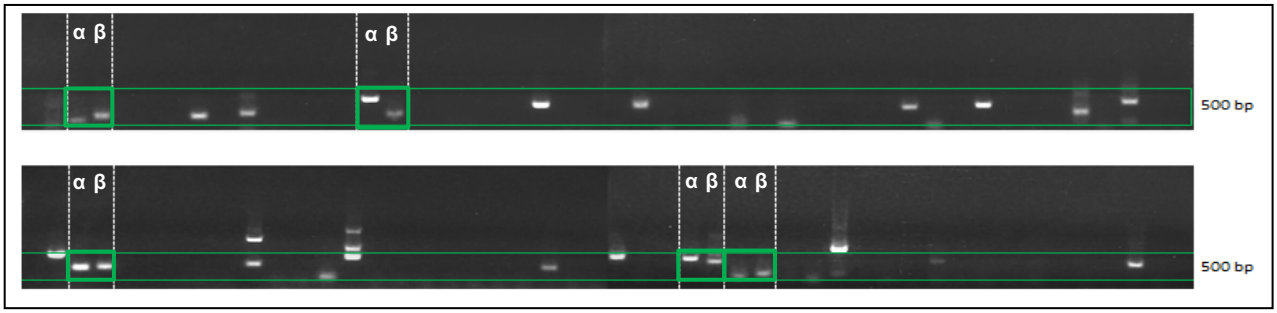


**Donor 2**

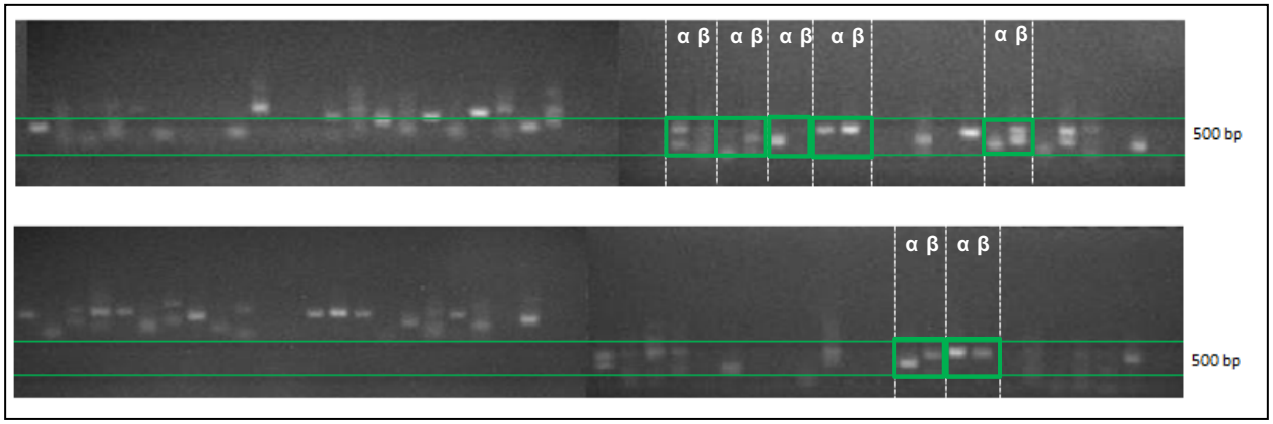


**B)**

| V-Segment | D-Segment | J-Segment | CDR3 Sequence | Label | Detected |
|---|---|---|---|---|---|

| | | | | | |
|---|---|---|---|---|---|
| TRAV12-2*01 F | - | TRAJ31*01 F | CAVNNARLMF | 2α | 2x |
| TRBV4-1*01 F | TRBD1*01 F | TRBJ2-7*01 F | CASSQEEGYEQYF | 2β | 2x |
| TRAV17*01 F | - | | CATGNSGGSNYKLTF | 40α | 1x |
| TRBV9*01 F | TRBD1*01 F | TRBD1*01 F | CASSAGTGGAYGYTF | 40β | 1x |
| TRAV21*01 F, or TRAV21*02 F | - | TRAJ32*01 F | CAVSLRRNYGGATNKLIF | 26α | 1x |
| TRBV12-3*01 F, or TRBV12-4*01 F | TRBD1*01 F | TRBJ2-7*01 F | CASSLGGGGYEQYF | 26β | 1x |
| TRAV12-2*01 F | - | TRAJ16*01 F | CAVPHGQKLLF | 38α | 1x |
| TRBV28*01 F | TRBD2*02 F | TRBJ1-5*01 F | CASSPMSQPQHF | 38β | 1x |

**Figure 4-8 : Sequence analysis of single cell PCR products from enriched YFV-specific TCRs.**

(A) Single PCR products were subjected to agarose gel electrophoresis. The results from the electrophoresis on the gel photography shows the white bands α- and β-chain adjacent to each other. White lines separate matched α- and β-chain products derived from same single cell and green boxes indicate TCR α- and β-chains with the expected size. The two white bands at the 500bp band indicate TCR chains with the expected size. (B) The table shows V-, D-, J-segment type and amino acid sequences of TCR CDR3 regions from sanger-sequenced YFV multimer positive T cells.

### NYESO1

NYESO1-specific T cells were MACS enriched and double multimer positive naïve T cells were FACS sorted onto slides for single cell PCR as described in the results (**Fig. 4-4 B**). Single sorted cells with detection of full-length TCR α- and β-chains are highlighted by green boxes (**Fig. 4-10 A**). After Sanger-sequencing and analysis of TCR pairs TCR 2 α / 2 β pairing occurred two times (**Fig. 4-10 B**).

**A)**


**B)**

| V-Segment | D-Segment | J-Segment | CDR3 Sequence | Label | Detected |
|---|---|---|---|---|---|
| TRAV13-2*01 F | - | TRAJ57*01 F | CAESTQGGSEKLVF | 2α | 1x |
| TRBV5-1*01 F | TRBD1*01 F | TRBJ1-3*01 F | CASSLAGLDSGNTIYF | 2β | 1x |

**Figure 4-9 : Sequence analysis of single cell PCR products from enriched NYESO1-specific TCRs.**

(A) Single cell PCR products were subjected to agarose gel electrophoresis. The results from the electrophoresis on the gel photography shows the white bands α- and β-chain adjacent to each other. White lines separate matched α- and β-chain products derived from same single cell and green boxes indicate TCR α- and β-chains with the expected size. The two white bands at the 500bp band indicate TCR chains with the expected size. (B) The table shows V-, D-, J-segment type and amino acid sequences of TCR CDR3 regions from sanger-sequenced NYESO1-multimer positive T cells.

**WT1**

WT1 HLA multimer-binding cells were MACS enriched and double MHC multimer-positive cells were single cell sorted. TCR α- and β-chains from single sorted cells with full-length are illustrated by green boxes. After Sanger-sequencing and analysis of TCR pairs TCR 33α / 33β pairing occurred two times (**Fig. 4-11B**).

**A)**

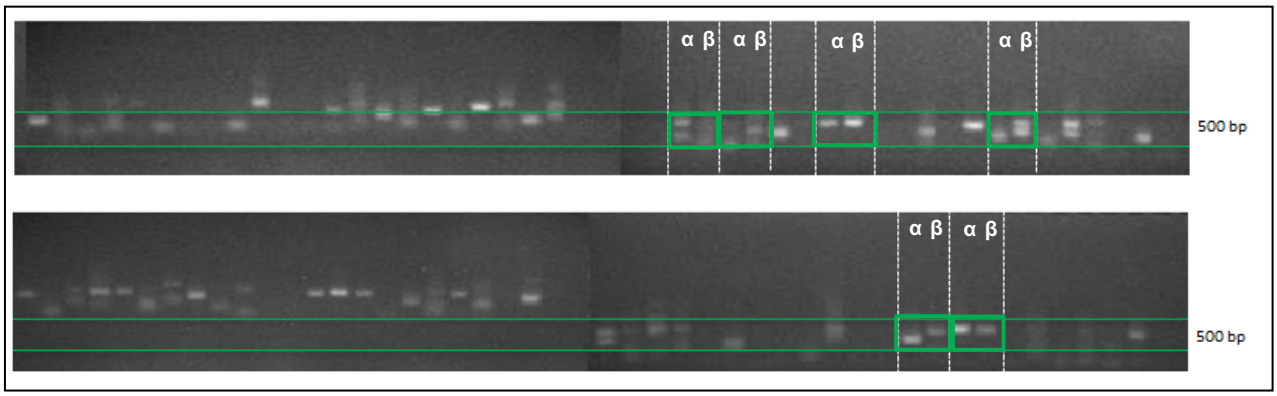


**B)**

| V-Segment | D-Segment | J-Segment | CDR3 Sequence | Label | Detected |
|---|---|---|---|---|---|
| TRAV12-1*01 F | - | TRAJ20*01 F | CVVNENDYKLSF | 33α | 2x |
| TRBV20-1*01 F, or TRBV20-1*02 F | TRBD2*01 F | TRBJ2-1*01 F | CSVAGASGGADYNEQFF | 33β | 2x |

**Figure 4-10 : Sequence analysis of single cell PCR products from enriched WT1-specific TCRs.**

(A) Single cell PCR products were subjected to agarose gel electrophoresis. The results from the electrophoresis on the gel photography shows the white bands α- and β-chain adjacent to each other. White lines separate matched α- and β-chain products derived from same single cell and green boxes indicate TCR α- and β-chains with the expected size. The two white bands at the 500bp band indicate TCR chains with the

expected size. (B) The table shows V-, D-, J-segment type and amino acid sequences of TCR CDR3 regions from sanger-sequenced WT1-multimer positive T cells.

### Her2Neu

Her2neu HLA multimer-binding cells were MACS enriched and double MHC multimer-positive cells were single cell sorted. TCR α- and β-chains from single sorted cells with full-length are illustrated by green boxes. After Sanger-sequencing and analysis of TCR pairs TCR 33α / 33β pairing occurred two times (**Fig. 4-11B**).

**A)**

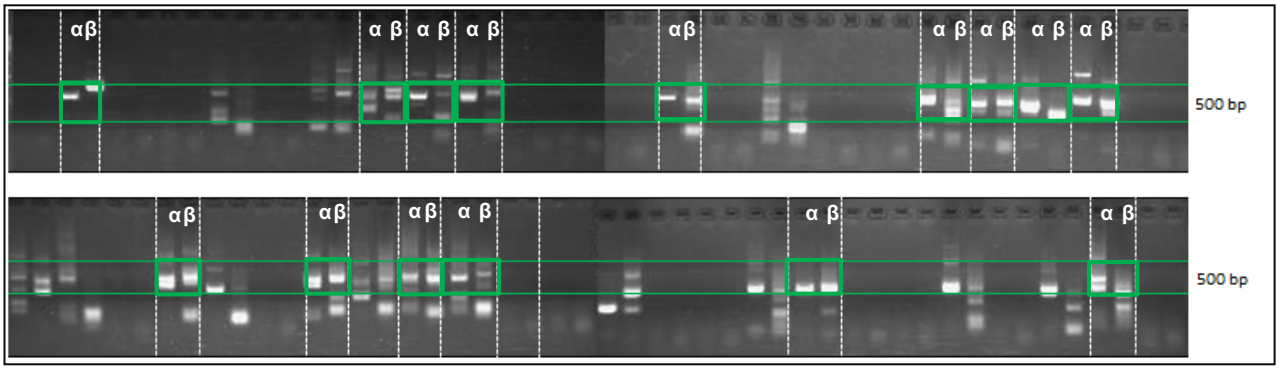


**B)**

| V-Segment | D-Segment | J-Segment | CDR3 Sequence | Label | Detected |
|---|---|---|---|---|---|
| TRAV9-2*02 F | | TRAJ42*01 F | CALSDDGGSQGNLIF | 2α | 3x |
| TRBV2*01 F | TRBD1*01 F | TRBJ1-4*01 F | CASSELVRGLEEKLFF | 2β | 3x |
| TRAV12-2*02 F | | TRAJ20*01 F | CAVTRSNDYKLSF | 42α | 4x |
| TRBV6-1*01 F | TRBD2*01 F | TRBJ2-3*01 F | CASSEGTHGTTQYF | 42β | 4x |

**Figure 4-11 : Sequence analysis of single cell PCR products from enriched Her2Neu specific TCRs.**

(A) Single cell PCR products were subjected to agarose gel electrophoresis. The results from the electrophoresis on the gel photography shows the white bands α- and β-chain adjacent to each other. White lines separate matched α- and β-chain products derived from same single cell the white bands with the right quantity of base pairs indicate TCR chains with the expected size. Green boxes indicate TCR α- and β-chains with the expected size. (B) The table shows V-, D-, J-segment type and amino acid sequences of TCR CDR3 regions from sanger-sequenced Her2Neu multimer positive T cells.

### Speed enrichment and parallel pool down

The precursor frequencies of the T cells specific for the chosen epitopes of interest was extremely low and the distribution was variable across donors. In order to be able to isolate T cells specific for different epitopes in a single step, we included a short-term expansion step after parallel pull down and enrichment. Parallel pull down with the help of speed enrichment was performed for all the T cells specific for epitopes of interest listed in the **Table 4-1**. MHC multimers specific for all the epitopes of interest conjugated to PE were generated before enrichment. For enrichment using parallel pull down from the healthy donor repertoire, T cells for different epitopes were all labelled together with MHC multimers conjugated to PE simultaneously. The labelled cells were then subjected to speed enrichment and the enriched MHC multimer-specific PE positive cells were directly sorted into a 24 well plate containing feeder cells. The sorted cells were then *in vitro* expanded with Okt3/ IL-2 stimulation (**Fig. 4-12 A**). After 12 days, the expanded cells were labeled with peptide specific MHC multimers for different epitopes in separate reactions. Double MHC multimer-positive cells were FACS sorted onto slides for single cell PCR. **Fig. 4-12 B** shows FACS plots from the final purity sort performed on the MoFlo-Legacy we can see the T cells double positive for pMHC multimers specific for all different epitopes of interest - WT1, Her2Neu, NYESO1, PRAME, PR1, HA1. Percentage of epitope-specific T cells are indicated in the right corner of the gates.

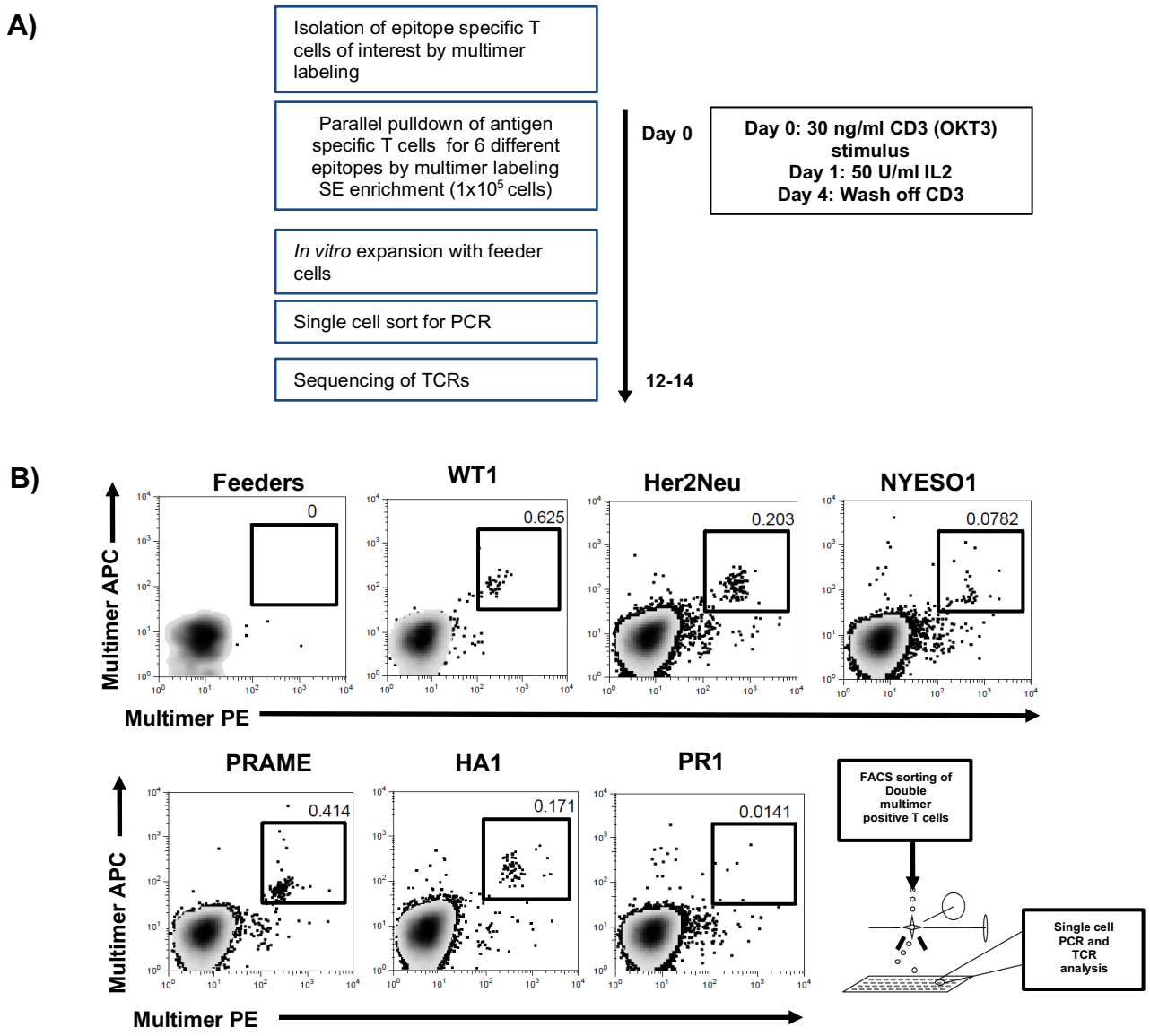


**Figure 4-12 : Speed enrichment and parallel pull down of MHC multimer-labelled epitope-specific T cells for 6 different specificities, short term cultured cells**. Speed enrichment of cells specific for epitopes of interest after parallel pool down and expansion. (A) Donor PBMCs were stained with PE- multimers specific for several epitopes labelled on PE and isolated using speed enrichment these epitope specific enriched cells were *in-vitro* cultured and Okt3/IL-2 stimulated with feeders. (B) Expanded cells after a 12-day culture, were screened for double multimer positive cells in separate reactions for different epitopes of interest. Dot plots show analyzed double multimer positive cells which were pre-gated on live lymphocytes, PI- , $CD3^+CD8^+$ lymphocytes. Double multimer positive cells were FACS sorted onto a single cell PCR slide.

The precursor frequencies for most of the epitopes of interest is known to occur at a frequency of < $1x10^{-6}$ in the healthy donor. As an example, from the donor shown in **Fig.4-12** the precursor frequency for $NYESO_{157-165}$ specific T cells: $3x10^{-6}$ (60 cells in 500ml of

blood) after parallel pool down and speed Enrichment: $7.8x10^{-2}$ cells were detected and sorted.

| Epitope | V-Segment | D-Segment | J-Segment | CDR3-Sequence: VN(D)NJ |
|---|---|---|---|---|
| WT1 126-137 | TRAV12-3*01 F | - | TRAJ39*01 F | CAMSEDNAGNMLTF |
| | TRBV2*01 F | TRBD1*01 F | TRBJ2-1*01 F | CASSTPGYGEQFF |
| | TRAV12-2*02(F) | - | TRAJ20*01 F | CAVNLNDYKLSF |
| | TRBV20-1*01 F | TRBD2*01 F | TRBJ2-3*01 F | CSAQTKGLAGISTDTQYF |
| NYESO1 157-165 | TRAV41*01 F | - | TRAJ33*01 F | CAVKSNYQLIW |
| | TRBV28*01 F | TRBD1*01 F | TRBJ1-5*01 F | CASSDDRENQPQHF |
| Her2Neu 369-377 | TRAV9-2*02 (F) | | TRAJ42*01 F | CALSDDGGSQGNLIF |
| | TRBV2*01 F | TRBD1*01 F | TRBJ1-4*01 F | CASSELVRGLEEKLFF |
| | TRAV12-2*02(F) | - | TRAJ20*01 F | CAVTRSNDYKLSF |
| | TRBV6-1*01 F | TRBD2*01 F | TRBJ2-3*01 F | CASSEGTHGTTQYF |
| PRAME 300-309 | TRAV1-2*01 F | - | TRAJ24*02 F | CAVRDDSWGKLQF |
| | TRBV24-1*01 F | - | TRBJ1-2*01 F | CATWLANYGYTF |
| YVF 214-222 | TRAV12-2*01 F | - | TRAJ16*01 F | CAVPHGQKLLF |
| | TRBV28*01 F | TRBD2*02 F | TRBJ1-5*01 F | CASSPMSQPQHF |
| | TRBV9*01 F | - | TRBJ1-2*01 F | CASSAGTGGAYGYTF |
| | TRBV9*01 F | TRBD1*01 F | TRBJ1-2*01 F | CASSAGTGGAYGYTF |

**Figure 4-13 : Sequences of identified TCRs for epitopes of interest**

The table shows V-, D-, J-segment type and amino acid sequences of CDR3 regions against the epitopes presented by HLA-A2 after sanger-sequencing. CDR3 indicates complementary determining region 3: TRAV: TCR α-chain variable region, TRBV: TCR β-chain variable region, TRBD: TCR β-chain D-Segment; TRAJ: TCR α-chain J-Segment, TRBJ: TCR β-chain J-Segment. The D region within the CDR3 is highlighted in red.

Full length TCR sequences extracted from single cell PCR for the epitopes of interest is summarized in the above table. Amino acid sequence of the CDR3 domain and V-, D and J- segment types are listed in the above figure**.** TCR sequences described in **Fig. 4-13** were re-expressed on healthy donor PBMCs by sleeping beauty mediated gene transfer system. However, for HA1 epitope-specific TCR we did not have complete pairs of α and β chain and for PR1 there were no sufficient MHC multimer positive cells for single cell PCR.

### 4.2.2 Transformation and TCR sequence analysis

Initially we tried to perform this assembly by a series of cloning steps using Gibson assembly. Due to the multiple cloning steps involved, lack of codon optimization, complexities involved with packaging huge cassette into a vector etc., TCRs could not be successfully re-expressed. After verification on IMGT database, the resulting TCR sequences were not complete and we had truncated sequences. We tried to clone the

chains individually by Gibson assembly into the complete cassette. The entire process was time consuming and technically challenging. Therefore, to successfully clone such a huge cassette, we subsequently decided to send it to a commercial provider for assembly. TCR sequences summarized in the **Fig. 4-13** were then *in silico* assembled and verified sequences were sent to a commercial provider (GeneArt®) for synthesis of a single gene string (Complete sequences of TCR cassettes are listed at the end of results section). In order to successfully express the TCRs and to overcome the competition with endogenous TCRs and increase the surface expression of TCRs, we modified the constant region to introduce murine constant region. After *in silico* verification for completeness, a total of 7 pairs of α/ β chains were sent for assembly (PRAME - 1 pair, Her2Neu - 2 pairs, YFV - 2 pairs, WT1 - 1 pair, NYESO1 - 1 pair). TCR cassette and pT2 backbone, both containing the same 5'- and 3'-homology regions, were ligated via Gibson Assembly. Adding equimolar amounts (0.02-0.5pmol) of linear TCR-cassette and pT2 backbone into a PCR vial, to this 5 µl of Gibson assembly mastermix was added as discussed in the methods section. Colony PCR revealed that most of the vectors contained full-length TCR cassette. The TCRs were Sanger-sequenced and analyzed. All the TCRs showed full integrity and there were no mutations when verified. The resulting gibson assembled pT2 TCR vector transposon in combination with SB100X transposase coded on a second plasmid, were used for gene transfer (electroporation) in order to transduce primary human PBMCs with engineered TCRs.

## 4.3 Transgenic expression of TCRs of interest using sleeping beauty mediated gene transfer system

Validating antigen specificity of the TCRs requires them to be expressed on healthy donor PBMCs. Sleeping beauty mediated gene transfer system was used for re-expression of TCRs on healthy donor PBMCs to further test the functionality of all the TCRs of interest. Although transduction using retroviral vectors was successfully used for validation of previously isolated TCRs, we chose to test more flexible methods for establishment of a reliable workflow. In this chapter, we discuss the results for re-expression of TCRs of interest using electroporation with sleeping beauty mediated gene transfer system **Fig. 4-3-1**.

### Transposon (TCR) based sleeping beauty mediated gene transfer system

Electroporation is a gene transfer technique based on the transient disruption of cell membrane after exposure to an electric field, allowing charged molecules to enter the cell in our case the transposon and transposase encoding plasmids by nucleofection (Fig. 4-15).

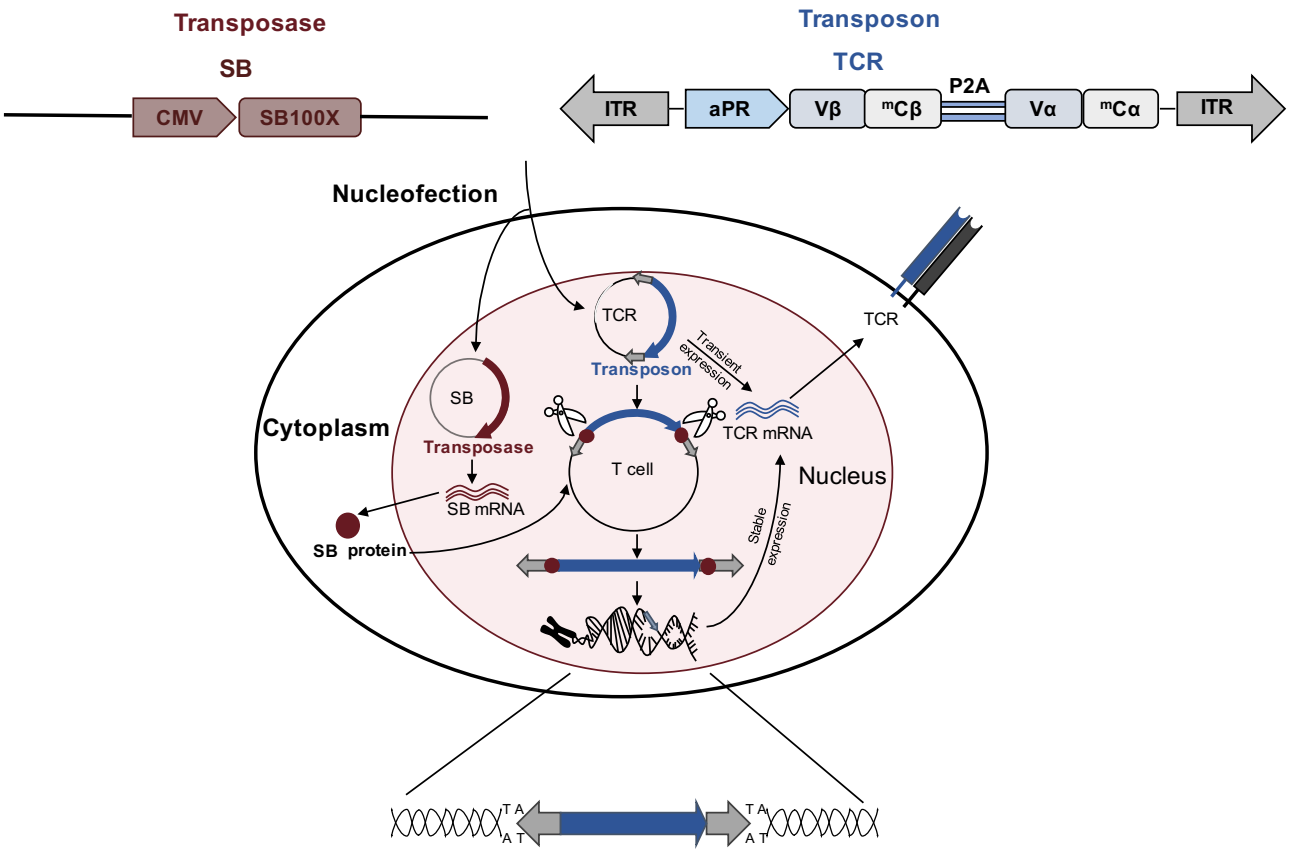


**Figure 4-3-1 : Sleeping beauty mediated gene transfer system and transposon (TCR) vector construct.**

Schematic representation of the Sleeping Beauty transposase (SB100x), the SB transposase SB100X is coded on a separate plasmid with CMV, cytomegalovirus promotor. pT2 transposon consisting of a transgene expression cassette, encoding the codon-optimized, chimeric human/murine TCR with specificity against various epitopes of interest. TCR α- and β- chains are linked via self-cleaving porcine teschovirus 2A sequence (P2A) (Yang et al. 2008; Wargo et al. 2009), flanked by inverted terminal repeats (ITRs) or the homology sequence, aPR indicates artificial promoter region; m, murine; In the two-plasmid SB system, a gene of interest (in this case a TCR) can be positioned between ITRs (gray arrows) of the transposon that is mobilized by the transposase protein SB100X (brown circle) supplemented in trans. ITRs contain transposase binding sites necessary for transposition. SB allows stable non-viral gene transfer through a “cut and paste” mechanism integrating the TCR of interest into the TA-dinucleotide sites of the host genome without unintended integration into transcriptional active sites (adapted from Singh et al. 2014).

**Establishment of a reliable protocol for electroporation of TCRs of interest**

Sleeping Beauty-mediated gene transfer was performed as described in the methods section. J76 cells and donor PBMCs were electroporated using Lonza Nucleofector™ II/2b along with compatible electroporation cuvettes which were tested for reusability. We used the protocols for the new set of generic buffers optimized for Lonza nucleofector II device as described in the protocols (65). We tested the conditions as described in the methods section for J76 and stimulated PBMCs on the Lonza nucleofector II.

### 4.3.1 TCR gene transfer and re-expression on J76 cells

We tested re-expression of TCRs of interest using sleeping beauty mediated gene transfer system on α β - TCR deficient jurkat cell lines and healthy donor PBMCs (65). J76 cells lack the expression of their endogenous TCR chains but possess all necessary CD3 molecules, which gets recruited in the presence of a functional TCR. One of the advantages of using J76 cells is that we can stably introduce transgenes and overcome the probable interference of endogenous TCRs. Surface expression of TCRs can be easily detected by anti-mTRBC staining and further analyzed by flow cytometry.

Higher concentration of DNA during gene transfer is known to affect the viability of cells post transfection. Therefore, it was important for us to titrate the right concentrations of transposon and transposase before we performed nucleofection of TCRs of interest. The electroporation mix is also known to be toxic for the cells so once the cells were resuspended in the mix they were electroporated immediately followed by dilution with pre-warmed RPMI complete media containing human serum, 25 U/ml IL-2 and taken into cell culture at 37°C and 5% CO2.

For efficient transfection, the J76 cells were taken into culture at least 2-3 days before electroporation. In case of electroporation on PBMCs the donor PBMCs were collected previous day of electroporation and subjected to polyclonal stimulation. Polyclonal stimulation of primary T cells is an important step in every transfection protocol. The main purpose of activating primary T cells is to obtain as many electrocompetent cells as possible. Moreover, stimulation with aCD3 and aCD28 increases the frequency of the $CD8^+$ T cell pool and hence enriches the main target population for TCR transfection. For successful electroporation and to attain maximum numbers of electrocompetent cells we stimulated the donor PBMCs with aCD3 and aCD28 to increase $CD8^+$ T cell pool and TCR transfection. Evaluation of efficiency and stimulation protocol optimization was performed together with Manuel Effenberger during the practical part of his Master thesis. Polyclonal stimulation of

primary T cells is an important step in every transfection protocol. The main purpose of activating primary T cells is to obtain as many electrocompetent cells as possible. Moreover, stimulation with aCD3 and aCD28 increases the frequency of the $CD8^+$ T cell pool and hence enriches the main target population for TCR transfection. For successful electroporation and to attain maximum numbers of electrocompetent cells, we stimulated the donor PBMCs with aCD3 and aCD28 to increase $CD8^+$ T cell pool and TCR transfection. Evaluation of efficiency, choice of electroporation method, stimulation protocol optimization was performed together with Manuel Effenberger during the practical part of his Master thesis. For successful re-expression of the TCRs on the surface, we also tried electroporation with different cell concentrations and re-evaluated the right concentrations of transposon and transposase for transfection **Fig.4-14**, **Fig.4-15**. We electroporated J76 cells with varying ratios of transposon and transposase to find the right concentration. We tried electroporation with different cell concentrations to re-evaluate the right concentrations of transposon and transposase for transfection (69). For detection of successfully transduced TCR-transgenic T cells, T cells were first only stained with an antibody directed against the murine constant region of the transgenic TCR β chain (referred to as mTrBC staining).

**A) Varying concentration of transposon and constant transposase concentration of 0.5 µg**

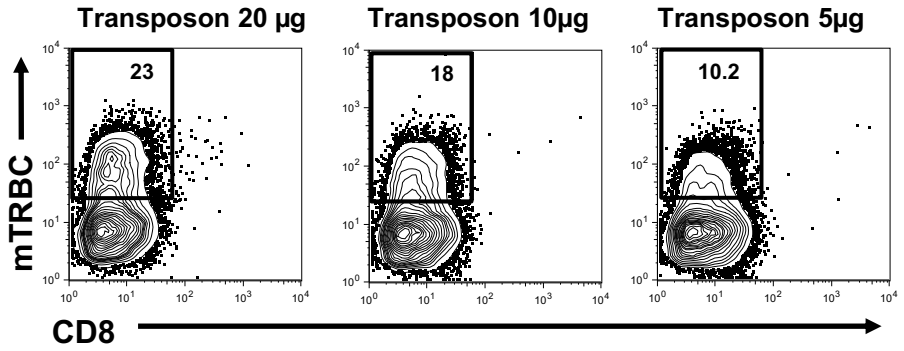


**B) Varying concentration of transposase and constant transposon concentration of 20 µg**

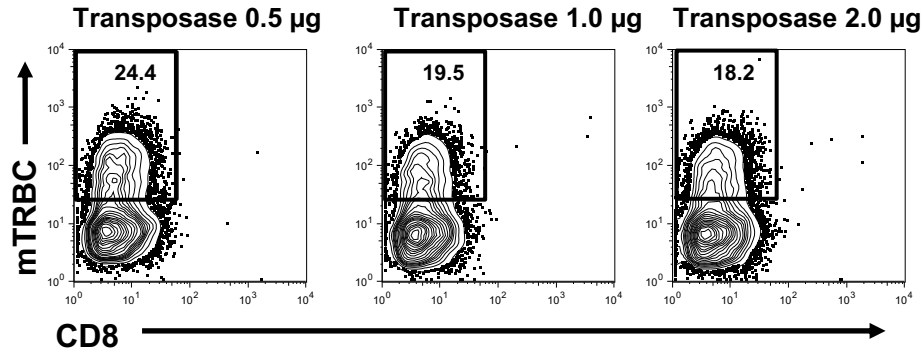


**Figure 4-14 : Titration of transposon-transposase ratio to determine optimum concentration using J76 cells Day 1 after electroporation.**

FACS plots showing mTrBC and CD8 Day 1 after electroporation. (A) Staining of J76 cells for surface expression of murine constant region (mTrBC) which may be transiently expressed at higher levels on the surface confirming TCR expression post electroporation with varying concentrations of transposon keeping the transposase concentration constant. (B) Staining of J76 cells for surface expression of murine constant region (mTrBC) post electroporation of J76 cells with varying concentrations of transposase keeping the transposon concentration constant.

It is notable that 0.5 µg of transposase and 20 µg of transposon seems to be the optimum concentrations for successful expression of TCRs on the surface. Optimum working concentrations was determined in order to avoid toxicity to the cells in culture due to higher concentrations of transposon. **Fig. 4-14 A** shows the mTrBc expression with varying concentration of transposase with a constant transposon concentration. **Fig. 4-14 B** shows the mTrBc expression with varying concentration of transposon with a constant transposase concentration. However, on Day 1 these are transient expressions and the cells were cultured further to test more stable expression. **Fig. 4-15 A** and **Fig. 4-15 B** shows Day 6

mTrBc expression with varying concentration of transposase with a constant transposon concentration.

**A) Varying concentration of transposon and constant transposase concentration of 0.5 µg**

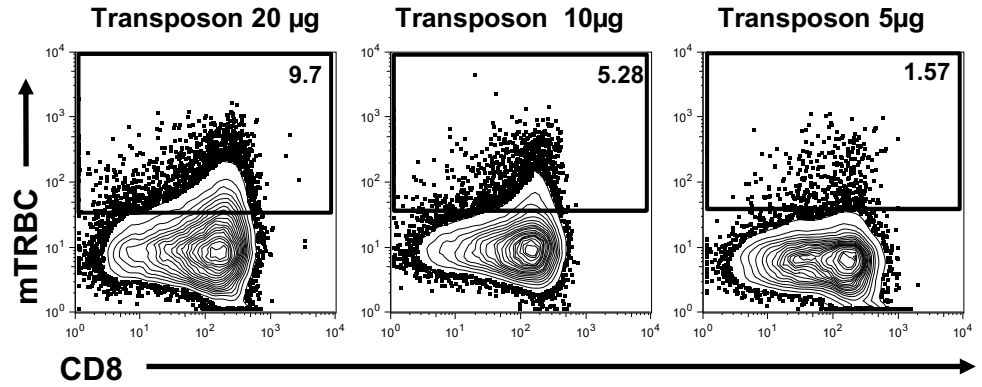


**B) Varying concentration of transposase and constant transposon concentration of 20 µg**

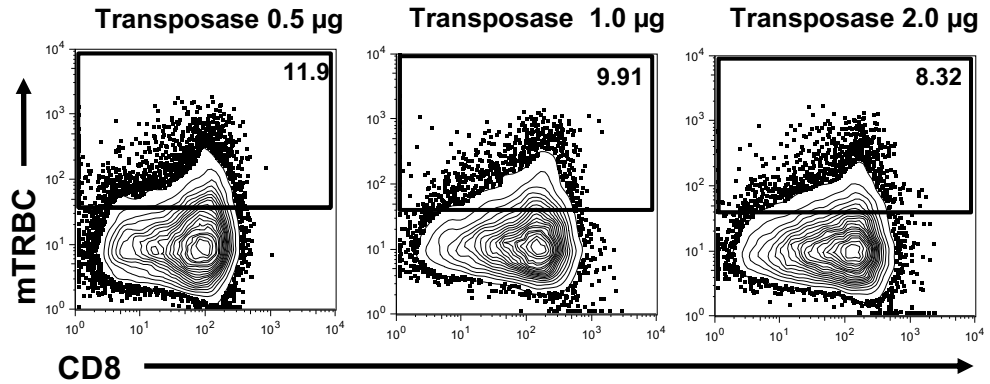


**Figure 4-15 : Titration of transposon-transposase ratio to determine optimum concentration using J76 cells Day 6 after electroporation.**

FACS plots showing mTrBC and CD8 6 days after electroporation to verify the stable expression of TCRs on the surface. (A) Staining of J76 cells for surface expression of murine constant region (mTrBC) which now are stably expressed on the surface confirming TCR expression post electroporation of J76 cells with varying concentrations of transposon keeping the transposase concentration constant. (B) Staining of J76 cells for surface expression of murine constant region (mTrBC) post electroporation of J76 cells with varying concentrations of transposase keeping the transposon concentration constant.

After determining the correct ratios of transposon and transposase concentrations, we performed several batches of electroporation with different donor PBMCs to verify consistent results. **Fig. 4-18** and **Fig. 4-19** are representative of several such electroporation experiments.

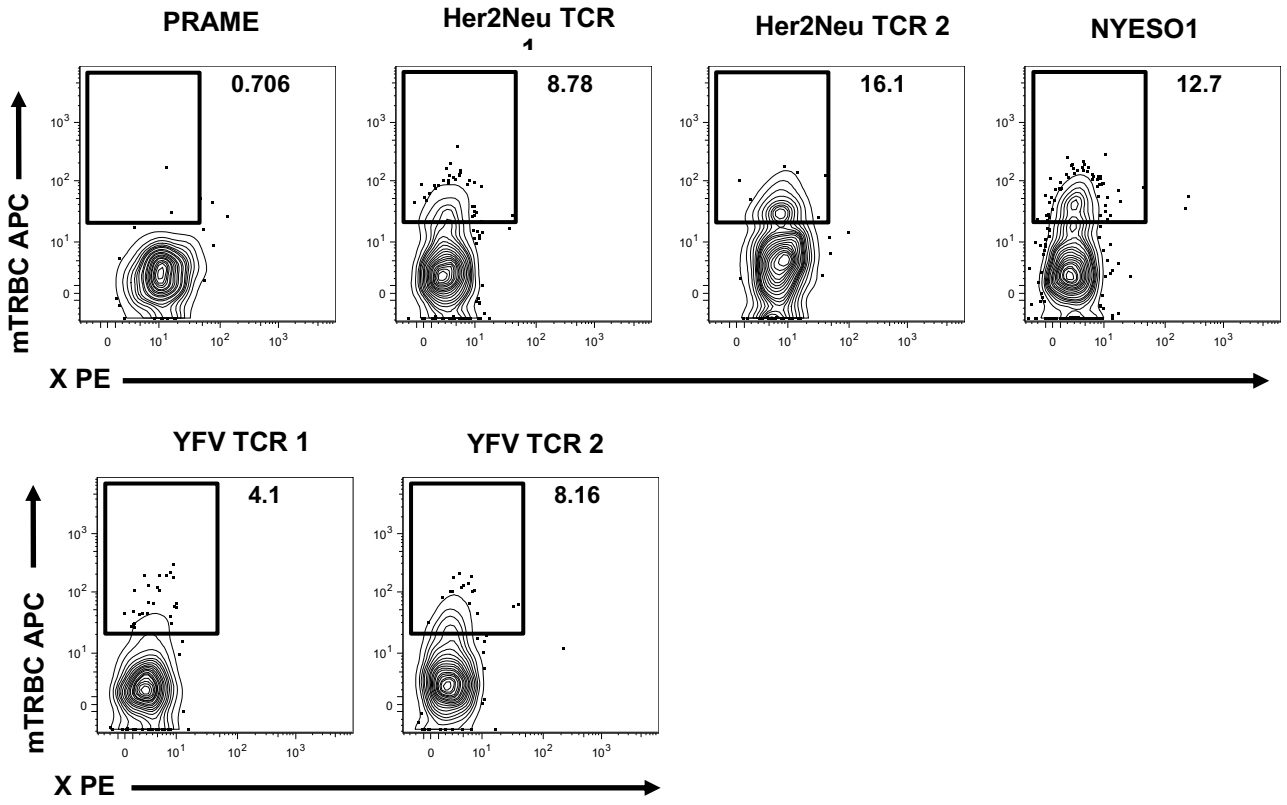


**Figure 4-16 : TCR expression on the surface of J76 cells determined by mTrBC expression day 1 post electroporation.**

FACS plots showing surface staining of murine constant region (mTrBC) on Day 1 after electroporation on J76 cells to determine surface expression which may be transiently expressed detected by antibody staining.

We first used α β - TCR deficient T - cell line J76 to re-express the TCRs of interest to test the specificity of the constructed TCR-chains. These cell lines express CD8 but lack their own TCRs. Other groups have shown high level functional expression of introduced TCR genes using J76 cells (61, 70). **Fig. 4-16** shows representative FACS plots for surface staining of mTRBC expression on J76 cells Day 1 after electroporation with all the TCRs of interest. However, functionality testing of TCRs transduced on J76 is not feasible. Therefore, for functionality testing we re-expressed the TCRs of interest (as listed in **Fig. 4-13**) on healthy donor PBMCs.

### 4.3.2 TCR gene transfer and re-expression on healthy donor PBMCs

Donor T cells were electroporated on U-014 program on the electroporator and then transferred into a single well of 12 well plate containing 2 mL of prewarmed RPMI media with human serum. Mock electroporation's without transposon (no TCR) was performed in parallel as negative control. As a positive control, healthy donor PBMCs were electroporated

with GFP-pT2 using the SB mediated gene transfer system. As a measure for efficient transduction we used sleeping beauty-mediated gene transfer system to transduce GFP-pT2 transposon under the same conditions. Per nucleofection, 0.5 µg SB100X was mixed with 4 µg pT2-GFP in 100 µl 1SM buffer. $GFP^+$ signal was measured using flow cytometry. We measured transient $GFP^+$ signal one day after electroporation and 60.9% of the cells showed successful transfection, for more stable expression these cells were kept in culture and we measured the $GFP^+$ signal 7 days post electroporation. We could show that around 30.3% of the cells were still $GFP^+$ after 7 days of transduction **Fig. 4-17** (FACS plot on the right). We also stained the untransduced cells for comparison and to exclude any background for actual TCR staining (**Fig. 4-18**).

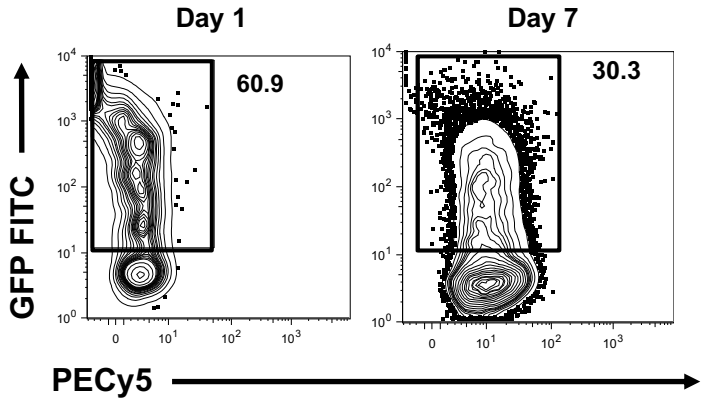


**Figure 4-17 : Electroporation with GFP-pT2 on healthy donor PBMCs**

Above are the FACS plots showing transient and stable GFP expression post electroporation. To the left FACS plot show GFP expression on Day 1 and on the right GFP expression on Day 7.

Prior to electroporation the donor PBMCs were cultured overnight in plates coated with OKT3/aCD3 and aCD28. Transient expression of 60.3% of GFP was obtained one day after electroporation following this protocol. Day 8 post electroporation a stable expression of 30% was notable as shown in **Fig. 4-17.** We then used this protocol to electroporate all the TCRs of interest. A reliable stimulation protocol was established with titrated amounts of transposon and transposase. The day after electroporation a small sample of electroporated cells was stained with anti mTCRβ antibody to test for surface expression. The surface expression of the TCRs was tested by mTrBC staining. Most of the TCRs showed the expression of TCRs on the surface **Fig. 4-18** and **Fig. 4-19.** However, for a few epitopes of interest using this protocol we could not detect any mTrBC staining indicating no TCR surface expression. There could be several factors influencing the surface expression of

TCRs like TCR internalization or presence of competing endogenous TCRs on the donor PBMCs. Mispairings between α/β chains and mismatched α/β chains could also affect successful surface expression of the TCRs of interest on the donor PBMCs. Nevertheless, we could detect both surface expression and multimer staining for NYESO1 TCR as shown in the **Fig. 4-21**.

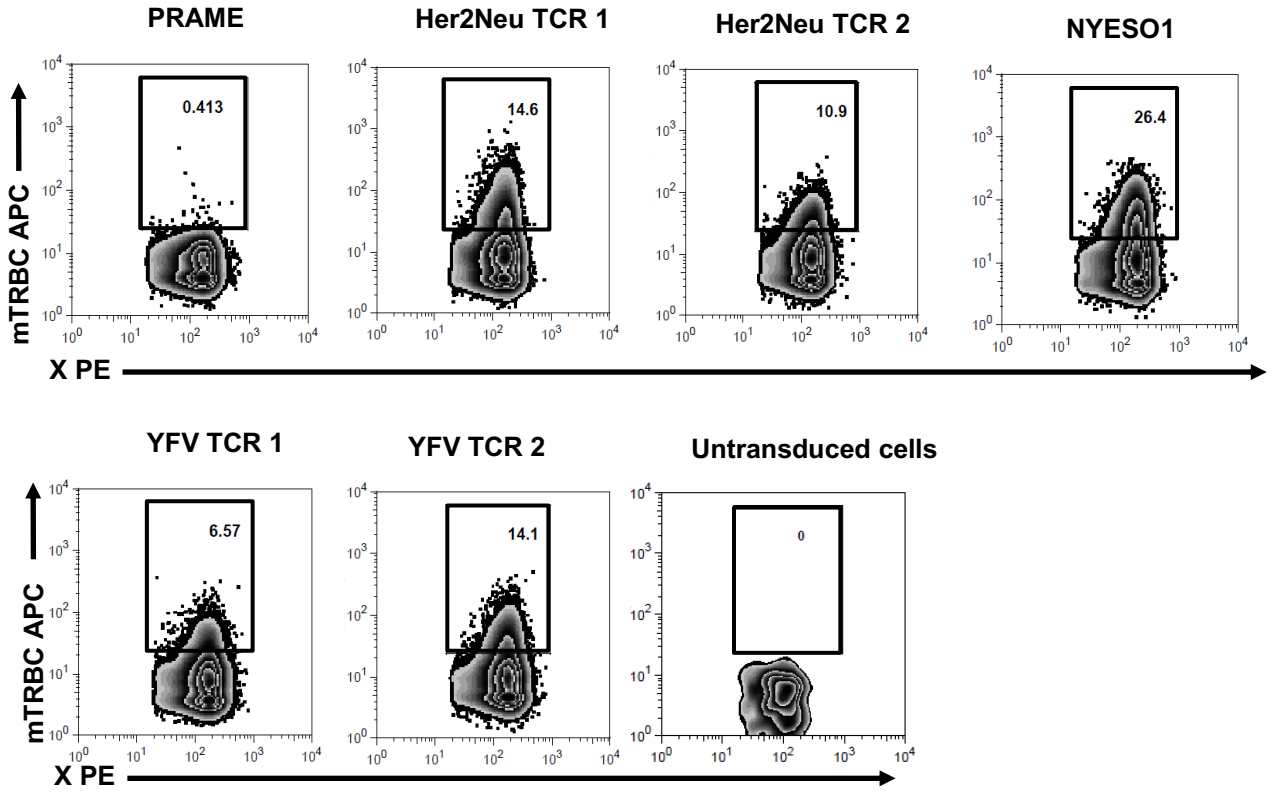


**Figure 4-18 : TCR expression on the surface determined by mTrBC expression day 1 post electroporation (Donor 1).**

FACS plots showing mTrBC staining with transient expression of TCRs on the surface for different TCRs of interest day 1 post electroporation.

In order to test for epitope specificity of TCRs expressed on the surface we tested for multimer staining day 1 post electroporation few epitopes of interest . As a control, we used MART1 TCR, which was previously optimized by the laboratory of Wolfgang Uckert (Berlin) and tested for multimer staining day 1 post electroporation for 2 other epitopes of interest (shown in the **Fig. 4-18-1**).

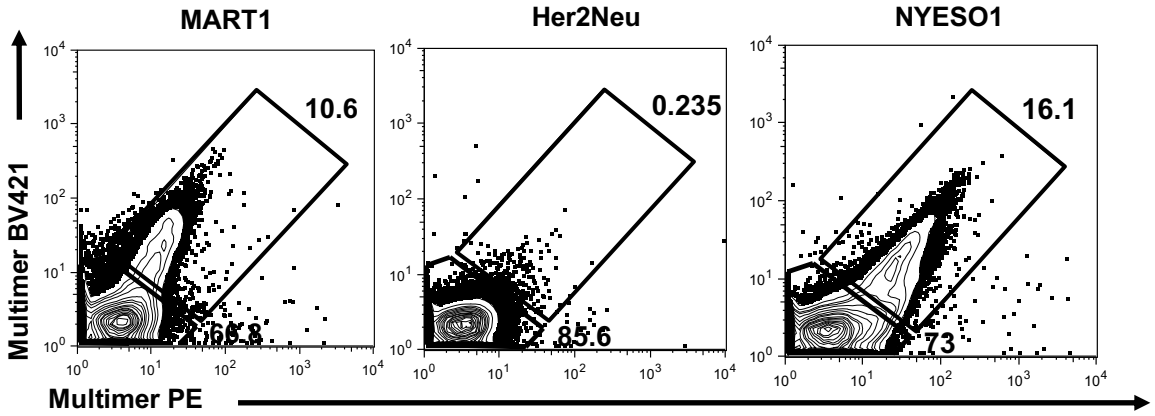


**Figure 4-18-1 . Detection of epitope specificity by double multimer staining Day 1 post electroporation (Donor 1)** Pre-gated on lymphocytes and live cells, FACS plots show transient expression of TCRs and double multimer positive cells confirming the epitope specificity of the TCRs of interest.

Healthy donor PBMCs were electroporated using the SB mediated gene transfer system. day 1 after electroporation, cells were tested to determine surface expression of TCRs on the donor PBMCs. As control GFP-pT2 transposon was transduced under the same conditions along with engineered TCRs-pT2 transposon vectors. **Fig. 4-18** shows the transient expression of TCRs on the surface measured by surface staining with antibody binding to mTrBC to determine TCR expression. The murine constant regions of transduced cells with all the different TCRs of interest were detectable with an exception for PRAME. These cells were further cultured to verify stable expression of TCRs. We performed several batches of electroporation's to test consistency in results with the same conditions. **Fig 4-19** shows FACS data for surface expression of TCRs from electroporation performed on different donor PBMCs (donor 2). We also stained for CD8 expression, the numbers indicate the percentage of cells positive for mTrBC confirming the surface expression of TCRs of interest. We could see a transient surface expression of TCRs via mTrBC staining for all the TCRs except for PRAME on day 1. In order to test for epitope specificity of TCRs expressed on the surface we tested for multimer staining day 1 post electroporation few epitopes of interest (shown in the **Fig. 4-19-1**). The mTrBC expression on day 8 was also detected as shown in the **Fig. 4-19-2**.

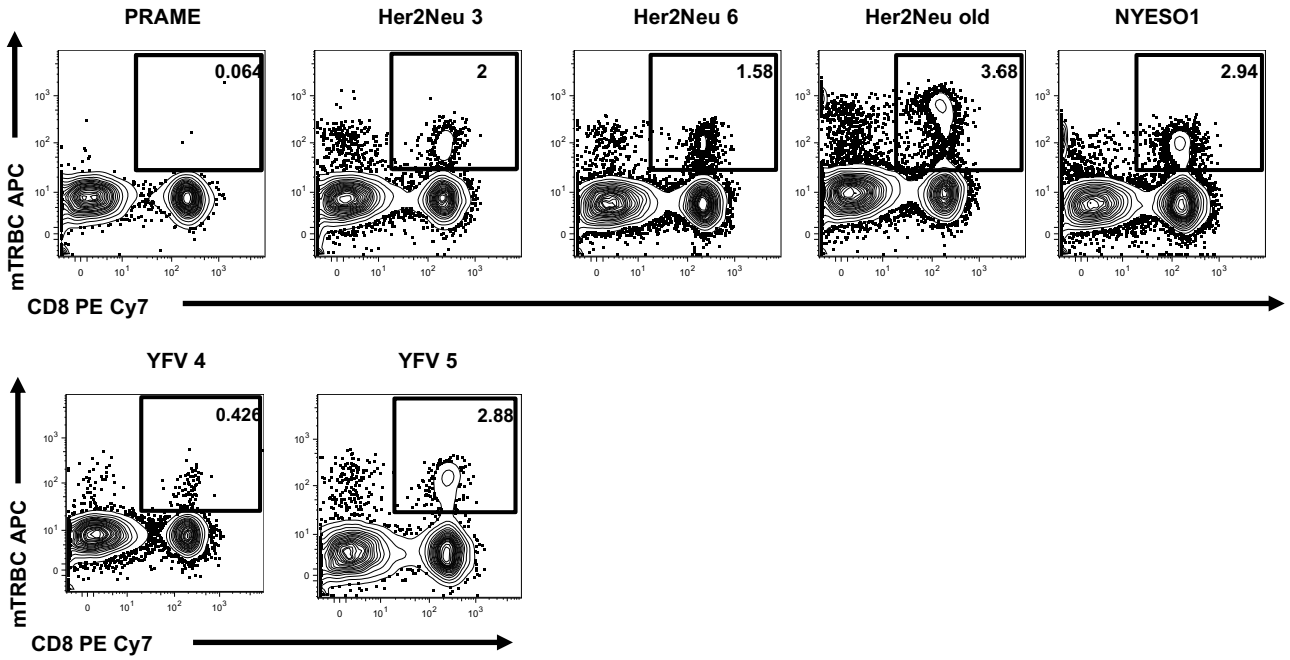


**Figure 4-19 : Transient TCR expression on the surface determined by mTrBC staining day 1 post electroporation (Donor 2).**

Pre-gated on lymphocytes and live cells, FACS plots show transient expression of mTrBC expression on the surface day 1 after electroporation, confirming the surface expression of most TCRs of interest.

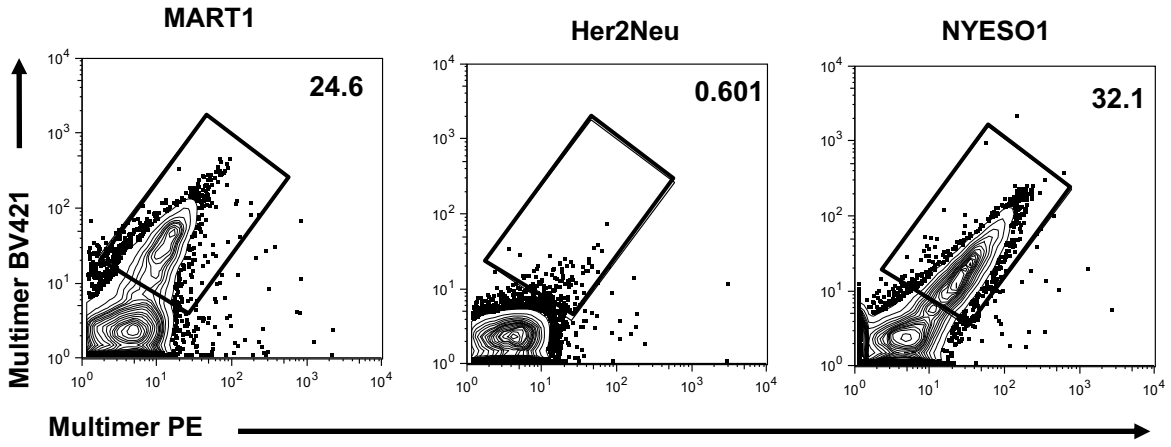


**Figure 4-19-1 . Detection of epitope specificity by double multimer staining Day 1 post electroporation (Donor 2)** Pre-gated on lymphocytes and live cells, FACS plots show transient expression of TCRs and double multimer positive cells confirming the epitope specificity of the TCRs of interest.

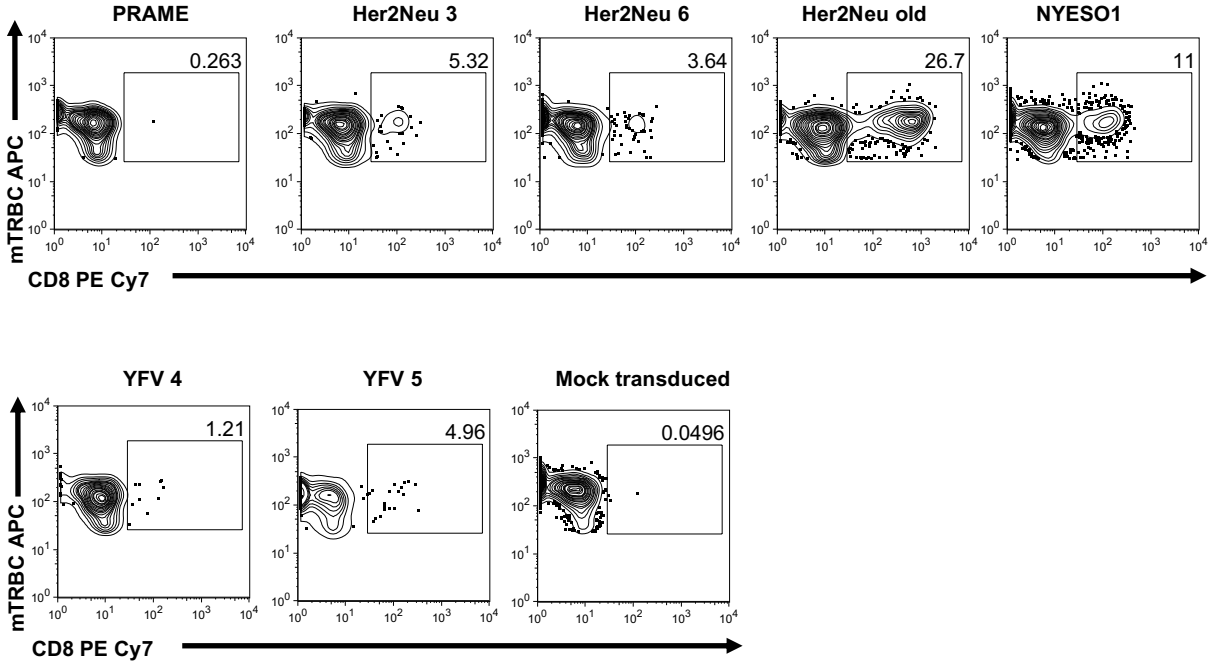


**Figure 4-19-2. Stable TCR expression on the surface determined by mTrBC staining 8 days post electroporation (Donor 2).**

Pre-gated on lymphocytes and live cells, FACS plots show stable expression of mTrBC expression on the surface day 8 after electroporation, confirming the surface expression of most TCRs of interest.

## 4.4 Functional evaluation of TCRs

In this chapter, we discuss the results post electroporation to determine the epitope specificity of the transduced TCRs on the surface. The surface expression on both jurkat cell line and donor PBMCs determined by mTrBC staining could be transient. In order to confirm stable expression of TCRs on the surface the cells were cultured for 7 days. On day 8 the epitope specificity was confirmed by double multimer staining for TCRs of interest **Fig. 4-22**. We then performed intracellular cytokine staining to determine their functionality.

### 4.4.1 Evaluation of epitope specificity

In order to evaluate the functionality and the specificity of the constructed TCR-chains they were initially re-expressed on αβ-TCR deficient J76 T-cell line. After 8 days in culture of all the transgenic TCRs expressed on J76 cells only NYESO1 TCR showed successful multimer staining on J76 cells. After electroporation and after 8 days in culture 1.57 % of the total live cells specifically bound to NYESO1 multimer **Fig. 4-20**. As J76 cells do not secrete cytokines or lyse target cells in response to TCR stimulation, we transgenically expressed all the TCRs of interest on healthy donor PBMCs by electroporation.

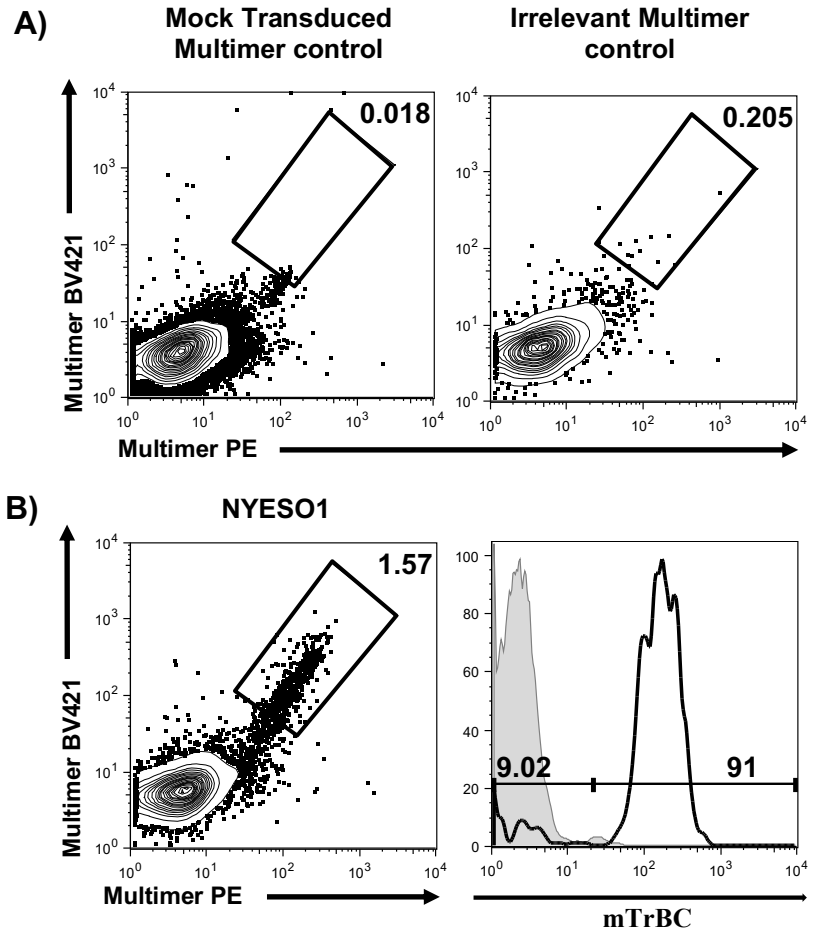


**Figure 4-20 : NYESO1 TCR expression on J76 cells day 8 post electroporation confirmed with MHC multimer staining and mTRBC staining**

Multimer staining of electroporated J76 cells day 8 after electroporation (A) On the left, FACS plot shows mock transduced sample with multimer staining. Right FACS plot shows multimer staining with an irrelevant MHC multimer. (B) FACS plot shows NYESO1 specific double multimer positive population on the left. On the right histogram shows surface staining with mTrBc antibody, all double multimer positive cells are also positive for mTrBC.

As NYESO1 TCR was the only one to show a positive multimer staining 8 days after transduction 7.29% of living lymphocytes were positive for the specific MHC multimer, but not for an irrelevant MHC multimer, which confirms the epitope-specificity as well as the capability for surface-expression despite competition with endogenous TCRs.

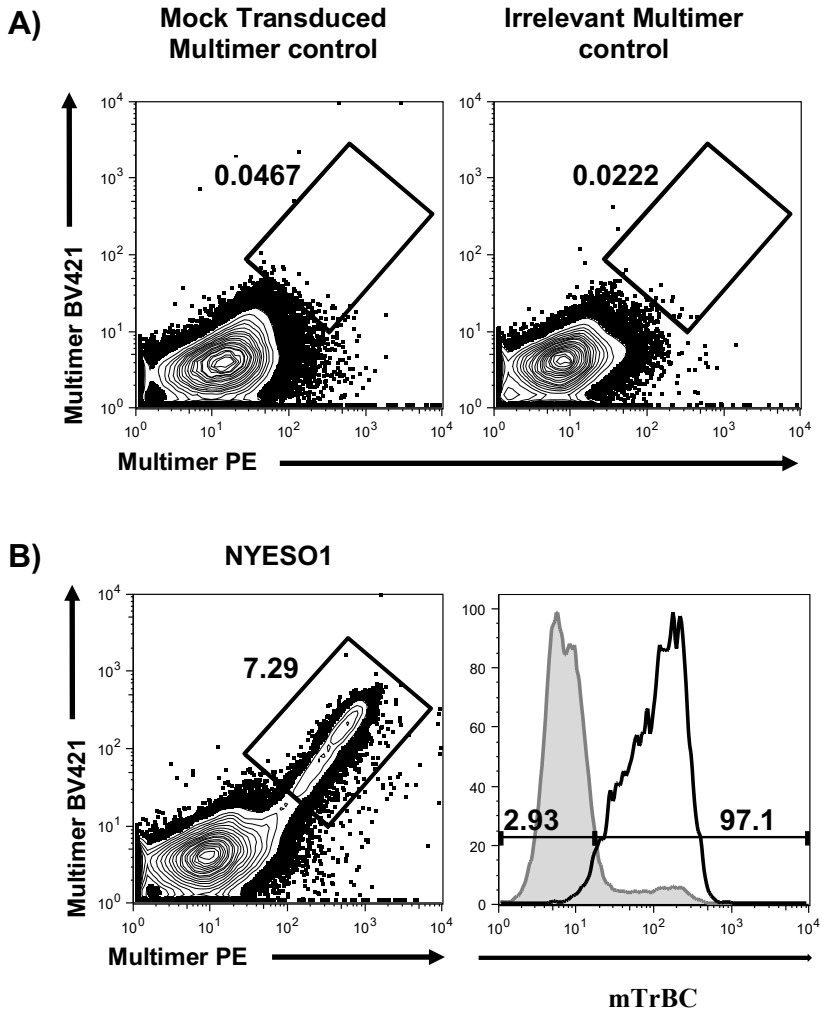


**Figure 4-21 : NYESO1 TCR expression on healthy donor PBMCs day 8 post electroporation confirmed with MHC multimer staining and mTRBC staining**

Multimer staining of electroporated donor PBMCs cells Day 8 after electroporation pre-gated on $CD8^+$ cells (A) On the left, FACS plot show mock transduced sample with multimer staining. Right FACS plot show multimer staining with an irrelevant MHC multimer. (B) FACS plot show NYESO1 specific double multimer positive population. On the right histogram shows surface staining with mTrBc antibody, all double multimer positive cells are also positive for mTrBC confirming the surface expression of TCRs.

Post electroporation on Day 8 the donor cells with transgenic TCRs in culture were tested to determine stable surface expression of TCRs via multimer staining as shown in the **Fig.4-22**. MHC multimer positive cells for different epitopes were tested and we noticed that Her2Neu old and NYESO1 TCRs showed cells that were true MHC multimer positive and with high expression as compared to the multimer staining with other TCRs. We also stained with an irrelevant multimer to avoid any cross-reactive background staining and also stained the mock transduced cells with the multimer of interest for the respective TCRs to eliminate any false positive staining (**Fig. 4-22-1**, **Fig. 4-22-2**).

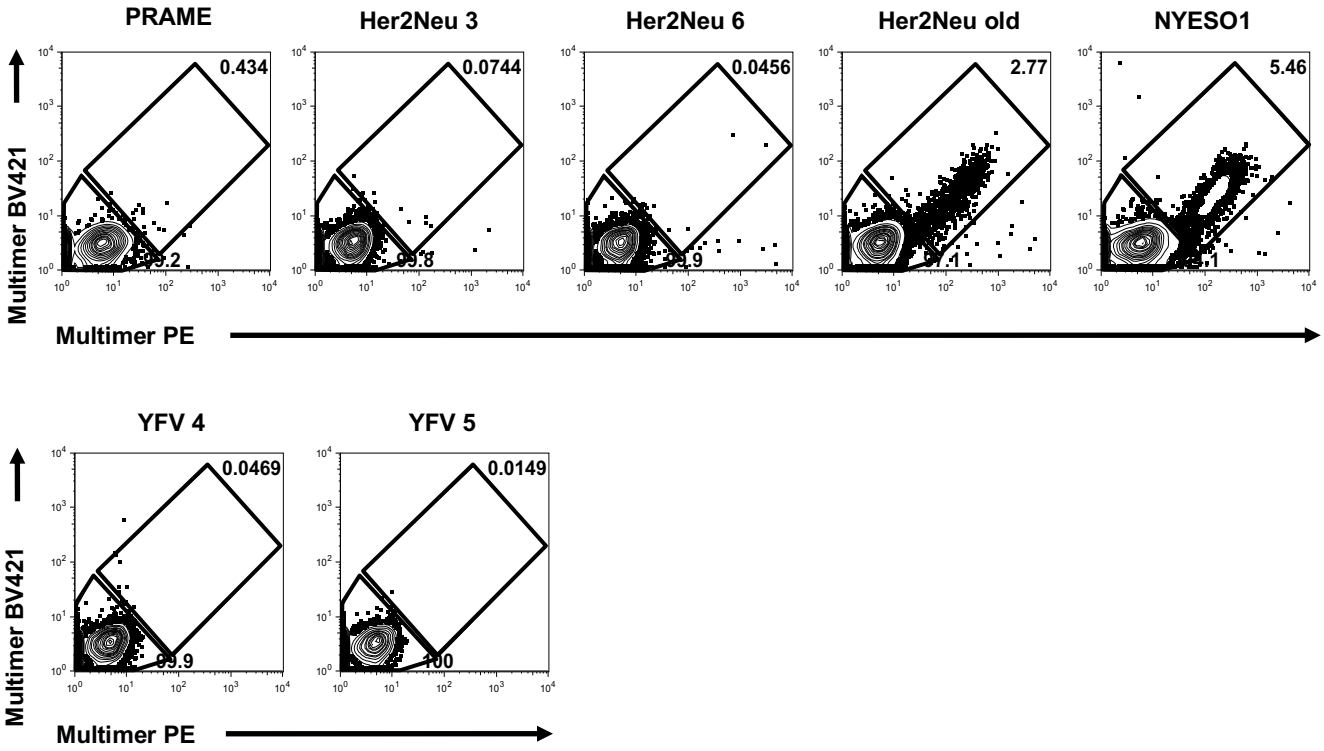


**Figure 4-22 : TCR expression on the surface determined by double multimer staining 8 days post electroporation.**

Pre-gated on $CD8^+$ cells FACS plots show double MHC multimer positive staining of electroporated cells with the TCRs of interest 8 days after electroporation.

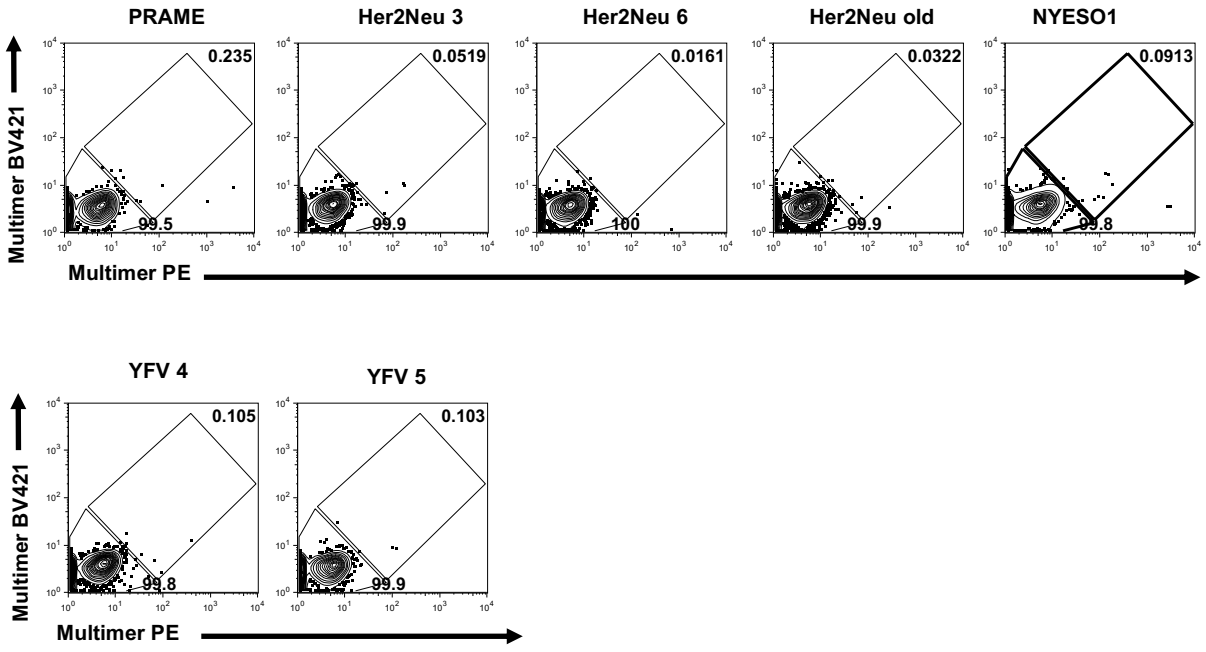


**Figure 4-22-1. Irrelevant multimer staining of the samples**

Pre gated on $CD8^+$ cells FACS plots show double multimer positive staining of electroporated cells with the TCRs of interest 8 days after electroporation.

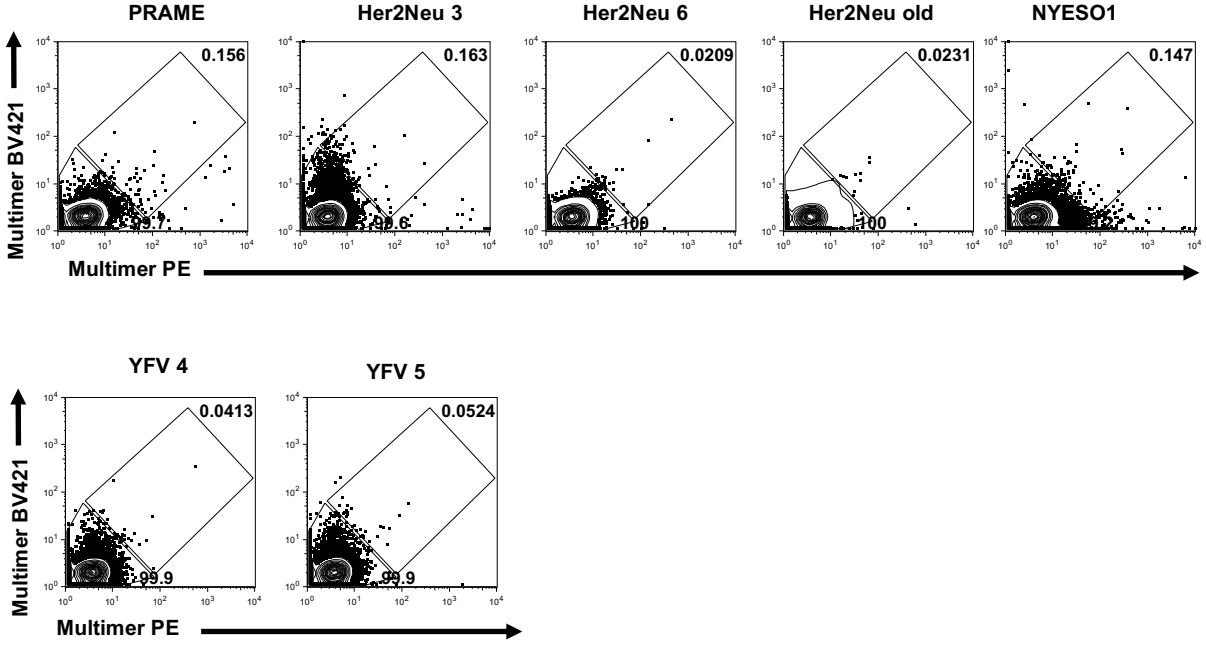


**Figure 4-22-2 . Mock control sample staining with respective multimers**

Pre gated on $CD8^+$ cells FACS plots show double multimer positive staining of electroporated cells with the TCRs of interest 8 days after electroporation.

We further confirmed the surface expression on all the cells that were double MHC multimer positive were also mTrBC positive as shown in **Fig.4-23**.

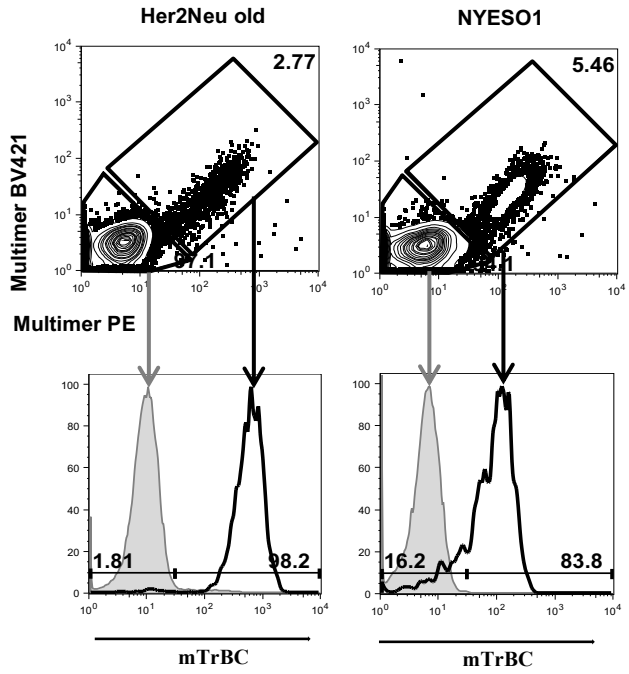


**Figure 4-23 : TCR expression on the surface determined by double MHC multimer staining and mTrBC expression day 8 post electroporation.**

Pre gated on CD8$^+$ cells FACS plots above show the double MHC multimer population of the electroporated cells with TCRs Her2Neu old and NYESO1 TCRs 8 days post electroporation.

From a total of 1x10$^7$ electroporated cells 5.46% of cells were multimer positive (36620 NYESO1 specific cells in culture). These were not sufficient cell numbers for functional assays. In order to obtain sufficient cell numbers for functionality testing we sorted the double MHC multimer positive cells (FACS plot on the left **Fig.4-24 B**) 12 days after electroporation**.** We further expanded them with their respective peptide stimulation for 10 days. After 10 days, we stained the cells again with MHC multimers to determine the cells with TCRs of interest. **Fig.4-24 B** on the right shows double MHC multimer staining for NYESO1 specific cells. Although, 5.46% of all the living cells were MHC multimer positive post electroporation, for function assays we needed more MHC multimer-positive epitope specific transgenic cells.

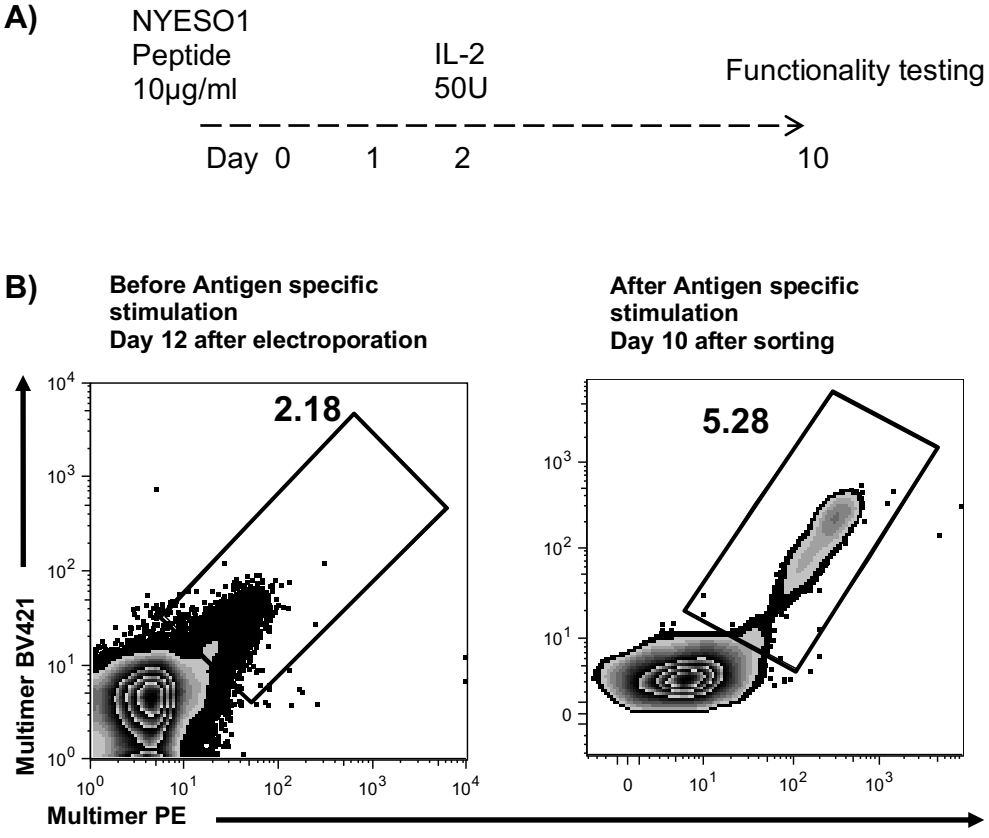


**Figure 4-24 : Expansion of successfully transfected cells to achieve sufficient cell numbers for functional assays.**

(A) Schematic representation of transgenic T cell expansion post electroporation. (B) Pre-gated on CD8$^+$ FACS plots (on the left) show the double multimer NYESO1 positive population of the electroporated cells sorted 12

days post electroporation. Sorted cells were then antigen stimulated, FACS plots on the right show double multimer staining of cells after antigen specific expansion.

As we can notice, the number of transgenic cells with NYESO1 specificity doubled after antigen specific expansion. Using this method, we could successfully expand cells with transgenic TCRs to sufficient cell numbers for functional assays. Once we had sufficient cell numbers we performed functional assays to determine the functionality of the transgenic TCRs.

### 4.4.2 Intracellular cytokine staining

Electroporated and *in vitro* cultured cells were then rested prior to functionality testing. After resting, transgenic T cells were tested for their potential to recognize target cells in an epitope specific manner by intracellular cytokine staining and also surface staining with degranulation marker CD107. Transgenic T cells were co-incubated with T2 cells pulsed with equal amount of the respective specific peptide or irrelevant peptide for the control. Unspecific stimulation with PMA/ionomycin served as a positive control. Transgenic T cells were co-incubated with unpulsed T2 cells as a negative control. After overnight culture, antigen specific cytokine release (Ifnγ, TNFα) as well as surface expression of CD107a were determined by FACS analysis with the respective fluorophore-labeled antibodies.
The FACS plots on the upper row **Fig.4-25, Fig.4-26,** show the controls, negative control with DMSO showed no staining for cytokines and the irrelevant peptide control showed no cytokine secretion or CD107a expression and therefore was used as the reference for setting up gates for other samples. As a contrast, the positive control with PMA/ionomycin stimulated transgenic cells were capable of producing both the cytokines and express CD107a. In response to the incubation with respective peptide pulsed T2 cells TCRs for different epitopes there was very little or no cytokine secretion or expression of CD107a. Transgenic TCRs tested positive for multimer staining and proved epitope specificity but there was no cytokine release. One of the several reasons for the low/no cytokine production was that the cells after electroporation were in culture for a long time. After being subjected to stimulation, electroporation and sorting the cells were characterized by substantial TCR internalization. Transgenic TCRs had also to overcome interference of endogenous TCRs competing for surface expression. All these factors could influence the functionality of the transgenic T cells. With successful CD8 and multimer staining we tried to proceed for avidity

measurement of the TCRs and even generated the reagents for avidity measurement directly after sorting but could not be follow up due to time constraint.

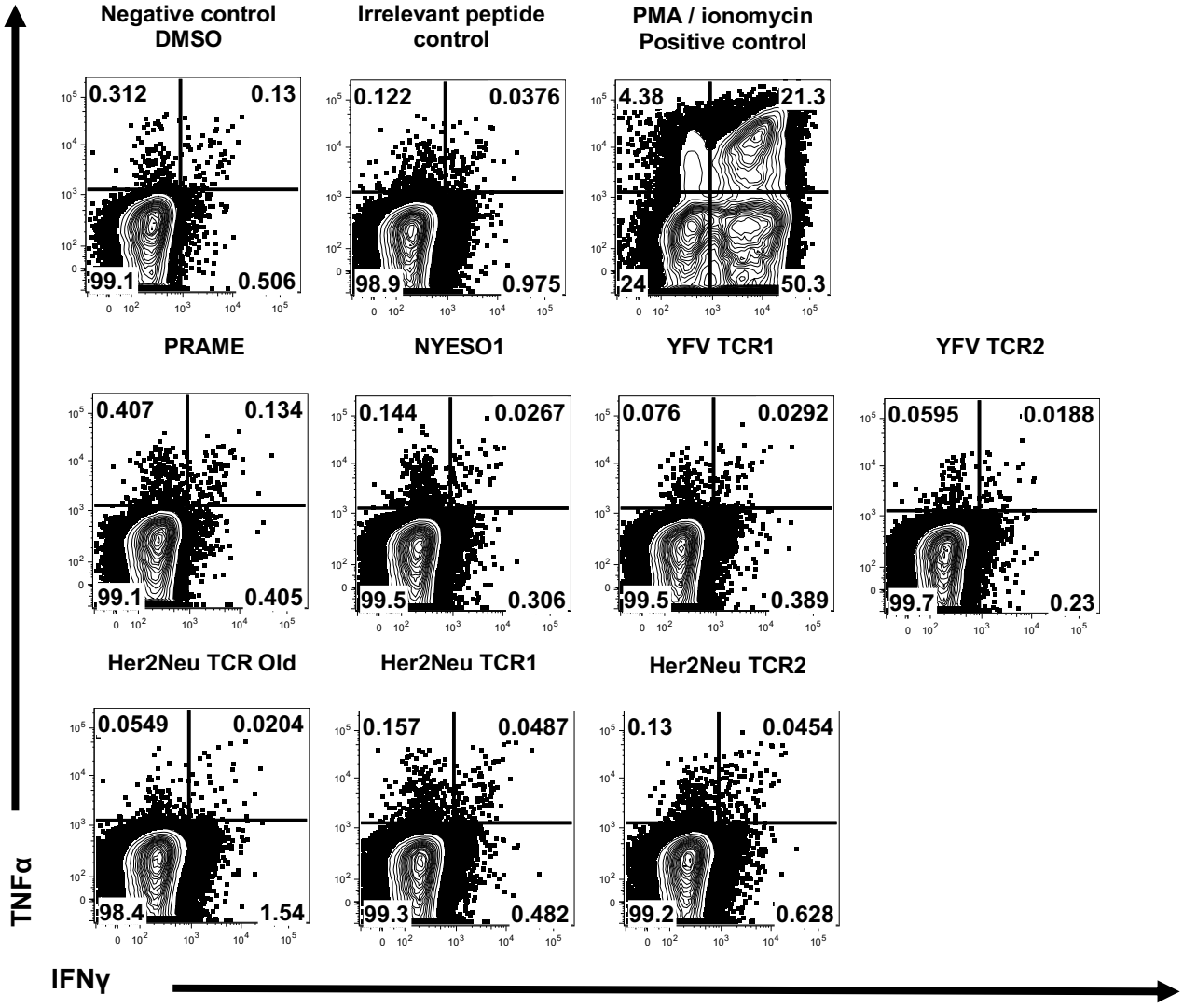


**Figure 4-25 : Intracellular cytokine release of single cell derived transgenic re-expressed TCRs.**

PBMCs electroporated with TCRs of interest were stimulated with their respective peptide-pulsed T2 (1 µM peptide) cells. As an irrelevant control electroporated PBMCs were incubated with T2 cells pulsed with 1 µM of the irrelevant peptide. As a positive control the electroporated cells were stimulated with PMA/ionomycin. As a negative control cells were stimulated with DMSO T cells cocultured with unpulsed T2 cells. Peptide-specific Ifnγ and Tnfα release of transduced PBMCs was detected via FACS analysis. Cells were pregated on live (PI-) CD8-positive lymphocytes. Numbers refer to peptide-stimulated T cells.

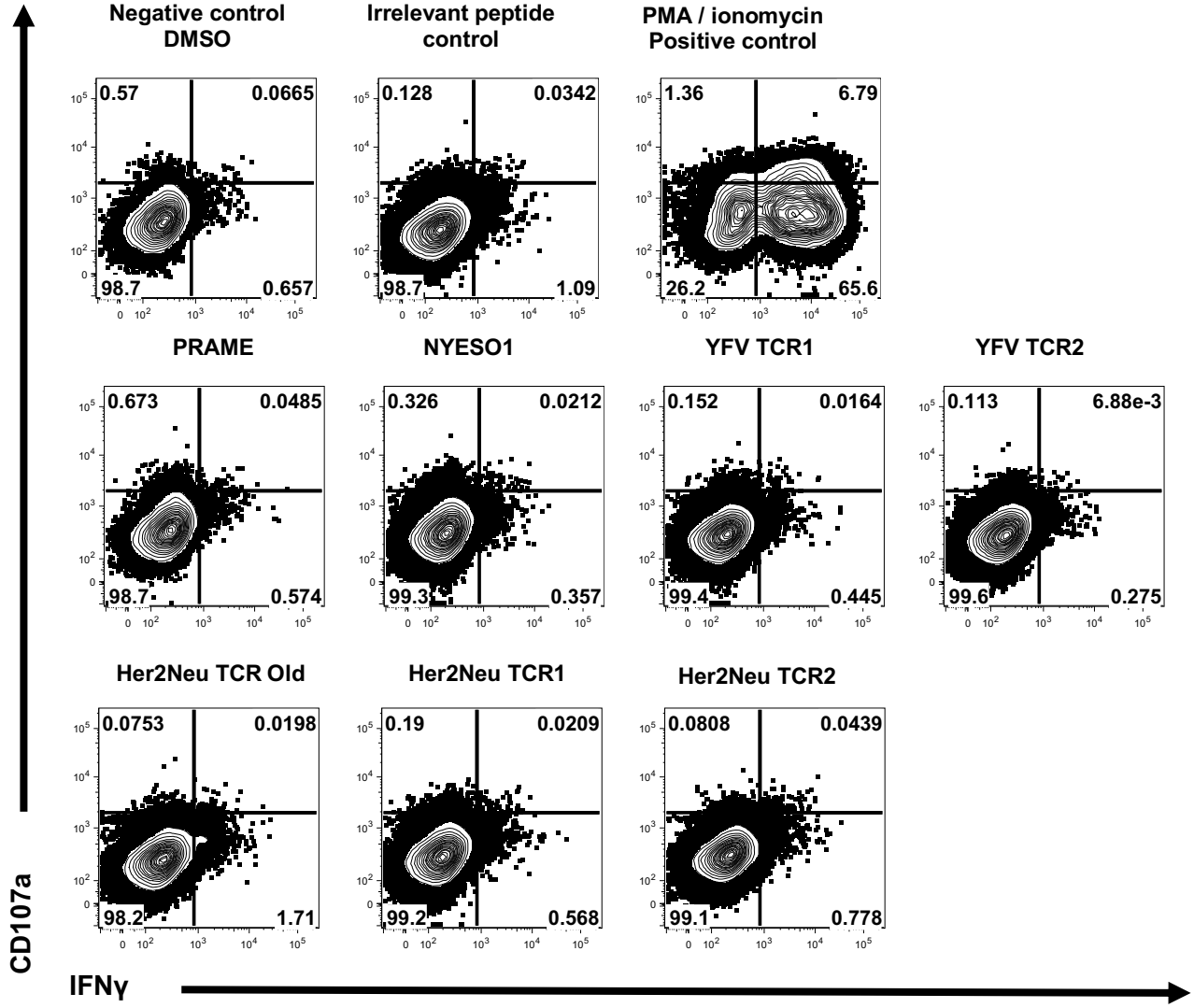


**Figure 4-26 : Intracellular cytokine release of single cell derived transgenic re-expressed TCRs.**

PBMCs electroporated with TCRs of interest were stimulated with their respective peptides (1 µM peptide) cells. As an irrelevant control electroporated PBMCs were incubated with 1 µM of the irrelevant peptide. As a positive control the electroporated cells were stimulated with PMA/ionomycin. As a negative control cells were stimulated with DMSO. Peptide-specific Ifnγ and Tnfα release of transduced PBMCs was detected via FACS analysis. Cells were pregated on live (PI-) CD8-positive lymphocytes. Numbers refer to peptide-stimulated T cells.

# 5. Discussion

T cells undergo a series of selection criteria before reaching circulation and subsequently build up a large pool of highly diverse naïve T cells. Within this large naïve T cell pool, T cells with a defined epitope-specificity represent only a minute fraction (often not more than a few hundred cells), which makes enrichment of rare epitope-specific T cells extremely challenging. Using techniques like MHC multimer staining followed by magnetic bead enrichment and flow cytometry to detect low frequency of T cells specific for a given MHC peptide complex, naïve $CD8^+$ T cells were isolated and studied. Developing a strategy to rapidly identify TCRs of potential clinical interest gives us a possibility for interrogating TCR repertoire. Enumeration of naïve T cells specific for different epitopes has been previously explored by different groups. They were able to detect frequencies varying between $5\times10^{-6}$ and $5\times10^{-3}$. We screened and performed enrichment and sorting of TCRs for several donors. We performed enrichment of different epitope-specific T cells and sequence analysis of TCR sequences for specific T cells using healthy donor PBMCs as a source for our TCRs of interest. Several repeated experiments revealed interesting facts about the source and choice of target epitopes. This in future will help us characterize the naive TCR repertoire and test its suitability as a source for TCRs for clinical application. In order to develop a reliable enrichment method, we tried to isolate T cells specific for different classes of epitopes. We found that distribution of the target population also varied based on the epitope of interest.

## 5.1 Rare epitope specific T cells detected and isolated from healthy donor repertoire

MHC multimers have emerged as a valuable tool for the identification and characterization of antigen-specific T cells (71). In this study, MHC multimers coupled to flurophores were used to label the T cells of interest. From a volume of 60ml buffy coat $2x10^8$ cells were stained with MHC multimers specific for epitopes of interest and we rare epitope-specific cells with a precursor frequency of $10^{-6}$ cells could be detected and isolated using our enrichment method.

In our experiments using MACS enrichment, T cells whose TCRs had a sufficient surface expression and binding capability to the HLA-multimers were retained as positive fraction.

After *in vitro* expansion of the enriched T cells, we were able to isolate extremely rare, epitope-specific subpopulations with the help of dual MHC multimer labeling. However, for a few epitopes of interest, like PRAME and PR1, detection of T cells was more difficult as compared to other epitopes like WT1 and Her2Neu. Due to the diversity of naïve T cell repertoires responding differently to a variety of antigens, distribution of antigen-specific T cells vary depending on the type of epitope (overexpressed, self, or autoantigen).

## 5.2 Enrichment technique - Speed enrichment

The most common techniques for single-cell isolation are fluorescent activated cell sorting (FACS), random seeding or limiting dilution, manual cell picking and different chip-based microfluidic systems. All of these techniques have advantages and limitations depending on the cell material and downstream applications after the isolation. Applications such as isolating single cells with a specific phonotype from a large heterogeneous cell mixture become more and more relevant. Only FACS and some chip-based microfluidic techniques have the capacity of high- throughput single-cell isolation (72). The basic principle of the FACS technology is to align and focus cells via hydrodynamic focusing in the nozzle through the sheath fluid so that the cells pass the interrogation point one by one and are thereby detected as separate events. These detected events can be sorted further for different applications. The upper speed limit for cell sorting is determined by the speed of data processing, the size of the sorted cells or particles and the frequency of the target population. For sorting, very rare populations with frequencies lower than 1:10,000 out of huge samples, conventional cell sorters reach their limits. As an example, a sort of $2x10^8$ cells at an event rate of 30,000 eps would take about 2hrs and that is the upper time limit for a sort, considering the capacity of sort facilities and the effects of the sorting process on cells. However, for experiments where the samples have even higher cell numbers a pre-enrichment of the target population is necessary. A new method to pre-enrich rare cell populations out of high cell numbers, called speed enrichment (SE), was used in our project.

The idea behind SE is to perform a pre-enrichment for rare cell populations using a flow cytometric approach. Using speed enrichment method, $NYESO_{157-165}$-specific T cells with a precursor frequency of as low as $3x10^{-6}$ (60 cells in 500ml of blood) could be detected. T cells for most of the epitopes of interest could be detected using speed enrichment and sorted for single cell PCR. However, for the epitopes HA1 and PR1 we had fewer cells for single cell sorting. TCR extraction was not complete for these epitopes of interest. With improvements and increased efficiency of single cell PCR, we can ensure retrieval of TCRs

even from these rare epitopes of interest.

Each donor had a different precursor frequency of T cells depending on the epitope of interest. In individual experiments for enrichment for overexpressed tumor antigens, like WT1 or Her2Neu, we were able to screen sufficiently higher numbers of T cells as compared to the cancer testis antigen NYESO1. The detected cells were then sorted onto single cell PCR slides and single cell PCR was performed to extract TCRs of interest. The extracted TCRs were then successfully expressed on J76 cell line and on healthy donor PBMCs and validated for epitope specificity by MHC multimer staining. The direct isolation of antigen-specific T cells from the naïve repertoire using SE is possible, which allows characterization of TCRs on a larger scale and help improve our understanding of the T cell repertoire.

## 5.3 Antigen-specificity of single-cell derived T cell receptors

To verify epitope specificity of the constructed TCR-chains post electroporation without interference by endogenous TCRs, we transgenically expressed them on jurkat cells (J76 cells) as described in the results section 4.3.1. We could see transient TCR surface expression (detected on day 1 post electroporation) for most of the epitopes of interest **Fig 4-16**. A few TCRs like PRAME did not show any surface expression even as early as on day 1 post electroporation. We tested for epitope specificity of the TCRs via MHC multimer staining but no signal was detected. We kept the cells in culture followed up and tested for more stable expression of TCRs with multimer staining on day 8 post electroporation. **Fig. 4-20** shows multimer staining for the NYESO1 TCR, which was the only TCR showing double MHC multimer-positive staining after 8 days in culture. J76 cells are not very stable in cultures for long term and they lost CD8 expression. However, we could still show a CD8 independent MHC multimer staining on these cells for NYESO1 epitope. The MHC multimer positive staining indeed indicates that the TCRs expressed on the J76 cells are capable of recognizing the epitope of interest independent of CD8 staining **Fig. 4-20**. Epitope specificity was confirmed for NYESO1 transgenic TCRs by transducing Jurkat T cells and human PBMCs. All Jurkat cells that expressed NYESO1 TCR after transduction could specifically bind to their respective MHC multimer. Successful multimer staining for NYESO1 transgenic cells confirmed the epitope specificity of the TCRs and surface expression of TCRs on J76 cells. As a next step, we electroporated all TCRs of interest on healthy donor PBMCs to test surface expression and epitope specificity of the TCRs of interest post electroporation. Using

the electroporation protocol for human stimulated PBMCs (program U014) on the lonza nucleofector II, we could also express most of the TCRs of interest on healthy donor PBMCs. Although there was a surface expression of the most TCRs of interest on day 1 and day 8 post electroporation, TCRs for Her2Neu and YFV epitope specificity could not be confirmed by multimer staining. The reason for absence of MHC mutimer staining could be that the TCRs had mismatched α/β chains, mispairings between α/β chains within the endogenous chains and the competition for surface expression with the endogenous TCRs.

## 5.4 Sleeping beauty mediated gene transfer

Sleeping beauty mediated system is a non-viral based transduction system and is of special interest for adoptive cell therapy since it is a non-immunogenic gene transfer system and is known to have a safer DNA integration profile. Non-viral TCR delivery platforms combine a stable transgene integration with a preferable safe profile and extended applicability (Peng, Cohen et al. 2009). Random integration profiles into the genome might help to reduce chances of insertional mutagenesis as compared to other gene transfer systems (69, 73).

In my project, sleeping beauty mediated gene transfer system was chosen instead of retroviral based gene transfer system for an efficient and safe transfection. We had to test the viability of cells post electroporation in order to confirm the efficiency of the electroporation. Manufacturers of the nucleofector claim upto 80% viability, 40–60% of successful expression of TCRs in human T cells post nucleofection (74). Lonza kits for nucleofection are efficient for electroporation but the cost and single time usage of the cuvettes and buffers included in the kits makes it far more expensive as compared to preparing the buffers in house. As per some recent study estimates, production of non-viral reagents may cost one-tenth that of GMP-grade virus. Presently, use of the Sleeping Beauty (SB) transposon/transposase system has advanced farthest in clinical development (69, 75). Another choice to be made was to either use the commercially available kits for transfection including the electroporation buffers or to prepare the electroporation buffer in house using the published protocols. We prepared our own transfection buffers as per the published protocols. 1SM buffer to be used for electroporation was prepared as described in the methods section. We even tested for re-usability of the cuvettes with several wash steps and overnight rinsing with alcohol saving us from buying the kits when we needed just cuvettes for electroporation’s which were more expensive. The programs were tested for Jurkat cells (program X-001) and stimulated donor PBMCs (program U-014) on the nucleofector II. The concentrations of the transposon and transposase was also titrated

before electroporation for establishment of a successfully working protocol. We could confirm the efficiency of the electroporation based on GFP to be 30%; however, based on the final MHC multimer-positive population the efficiency is roughly around 5%, which is a good starting step. In future studies, one could also increase the efficiency by using ultraclean DNA and using modifications of transposons with alternate promotors to maximize the production and stability of transgenes (76). We could also increase the transgenic T cell numbers by electroporating large cell numbers in one step with the MaxCyte system (74, 77).

## 5.5 Functionality of Transduced TCRs

To test the functionality and the potential of our transgenic T cells to recognize their specific epitopes, we performed functional assays. After *in vitro* re-stimulation using functional readouts of cytokine secretion and surface expression of CD107a we tested for functionality. These molecules are produced or surface exposed upon antigen-specific stimulation of T cells and are therefore regarded as markers for T cell functionality. T cells were co-cultured with their respective specific peptide or irrelevant peptide-pulsed T2 cells. Upon stimulation with their respective target epitopes, there was no significant amount of cytokines released to make a reliable statement about their functionality. Antigen-specific reactivity could not be detected even with degranulation results. An explanation for the failed functionality results could be due to cells being in culture for too long post electroporation and also being subjected to stress caused due to external factors like sorting and stimulation, by the time we performed functional assays these cells were characterized by extensive TCR internalization. Perhaps we also would have needed higher numbers of TCR-engineered T cells for receiving more convincing functional assay results. We could have achieved this for example by performing several electroporation's for a TCR of interest (electroporation's in multiple cuvettes) and pooling them all together post electroporation. Currently we electroporate $1x10^7$ cells per sample; by performing 10 separate electroporation's simultaneously using 10 different cuvettes, this could yield in a total of approximately $1x10^8$ cells. Alternatively, we could speed enrich mTrBC positive cells day 1 post electroporation and perform a rapid expansion (REP) with the increased transgenic T cells for REP we can boost the cell counts by expansion. After one REP cycle, we can recover TCR surface expression by resting and if needed we could further increase the cell numbers by performing a second REP to have sufficient cell counts for functional assays .

## 5.6 Concluding Remarks and Outlook

Using speed enrichment as a fast detection and reliable enrichment method it is now possible to isolate even extremely rare epitope specific cells. With these convincing results from enrichment, we provide first experimental data that using speed enrichment we can detect, enrich and extract rare epitope-specific TCRs from a healthy donor repertoire.

We could also demonstrate successful TCR transfer into primary human PBMCs mediated by non-viral SB gene transfer system and stable surface expression of the introduced transgenes. Furthermore, we verified epitope specificity of these TCRs of interest by target antigen-specific MHC multimer staining.

We extracted TCRs for 5 different epitopes: WT1, NYESO1, Her2Neu, YFV, FluMP from a total of 8 epitopes of interest. Although more extensive experiments on their functionality still have to be performed, the basic concept or reaching out for clinically relevant TCRs from the naïve repertoire of healthy donors seems to be a promising approach. Moreover, incorporating recent advances in methods for transgenic expression of TCRs (including efficient knockout of the endogenous TCR sequences) will probably drastically improve TCR surface expression and T cell engineering in future experiments. With improved efficiency in electroporation and successful re-expression on donor PBMCs, these TCRs should especially be tested for their functional as well as structural avidity, as these parameters seem to be predictive for *in vivo* functionality and protectivity (39).

## TCR sequences for the epitopes of interest

In silico assembled TCR cassette sequences are illustrated as following:

**5' homology region in orange**

TCR β chain in black

**P2A linker in green**

TCR α chain in blue

**3' homology region in orange**

Different regions are separated by a paragraph.

### PRAME

**TATAGCAGTAGCAGCAGTTCGATAA**

ATGGCCAGCCTGCTGTTCTTCTGCGGCGCCTTCTACCTGCTGGGCACCGGCAGCATGGACGCCGACGT
GACCCAGACCCCCCGGAACAGAATCACCAAGACCGGCAAGCGGATCATGCTGGAATGCAGCCAGACC
AAGGGCCACGACCGGATGTACTGGTACAGACAGGACCCCGGCCTGGGCCTGCGGCTGATCTACTACA
GCTTCGACGTGAAGGACATCAACAAGGGCGAGATCAGCGACGGCTACAGCGTGTCCCGGCAGGCTCA
GGCCAAGTTCAGCCTGAGCCTGGAAAGCGCCATCCCCAACCAGACCGCCCTGTACTTCTGCGCCACCT
GGCTGGCCAACTACGGCTACACCTTCGGCAGCGGCACCCGGCTGACCGTGGTGGAAGATCTGAACAA
GGTGTTCCCCCCAGAGGTGGCCGTGTTCGAGCCCAGCAAGGCCGAGATCGCCAACAAGCAGAAAGCC
ACCCTCGTGTGCCTGGCCAGAGGCTTCTTCCCCGACCACGTGGAACTGTCTTGGTGGGTCAACGGCAA
AGAGGTGCACAGCGGCGTCTGCACCGACCCCCAGGCCTACAAAGAGAGCAACTACAGCTACTGCCTGA
GCAGCCGGCTGAGAGTGTCCGCCACCTTCTGGCACAACCCCCGGAACCACTTCAGATGCCAGGTGCA
GTTCCACGGCCTGAGCGAAGAGGACAAGTGGCCCGAGGGCAGCCCCAAGCCTGTGACCCAGAATATC
AGCGCCGAGGCCTGGGGCAGAGCCGACTGTGGCATCACCAGCGCCAGCTACCACCAGGGCGTGCTG
AGCGCCACCATCCTGTACGAGATCCTGCTGGGAAAGGCCACCCTGTACGCCGTGCTGGTGTCCGGCCT
GGTGCTGATGGCCATGGTCAAGAAGAAGAACAGCGGCAGCGGCGCCACC

**AACTTCAGCCTGCTGAAACAGGCCGGCGACGTGGAAGAGAACCCTGGCCCTATGTGGGGCGTGTTC**
**CTGCTGTACGTGTCCATGAAGATGGGCGGCACCACCGGCCAGAACATCGACCAGCCTACCGAGATG**
**ACCGCCACCGAGGGCGCCATCGTGCAGATCAACTGCACCT**

ACCAGACCAGCGGCTTCAACGGCCTGTTCTGGTATCAGCAGCACGCCGGCGAGGCCCCCACCTTCCT
GAGCTACAACGTGCTGGACGGCCTGGAAGAGAAGGGCCGGTTCAGCAGCTTCCTGAGCAGAAGCAAG
GGCTACAGCTACCTGCTGCTGAAAGAACTGCAGATGAAGGACAGCGCCTCCTACCTGTGCGCCGTGCG
GGACGATAGCTGGGGCAAGCTGCAGTTCGGAGCCGGCACCCAGGTGGTGGTCACCCCCGACATCCAG
AACCCCGACCCCGCCGTGTACCAGCTGAAGGACCCCAGAAGCCAGGACAGCACCCTGTGCCTGTTCA
CCGACTTCGACAGCCAGATCAACGTGCCCAAGACCATGGAAAGCGGCACCTTCATCACCGATAAGTGC
GTGCTGGACATGAAGGCCATGGACAGCAAGAGCAACGGCGCCATTGCCTGGTCCAATCAGACCAGCTT
CACATGCCAGGACATCTTCAAAGAGACAAACGCCACCTACCCCAGCAGCGACGTGCCCTGTGACGCCA
CCCTGACCGAGAAGTCCTTCGAGACAGACATGAACCTGAACTTCCAGAACCTGAGCGTGATGGGCCTG
AGAATCCTGCTGCTCAAGGTGGCCGGCTTCAACCTGCTGATGACCCTGCGGCTGTGGTCCAGCTGA
**GAATTCGAGCATCTTACCGCCATTTAT**

## NY-ESO1

**TATAGCAGTAGCAGCAGTTCGATAA**

ATGGGCATCCGGCTGCTGTGCCGGGTGGCCTTCTGTTTCCTGGCCGTGGGCCTGGTGGACGTGAAAG
TGACCCAGAGCAGCAGATACCTGGTCAAGCGGACCGGCGAGAAGGTGTTCCTGGAATGCGTGCAGGA
CATGGACCACGAGAATATGTTCTGGTACAGACAGGACCCCGGCCTGGGCCTGCGGCTGATCTACTTCA
GCTACGACGTGAAGATGAAGGAAAAGGGCGACATCCCCGAGGGCTACAGCGTGTCCAGAGAGAAGAA
AGAGCGGTTCAGCCTGATCCTGGAAAGCGCCAGCACCAACCAGACCAGCATGTACCTGTGCGCCAGCA
GCGACGACAGAGAGAACCAGCCCCAGCACTTCGGCGACGGCACCCGGCTGAGCATCCTGGAAGATCT
GAACAAGGTGTTCCCCCCAGAGGTGGCCGTGTTCGAGCCCAGCAAGGCCGAGATCGCCAACAAGCAG
AAAGCCACCCTCGTGTGCCTGGCCAGAGGCTTCTTCCCCGACCACGTGGAACTGTCTTGGTGGGTCAA
CGGCAAAGAGGTGCACAGCGGCGTCTGCACCGACCCCCAGGCCTACAAAGAGAGCAACTACAGCTAC
TGCCTGAGCAGCCGGCTGAGAGTGTCCGCCACCTTCTGGCACAACCCCCGGAACCACTTCAGATGCCA
GGTGCAGTTCCACGGCCTGAGCGAAGAGGACAAGTGGCCCGAGGGCAGCCCCAAGCCCGTGACCCA
GAATATCAGCGCCGAGGCCTGGGGCAGAGCCGACTGTGGCATCACCTCCGCCAGCTACCACCAGGGC
GTGCTGAGCGCCACCATCCTGTACGAGATCCTGCTGGGCAAGGCCACCCTGTACGCCGTGCTGGTGTC
CGGCCTGGTGCTGATGGCCATGGTCAAGAAGAAGAACAGCGGCAGCGGCGCCACC
**AACTTCAGCCTGCTGAAACAGGCCGGCGACGTGGAAGAGAACCCTGGCCCTATGGTCAAGATCCGG**
**CAGTTCCTGCTGGCCATCCTGTGGCTGCAGCTGAGCTGCGTGTCCGCCGCCAAGAACGAGGTGGAAC**
**AGAGCCCCCAGAACCTGACCGCCCAGGAAGGCGAGTTCATCACCATCAACT**

GCAGCTACTCCGTGGGCATCAGCGCCCTGCACTGGCTGCAGCAGCACCCTGGCGGCGGAATCGTGTC
CCTGTTCATGCTGAGCAGCGGCAAGAAGAAGCACGGCCGGCTGATCGCCACAATCAACATCCAGGAAA
AGCACAGCAGCCTGCACATCACCGCCAGCCACCCCAGAGACAGCGCCGTGTACATCTGCGCCGTGAA
GTCCAACTACCAGCTGATCTGGGGAGCCGGCACCAAGCTGATCATCAAGCCCGACATCCAGAACCCCG
ACCCCGCCGTGTACCAGCTGAAGGACCCCAGAAGCCAGGACAGCACCCTGTGCCTGTTCACCGACTTC
GACAGCCAGATCAACGTGCCCAAGACCATGGAAAGCGGCACCTTCATCACCGATAAGTGCGTGCTGGA
TATGAAGGCCATGGACAGCAAGAGCAACGGCGCCATTGCCTGGTCCAATCAGACCAGCTTCACATGCC
AGGACATCTTCAAAGAGACAAACGCCACCTACCCCAGCTCCGACGTGCCCTGTGACGCCACCCTGACC
GAGAAGTCCTTCGAGACAGACATGAACCTGAACTTCCAGAACCTGTCCGTGATGGGCCTGAGAATCCT
GCTGCTGAAGGTGGCCGGCTTCAACCTGCTGATGACCCTGCGGCTGTGGTCCAGCTGA
**GAATTCGAGCATCTTACCGCCATTTAT**

## Her 2 Neu_TCR_1

**TATAGCAGTAGCAGCAGTTCGATAA**

ATGAGCATCGGCCTGCTGTGCTGCGTGGCCTTCAGCCTGCTGTGGGCCAGCCCTGTGAATGCCGGCG
TGACCCAGACCCCCAAGTTCCAGGTGCTGAAAACCGGCCAGAGCATGACCCTGCAGTGCGCCCAGGA
CATGAACCACAACAGCATGTACTGGTACAGACAGGACCCCGGCATGGGCCTGCGGCTGATCTACTACA
GCGCCAGCGAGGGCACCACCGACAAGGGCGAGGTGCCCAACGGCTACAACGTGTCCCGGCTGAACAA
GAGAGAGTTCAGCCTGAGACTGGAAAGCGCCGCTCCCAGCCAGACCAGCGTGTACTTCTGTGCCAGCT
CCGAGGGCACCCACGGCACCACCCAGTACTTCGGCCCTGGCACCAGACTGACCGTGCTGGAAGATCT
GAAGAACGTGTTCCCCCCAGAGGTGGCCGTGTTCGAGCCCAGCAAGGCCGAGATCGCCAACAAGCAG
AAAGCCACCCTCGTGTGCCTGGCCAGAGGCTTCTTCCCCGACCACGTGGAACTGTCTTGGTGGGTCAA

CGGCAAAGAGGTGCACAGCGGCGTCTGCACCGACCCCCAGGCCTACAAAGAGAGCAACTACAGCTAC
TGCCTGAGCAGCCGGCTGAGAGTGTCCGCCACCTTCTGGCACAACCCCCGGAACCACTTCAGATGCCA
GGTGCAGTTCCACGGCCTGAGCGAAGAGGACAAGTGGCCCGAGGGCAGCCCCAAGCCTGTGACCCAG
AATATCAGCGCCGAGGCCTGGGGCAGAGCCGACTGTGGCATCACCAGCGCCAGCTACCACCAGGGCG
TGCTGAGCGCCACCATCCTGTACGAGATCCTGCTGGGCAAGGCCACCCTGTACGCCGTGCTGGTGTCC
GGCCTGGTGCTGATGGCCATGGTCAAGAAGAAGAACAGCGGCAGCGGCGCCACC
**AACTTTAGCCTGCTGAAGCAGGCCGGCGACGTGGAAGAGAACCCTGGCCCCATGATGAAGTCCCTG**
**CGGGTGCTGCTGGTCATCCTGTGGCTGCAGCTGAGCTGGGTCTGGTCCCAGCAGAAAGAGGTGGAA**
**CAGAACTCCGGCCCTCTGAGCGTGCCCGAGGGCGCCATTGCCAGCCTGAACTGCACCT**
ACAGCGACCGGGGCTCCCAGAGCTTCTTCTGGTATCGGCAGTACAGCGGCAAGAGCCCCGAGCTGAT
CATGAGCATCTACAGCAACGGCGACAAAGAGGACGGCCGGTTCACCGCCCAGCTGAACAAGGCCAGC
CAGTATGTGTCCCTGCTGATCCGGGACAGCCAGCCCAGCGACAGCGCCACCTACCTGTGCGCCGTGA
CCAGAAGCAACGACTACAAGCTGAGCTTCGGAGCCGGCACCACCGTGACCGTGCGGGCCAACATCCA
GAACCCCGACCCCGCCGTGTACCAGCTGAAGGACCCCAGAAGCCAGGACAGCACCCTGTGCCTGTTC
ACCGACTTCGACAGCCAGATCAACGTGCCCAAGACCATGGAAAGCGGCACCTTCATCACCGATAAGTG
CGTGCTGGACATGAAGGCCATGGACAGCAAGAGCAACGGCGCTATCGCCTGGTCCAACCAGACCAGC
TTCACATGCCAGGACATCTTCAAAGAGACAAACGCCACATACCCCAGCAGCGACGTGCCCTGCGACGC
CACCCTGACCGAGAAGTCCTTCGAGACAGACATGAACCTGAACTTCCAGAACCTGAGCGTGATGGGCC
TGAGAATCCTGCTGCTGAAGGTGGCCGGCTTCAACCTGCTGATGACCCTGCGGCTGTGGTCCAGCTGA
**GAATTCGAGCATCTTACCGCCATTTAT**

### Her 2 neu_TCR_2

**TATAGCAGTAGCAGCAGTTCGATAA**
ATGGACACCTGGCTCGTGTGCTGGGCCATCTTCAGCCTGCTGAAGGCCGGCCTGACCGAGCCCGAAG
TGACCCAGACACCCAGCCACCAGGTCACACAGATGGGCCAGGAAGTGATCCTGCGCTGCGTGCCCAT
CAGCAACCACCTGTACTTCTACTGGTACAGACAGATCCTGGGCCAGAAGGTGGAATTCCTCGTCAGCTT
CTACAACAACGAGATCAGCGAGAAGTCCGAGATCTTCGACGACCAGTTCAGCGTGGAACGGCCCGACG
GCAGCAACTTCACCCTGAAGATCAGAAGCACCAAGCTCGAGGACAGCGCCATGTACTTTTGCGCCAGC
AGCGAACTCGTGCGGGGCCTGGAAGAGAAGCTGTTCTTCGGCAGCGGCACCCAGCTGAGCGTGCTGG
AAGATCTGAACAAGGTGTTCCCCCCAGAGGTGGCCGTGTTCGAGCCCAGCAAGGCCGAGATCGCCAAC
AAGCAGAAAGCCACCCTCGTGTGCCTGGCCAGAGGCTTCTTCCCCGACCACGTGGAACTGTCTTGGTG
GGTCAACGGCAAAGAGGTGCACAGCGGCGTCTGCACCGACCCCCAGGCCTACAAAGAGAGCAACTAC
AGCTACTGCCTGAGCAGCCGGCTGAGAGTGTCCGCCACCTTTTGGCACAACCCCCGGAACCACTTCAG
ATGCCAGGTGCAGTTCCACGGCCTGAGCGAAGAGGACAAGTGGCCCGAGGGCAGCCCCAAGCCCGTG
ACCCAGAATATCAGCGCCGAGGCCTGGGGCAGAGCCGACTGTGGCATCACCAGCGCCAGCTACCACC
AGGGCGTGCTGAGCGCCACCATCCTGTACGAGATCCTGCTGGGCAAGGCCACCCTGTACGCCGTGCT
GGTGTCCGGCCTGGTGCTGATGGCCATGGTCAAGAAGAAGAACAGCGGCAGCGGCGCCACC
**AACTTTAGTCTGCTGAAGCAGGCCGGCGACGTGGAAGAGAACCCTGGCCCCATGAACTACAGCCCT**
**GGCCTGGTGTCCCTGATTCTGCTGCTGCTGGGCCGGACCAGAGGCGACAGCGTGACACAGATGGAA**
**GGCCCCGTGACCCTGAGCGAGGAAGCCTTCCTGACCATCAACTGCACCT**

ACACCGCCACCGGCTACCCCAGCCTGTTTTGGTACGTGCAGTACCCCGGCGAGGGCCTGCAGCTGCT
GCTGAAAGCCACCAAGGCCGACGACAAGGGCAGCAACAAGGGCTTCGAGGCCACCTACCGGAAAGAG
ACAACCAGCTTCCACCTGGAAAAGGGCAGCGTCCAGGTGTCCGACTCCGCCGTGTACTTCTGTGCCCT
GAGCGACGATGGCGGCAGCCAGGGCAACCTGATCTTCGGCAAGGGCACAAAGCTGTCCGTGAAGCCC
AACATCCAGAACCCCGACCCTGCCGTGTACCAGCTGAAGGACCCCAGAAGCCAGGACAGCACCCTGTG
CCTGTTCACCGACTTCGACAGCCAGATCAACGTGCCCAAGACCATGGAAAGCGGCACCTTCATCACCG
ATAAGTGCGTGCTGGACATGAAGGCCATGGACAGCAAGAGCAACGGCGCCATTGCCTGGTCCAACCAG
ACCAGCTTCACATGCCAGGACATCTTCAAAGAGACAAACGCCACCTACCCCAGCAGCGACGTGCCCTG
TGACGCCACCCTGACCGAGAAGTCCTTCGAGACAGACATGAACCTGAACTTCCAGAACCTGAGCGTGA
TGGGCCTGCGGATCCTGCTGCTCAAGGTGGCCGGCTTCAACCTGCTGATGACCCTGCGGCTGTGGTC
CAGCTGA
**GAATTCGAGCATCTTACCGCCATTTAT**

## YFV_TCR_1

**TATAGCAGTAGCAGCAGTTCGATAA**
ATGGGCTTCCGGCTGCTGTGCTGCGTGGCCTTCTGTCTGCTGGGAGCCGGCCCTGTGGATAGCGGCG
TGACCCAGACCCCCAAGCACCTGATCACCGCCACCGGCCAGCGCGTGACCCTGAGATGTAGCCCCAG
ATCCGGCGACCTGAGCGTGTACTGGTATCAGCAGAGCCTGGACCAGGGCCTGCAGTTCCTGATCCAGT
ACTACAACGGCGAGGAACGGGCCAAGGGCAACATCCTGGAACGGTTCAGCGCCCAGCAGTTCCCCGA
CCTGCACAGCGAGCTGAACCTGAGCAGCCTGGAACTGGGCGACAGCGCCCTGTACTTCTGTGCCAGCT
CTGCCGGCACAGGCGGAGCCTACGGCTACACCTTTGGCAGCGGCACCCGGCTGACCGTGGTGGAAGA
TCTGAACAAGGTGTTCCCCCCAGAGGTGGCCGTGTTCGAGCCCAGCAAGGCCGAGATCGCCAACAAG
CAGAAAGCCACCCTCGTGTGCCTGGCCAGAGGCTTCTTCCCCGACCACGTGGAACTGTCTTGGTGGGT
CAACGGCAAAGAGGTGCACAGCGGCGTCTGCACCGACCCCCAGGCCTACAAAGAGAGCAACTACAGC
TACTGCCTGAGCAGCAGACTGCGGGTGTCCGCCACCTTCTGGCACAACCCCCGGAACCACTTCAGATG
CCAGGTGCAGTTCCACGGCCTGAGCGAAGAGGACAAGTGGCCCGAGGGCAGCCCCAAGCCTGTGACC
CAGAATATCAGCGCCGAGGCCTGGGGCAGAGCCGACTGTGGCATCACCAGCGCCAGCTACCACCAGG
GCGTGCTGAGCGCCACCATCCTGTACGAGATCCTGCTGGGCAAGGCCACCCTGTACGCCGTGCTGGT
GTCCGGCCTGGTGCTGATGGCCATGGTCAAGAAGAAGAACAGCGGCAGCGGCGCCACC
**AACTTCAGCCTGCTGAAACAGGCCGGCGACGTGGAAGAGAACCCTGGCCCCATGGAAACCCTGCTG**
**GGCGTGTCCCTGGTCATCCTGTGGCTGCAGCTGGCCAGAGTGAACAGCCAGCAGGGCGAGGAAGAT**
**CCCCAGGCCCTGAGCATCCAGGAAGGCGAGAACGCCACCATGAACTGCAGCTACAAGACCAGCATC**
**AACAACCT**
GCAGTGGTACAGACAGAACTCCGGCAGAGGCCTGGTGCACCTGATCCTGATCAGAAGCAACGAGAGA
GAGAAGCACTCCGGCAGGCTGAGAGTGACCCTGGACACCAGCAAGAAGTCCAGCTCCCTGCTGATTAC
CGCCAGCAGAGCCGCCGATACCGCCAGCTACTTCTGCGCCACCGGCAACAGCGGCGGCAGCAACTAC
AAGCTGACCTTCGGCAAGGGCACACTGCTGACAGTGAACCCCAACATCCAGAACCCCGACCCCGCCGT
GTACCAGCTGAAGGACCCCAGAAGCCAGGACAGCACCCTGTGCCTGTTCACCGACTTCGACAGCCAGA
TCAACGTGCCCAAGACCATGGAAAGCGGCACCTTCATCACCGATAAGTGCGTGCTGGACATGAAGGCC
ATGGACAGCAAGAGCAACGGCGCCATTGCCTGGTCCAACCAGACCAGCTTCACATGCCAGGACATCTT
CAAAGAGACAAACGCCACCTACCCCAGCAGCGACGTGCCCTGTGACGCCACCCTGACCGAGAAGTCCT

TCGAGACAGACATGAACCTGAACTTCCAGAACCTGTCCGTGATGGGCCTGCGGATCCTGCTGCTGAAG
GTGGCCGGCTTCAACCTGCTGATGACCCTGCGGCTGTGGTCCAGCTGA
**GAATTCGAGCATCTTACCGCCATTTAT**

### YFV_TCR_2

**TATAGCAGTAGCAGCAGTTCGATAA**
ATGGGCATCCGGCTGCTGTGCCGGGTGGCCTTCTGTTTCCTGGCCGTGGGCCTGGTGGACGTGAAAG
TGACCCAGAGCAGCAGATACCTGGTCAAGCGGACCGGCGAGAAGGTGTTCCTGGAATGCGTGCAGGA
CATGGACCACGAGAATATGTTCTGGTACAGACAGGACCCCGGCCTGGGCCTGCGGCTGATCTACTTCA
GCTACGACGTGAAGATGAAGGAAAAGGGCGACATCCCCGAGGGCTACAGCGTGTCCAGAGAGAAGAA
AGAGCGGTTCAGCCTGATCCTGGAAAGCGCCAGCACCAACCAGACCAGCATGTACCTGTGCGCCAGCA
GCCCCATGAGCCAGCCCCAGCACTTTGGCGACGGCACCCGGCTGAGCATCCTGGAAGATCTGAACAA
GGTGTTCCCCCCAGAGGTGGCCGTGTTCGAGCCCAGCAAGGCCGAGATCGCCAACAAGCAGAAAGCC
ACCCTCGTGTGCCTGGCCAGAGGCTTCTTCCCCGACCACGTGGAACTGTCTTGGTGGGTCAACGGCAA
AGAGGTGCACAGCGGCGTCTGCACCGACCCCCAGGCCTACAAAGAGAGCAACTACAGCTACTGCCTGA
GCAGCCGGCTGAGAGTGTCCGCCACCTTCTGGCACAACCCCCGGAACCACTTCAGATGCCAGGTGCA
GTTCCACGGCCTGAGCGAAGAGGACAAGTGGCCCGAGGGCAGCCCCAAGCCCGTGACCCAGAATATC
AGCGCCGAGGCCTGGGGCAGAGCCGACTGTGGCATCACCTCCGCCAGCTACCACCAGGGCGTGCTGA
GCGCCACCATCCTGTACGAGATCCTGCTGGGCAAGGCCACCCTGTACGCCGTGCTGGTGTCCGGCCT
GGTGCTGATGGCCATGGTCAAGAAGAAGAACAGCGGCAGCGGCGCCACC
**AACTTCAGCCTGCTGAAACAGGCCGGCGACGTGGAAGAGAACCCTGGCCCCATGATGAAGTCCCTG**
**CGGGTGCTGCTGGTCATCCTGTGGCTGCAGCTGAGCTGGTGGTCCCAGCAGAAAGAGGTGGAACAG**
**AACTCCGGCCCTCTGAGCGTGCCCGAGGGCGCCATTGCCAGCCTGAACTGCACCT**
ACAGCGACCGGGGCTCCCAGAGCTTCTTCTGGTATCGGCAGTACAGCGGCAAGAGCCCCGAGCTGAT
CATGTTCATCTACAGCAACGGCGACAAAGAGGACGGCCGGTTCACCGCCCAGCTGAACAAGGCCAGCC
AGTACGTGTCCCTGCTGATCCGGGACAGCCAGCCCAGCGACAGCGCCACCTATCTGTGTGCCGTGCC
CCACGGCCAGAAGCTGCTGTTCGCCAGAGGCACCATGCTGAAGGTGGACCTGAACATCCAGAAACCCG
ACCCCGCCGTGTACCAGCTGAAGGACCCCAGAAGCCAGGACAGCACCCTGTGCCTGTTCACCGACTTC
GACAGCCAGATCAACGTGCCCAAGACCATGGAAAGCGGCACCTTCATCACCGATAAGTGCGTGCTGGA
TATGAAGGCCATGGACAGCAAGAGCAACGGCGCTATCGCCTGGTCCAATCAGACCAGCTTCACATGCC
AGGACATCTTCAAAGAGACAAACGCCACCTACCCCAGCAGCGACGTGCCCTGTGACGCCACCCTGACC
GAGAAGTCCTTCGAGACAGACATGAACCTCAACTTCCAGAACCTGAGCGTGATGGGCCTGAGAATCCT
GCTGCTGAAAGTGGCCGGCTTCAACCTGCTGATGACCCTGCGGCTGTGGTCCAGCTGA
**GAATTCGAGCATCTTACCGCCATTTAT**

### WT1_TCR

**TATAGCAGTAGCAGCAGTTCGATAA**
ATGGACACCTGGCTCGTGTGCTGGGCCATCTTCAGCCTGCTGAAGGCCGGCCTGACCGAGCCCGAAG
TGACCCAGACACCCAGCCACCAGGTCACACAGATGGGCCAGGAAGTGATCCTGCGCTGCGTGCCCAT
CAGCAACCACCTGTACTTCTACTGGTACAGACAGATCCTGGGCCAGAAGGTGGAATTCCTCGTCAGCTT

CTACAACAACGAGATCAGCGAGAAGTCCGAGATCTTCGACGACCAGTTCAGCGTGGAACGGCCCGACG
GCAGCAACTTCACCCTGAAGATCAGAAGCACCAAGCTCGAGGACAGCGCCATGTACTTTTGCGCCAGC
AGCACCCCCGGCTACGGCGAGCAGTTTTTCGGCCCTGGCACCCGGCTGACCGTGCTGGAAGATCTGA
AGAACGTGTTCCCCCCAGAGGTGGCCGTGTTCGAGCCCAGCAAGGCCGAGATCGCCAACAAGCAGAA
AGCCACCCTCGTGTGCCTGGCCAGAGGCTTCTTCCCCGACCACGTGGAACTGTCTTGGTGGGTCAACG
GCAAAGAGGTGCACAGCGGCGTCTGCACCGACCCCCAGGCCTACAAAGAGAGCAACTACAGCTACTG
CCTGAGCAGCCGGCTGAGAGTGTCCGCCACCTTTTGGCACAACCCCCGGAACCACTTCAGATGCCAGG
TGCAGTTCCACGGCCTGAGCGAAGAGGACAAGTGGCCCGAGGGCAGCCCCAAGCCCGTGACCCAGAA
TATCAGCGCCGAGGCCTGGGGCAGAGCCGACTGTGGCATCACCAGCGCCAGCTACCACCAGGGCGTG
CTGAGCGCCACCATCCTGTACGAGATCCTGCTGGGCAAGGCCACCCTGTACGCCGTGCTGGTGTCCG
GCCTGGTGCTGATGGCCATGGTCAAGAAGAAGAACAGCGGCAGCGGCGCCACC
**AACTTTAGTCTGCTGAAGCAGGCCGGCGACGTGGAAGAGAACCCTGGCCCCATGATGAAGTCCCTGC**
**GGGTGCTGCTCGTGATCCTGTGGCTGCAGCTGAGCTGGGTCTGGTCCCAGCAGAAAGAGGTGGAAC**
**AGGACCCAGGCCCCCTGAGCGTGCCAGAGGGCGCCATCGTGTCCCTGAACTGCACCT**
ACAGCAACAGCGCCTTCCAGTACTTCATGTGGTACAGGCAGTACAGCCGGAAGGGCCCCGAGCTGCTG
ATGTACACCTACAGCTCCGGCAACAAAGAGGACGGCCGGTTCACCGCCCAGGTGGACAAGAGCAGCA
AGTACATCAGCCTGTTCATCCGGGACAGCCAGCCCAGCGACAGCGCCACCTACCTGTGCGCCATGAGC
GAGGACAACGCCGGCAACATGCTGACCTTCGGCGGAGGCACCAGACTGATGGTCAAGCCCCACATCC
AGAACCCCGACCCCGCCGTGTACCAGCTGAAGGACCCCAGAAGCCAGGACAGCACCCTGTGCCTGTT
CACCGACTTCGACAGCCAGATCAACGTGCCCAAGACCATGGAAAGCGGCACCTTCATCACCGATAAGT
GCGTGCTGGACATGAAGGCCATGGACAGCAAGAGCAACGGCGCCATTGCCTGGTCCAACCAGACCAG
CTTCACATGCCAGGACATCTTCAAAGAGACAAACGCCACATACCCCAGCAGCGACGTGCCCTGCGACG
CCACCCTGACCGAGAAGTCCTTCGAGACAGACATGAACCTGAACTTCCAGAACCTGAGCGTGATGGGC
CTGCGGATCCTGCTGCTGAAGGTGGCCGGCTTCAACCTGCTGATGACCCTGCGGCTGTGGTCCAGCTG
A
**GAATTCGAGCATCTTACCGCCATTTAT**

# 6. List of references

1. Robins HS, Campregher PV, Srivastava SK, Wacher A, Turtle CJ, Kahsai O, et al. Comprehensive assessment of T-cell receptor beta-chain diversity in alphabeta T cells. Blood. 2009;114(19):4099-107.

2. Rudolph MG, Stanfield RL, Wilson IA. How TCRs bind MHCs, peptides, and coreceptors. Annu Rev Immunol. 2006;24:419-66.

3. Blum JS, Wearsch PA, Cresswell P. Pathways of antigen processing. Annu Rev Immunol. 2013;31:443-73.

4. Xing Y, Hogquist KA. T-cell tolerance: central and peripheral. Cold Spring Harb Perspect Biol. 2012;4(6).

5. Arstila TP. A Direct Estimate of the Human T Cell Receptor Diversity. Science. 1999;286(5441):958-61.

6. Nikolich-Zugich J, Slifka MK, Messaoudi I. The many important facets of T-cell repertoire diversity. Nat Rev Immunol. 2004;4(2):123-32.

7. Bousso PC, A .; et al. Individual variations in the murine T cell response to a specific peptide reflect variability in naive repertoire. Immunity. 1998;Immunity, Vol. 9, 169–178.

8. Price DA, Brenchley JM, Ruff LE, Betts MR, Hill BJ, Roederer M, et al. Avidity for antigen shapes clonal dominance in CD8+ T cell populations specific for persistent DNA viruses. J Exp Med. 2005;202(10):1349-61.

9. Day EK, Carmichael AJ, ten Berge IJM, Waller ECP, Sissons JGP, Wills MR. Rapid CD8+ T Cell Repertoire Focusing and Selection of High-Affinity Clones into Memory Following Primary Infection with a Persistent Human Virus: Human Cytomegalovirus. The Journal of Immunology. 2007;179(5):3203-13.

10. Alanio C, Lemaitre F, Law HK, Hasan M, Albert ML. Enumeration of human antigen-specific naive CD8+ T cells reveals conserved precursor frequencies. Blood. 2010;115(18):3718-25.

11. Simon P, Omokoko TA, Breitkreuz A, Hebich L, Kreiter S, Attig S, et al. Functional TCR retrieval from single antigen-specific human T cells reveals multiple novel epitopes 2014.

12. Wiley JHaDC. T Cell Receptor–MHC Minireview
Interactions up Close.

13. Chowell D, Krishna S, Becker PD, Cocita C, Shu J, Tan X, et al. TCR contact residue hydrophobicity is a hallmark of immunogenic CD8+ T cell epitopes. Proc Natl Acad Sci U S A. 2015;112(14):E1754-62.

14. al. Le. IMGT, the international ImMunoGeneTics database. 1999.

15. PJ DMaB. T-cell antigen receptor genes and T-cell recognition. Nature. 1988(334).

16. Davis MM, Altman JD, Newell EW. Interrogating the repertoire: broadening the scope of peptide-MHC multimer analysis. Nat Rev Immunol. 2011;11(8):551-8.

17. Salmond RJ, Filby A, Qureshi I, Caserta S, Zamoyska R. T-cell receptor proximal signaling via the Src-family kinases, Lck and Fyn, influences T-cell activation, differentiation, and tolerance. Immunological reviews. 2009;228(1):9-22.

18. Greenwald RJ, Freeman GJ, Sharpe AH. The B7 family revisited. Annu Rev Immunol. 2005;23:515-48.

19. Watts TH. TNF/TNFR family members in costimulation of T cell responses. Annu Rev Immunol. 2005;23:23-68.

20. Curtsinger JM, Schmidt CS, Mondino A, Lins DC, Kedl RM, Jenkins MK, et al. Inflammatory cytokines provide a third signal for activation of naive CD4+ and CD8+ T cells. J Immunol. 1999;162(6):3256-62.

21. Bromley SK, Thomas SY, Luster AD. Chemokine receptor CCR7 guides T cell exit from peripheral tissues and entry into afferent lymphatics. Nat Immunol. 2005;6(9):895-901.

22. Harty JT, Tvinnereim AR, White DW. CD8+ T cell effector mechanisms in resistance to infection. Annu Rev Immunol. 2000;18:275-308.

23. Klebanoff CA, Rosenberg SA, Restifo NP. Prospects for gene-engineered T cell immunotherapy for solid cancers. Nat Med. 2016;22(1):26-36.

24. June C RS, Schumacher T. Adoptive cellular therapy a race to the finish line. 2015.

25. Fesnak AD, June CH, Levine BL. Engineered T cells: the promise and challenges of cancer immunotherapy. Nat Rev Cancer. 2016;16(9):566-81.

26. Rapoport AP, Stadtmauer EA, Binder-Scholl GK, Goloubeva O, Vogl DT, Lacey SF, et al. NY-ESO-1-specific TCR-engineered T cells mediate sustained antigen-specific antitumor effects in myeloma. Nat Med. 2015;21(8):914-21.

27. al Me. Cancer regression in patients after transfer of genetically engineered lymphocytes. 2006.

28. Robbins PF, Morgan RA, Feldman SA, Yang JC, Sherry RM, Dudley ME, et al. Tumor regression in patients with metastatic synovial cell sarcoma and melanoma using genetically engineered lymphocytes reactive with NY-ESO-1. J Clin Oncol. 2011;29(7):917-24.

29. Rosenberg SA, Dudley ME, Restifo NP. Cancer immunotherapy. N Engl J Med. 2008;359(10):1072.

30. al Me. Cancer regression in patients after transfer of genetically engineered lymphocytes. 2006

31. ROSA SCD, LAH, ROEDERER1 M. 11-color, 13-parameter flow cytometry: Identification of human naive T cells by phenotype, function, and T-cell receptor diversity. 2001.

32. Ciucci T, Bosselut R. A long journey coming to fruition: In sight of the preselection T-cell repertoire. Eur J Immunol. 2016;46(3):539-42.

33. Lucas S, Coulie PG. About human tumor antigens to be used in immunotherapy. Semin Immunol. 2008;20(5):301-7.

34. Hinrichs CS, Restifo NP. Reassessing target antigens for adoptive T-cell therapy. Nature biotechnology. 2013;31(11):999-1008.

35. Simpson AJ, Caballero OL, Jungbluth A, Chen YT, Old LJ. Cancer/testis antigens, gametogenesis and cancer. Nat Rev Cancer. 2005;5(8):615-25.

36. Kunert A, Straetemans T, Govers C, Lamers C, Mathijssen R, Sleijfer S, et al. TCR-Engineered T Cells Meet New Challenges to Treat Solid Tumors: Choice of Antigen, T Cell Fitness, and Sensitization of Tumor Milieu. Front Immunol. 2013;4:363.

37. Baitsch L, Baumgaertner P, Devevre E, Raghav SK, Legat A, Barba L, et al. Exhaustion of tumor-specific CD8(+) T cells in metastases from melanoma patients. J Clin Invest. 2011;121(6):2350-60.

38. Wherry EJ, Ha SJ, Kaech SM, Haining WN, Sarkar S, Kalia V, et al. Molecular signature of CD8+ T cell exhaustion during chronic viral infection. Immunity. 2007;27(4):670-84.

39. Nauerth M, Weissbrich B, Knall R, Franz T, Dossinger G, Bet J, et al. TCR-ligand koff rate correlates with the protective capacity of antigen-specific CD8+ T cells for adoptive transfer. Sci Transl Med. 2013;5(192):192ra87.

40. Morgan RA, Chinnasamy N, Abate-Daga D, Gros A, Robbins PF, Zheng Z, et al. Cancer regression and neurological toxicity following anti-MAGE-A3 TCR gene therapy. Journal of immunotherapy. 2013;36(2):133-51.

41. Johnson LA, Morgan RA, Dudley ME, Cassard L, Yang JC, Hughes MS, et al. Gene therapy with human and mouse T-cell receptors mediates cancer regression and targets normal tissues expressing cognate antigen. Blood. 2009;114(3):535-46.

42. Linette GP, Stadtmauer EA, Maus MV, Rapoport AP, Levine BL, Emery L, et al. Cardiovascular toxicity and titin cross-reactivity of affinity-enhanced T cells in myeloma and melanoma. Blood. 2013;122(6):863-71.

43. Robbins PF, Li YF, El-Gamil M, Zhao Y, Wargo JA, Zheng Z, et al. Single and dual amino acid substitutions in TCR CDRs can enhance antigen-specific T cell functions. J Immunol. 2008;180(9):6116-31.

44. Stone JD, Kranz DM. Role of T cell receptor affinity in the efficacy and specificity of adoptive T cell therapies. Front Immunol. 2013;4:244.

45. Zoete V, Michielin O. Comparison between computational alanine scanning and per-residue binding free energy decomposition for protein-protein association using MM-GBSA: application to the TCR-p-MHC complex. Proteins. 2007;67(4):1026-47.

46. Gronski MA, Boulter JM, Moskophidis D, Nguyen LT, Holmberg K, Elford AR, et al. TCR affinity and negative regulation limit autoimmunity. Nat Med. 2004;10(11):1234-9.

47. Buchholz VR, Neuenhahn M, Busch DH. CD8+ T cell differentiation in the aging immune system: until the last clone standing. Curr Opin Immunol. 2011;23(4):549-54.

48. Blackburn SD, Shin H, Haining WN, Zou T, Workman CJ, Polley A, et al. Coregulation of CD8+ T cell exhaustion by multiple inhibitory receptors during chronic viral infection. Nat Immunol. 2009;10(1):29-37.

49. Neuenhahn M, Albrecht J, Odendahl M, Schlott F, Dossinger G, Schiemann M, et al. Transfer of minimally manipulated CMV-specific T cells from stem cell or third-party donors to treat CMV infection after alloHSCT. Leukemia. 2017.

50. Adams JJ, Narayanan S, Birnbaum ME, Sidhu SS, Blevins SJ, Gee MH, et al. Structural interplay between germline interactions and adaptive recognition determines the bandwidth of TCR-peptide-MHC cross-reactivity. Nat Immunol. 2016;17(1):87-94.

51. Dossinger G, Bunse M, Bet J, Albrecht J, Paszkiewicz PJ, Weissbrich B, et al. MHC multimer-guided and cell culture-independent isolation of functional T cell receptors from single cells facilitates TCR identification for immunotherapy. PLoS One. 2013;8(4):e61384.

52. Purbhoo MA, Sutton DH, Brewer JE, Mullings RE, Hill ME, Mahon TM, et al. Quantifying and imaging NY-ESO-1/LAGE-1-derived epitopes on tumor cells using high affinity T cell receptors. J Immunol. 2006;176(12):7308-16.

53. Schmitt TM, Stromnes IM, Chapuis AG, Greenberg PD. New Strategies in Engineering T-cell Receptor Gene-Modified T cells to More Effectively Target Malignancies. Clin Cancer Res. 2015;21(23):5191-7.

54. Matthias Peiper DCL, Eric Ganguly, al. e. The HER2heu-derived peptide p654-662 is a tumor-associated antigen in human pancreatic cancer recognized by cytotoxic T lymphocytes. 1997.

55. Bryan Fisk TLBea. Identification of an Immunodominant Peptide of HER-2/neu Protooncogene Recognized by Ovarian Tumor-specific Cytotoxic T Lymphocyte Lines. 1995.

56. Amir AL, van der Steen DM, van Loenen MM, Hagedoorn RS, de Boer R, Kester MD, et al. PRAME-specific Allo-HLA-restricted T cells with potent antitumor reactivity useful for therapeutic T-cell receptor gene transfer. Clin Cancer Res. 2011;17(17):5615-25.

57. Pollack SM, Li Y, Blaisdell MJ, Farrar EA, Chou J, Hoch BL, et al. NYESO-1/LAGE-1s and PRAME are targets for antigen specific T cells in chondrosarcoma following treatment with 5-Aza-2-deoxycitabine. PLoS One. 2012;7(2):e32165.

58. Klebanoff CA, Scott CD, Leonardi AJ, Yamamoto TN, Cruz AC, Ouyang C, et al. Memory T cell-driven differentiation of naive cells impairs adoptive immunotherapy. J Clin Invest. 2016;126(1):318-34.

59. Khan N, Shariff N, Cobbold M, Bruton R, Ainsworth JA, Sinclair AJ, et al. Cytomegalovirus Seropositivity Drives the CD8 T Cell Repertoire Toward Greater Clonality in Healthy Elderly Individuals. The Journal of Immunology. 2002;169(4):1984-92.

60. Spielmann G, Bollard CM, Kunz H, Hanley PJ, Simpson RJ. A single exercise bout enhances the manufacture of viral-specific T-cells from healthy donors: implications for allogeneic adoptive transfer immunotherapy. Sci Rep. 2016;6:25852.

61. Berdien B, Reinhard H, Meyer S, Spock S, Kroger N, Atanackovic D, et al. Influenza virus-specific TCR-transduced T cells as a model for adoptive immunotherapy. Hum Vaccin Immunother. 2013;9(6):1205-16.

62. Hebeisen M, Schmidt J, Guillaume P, Baumgaertner P, Speiser DE, Luescher I, et al. Identification of Rare High-Avidity, Tumor-Reactive CD8+ T Cells by Monomeric TCR-Ligand Off-Rates Measurements on Living Cells. Cancer Res. 2015;75(10):1983-91.

63. Busch DH, Pilip I, Pamer EG. Evolution of a complex T cell receptor repertoire during primary and recall bacterial infection. The Journal of experimental medicine. 1998;188(1):61-70.

64. Rodenko B, Toebes M, Hadrup SR, van Esch WJ, Molenaar AM, Schumacher TN, et al. Generation of peptide-MHC class I complexes through UV-mediated ligand exchange. Nature protocols. 2006;1(3):1120-32.

65. Chicaybam L, Sodre AL, Curzio BA, Bonamino MH. An efficient low cost method for gene transfer to T lymphocytes. PLoS One. 2013;8(3):e60298.

66. Mates L, Chuah MK, Belay E, Jerchow B, Manoj N, Acosta-Sanchez A, et al. Molecular evolution of a novel hyperactive Sleeping Beauty transposase enables robust stable gene transfer in vertebrates. Nat Genet. 2009;41(6):753-61.

67. Zweerink HJ, Gammon MC, Utz U, Sauma SY, Harrer T, Hawkins JC, et al. Presentation of endogenous peptides to MHC class I-restricted cytotoxic T lymphocytes in transport deletion mutant T2 cells. J Immunol. 1993;150(5):1763-71.

68. Wooldridge L, Lissina A, Cole DK, van den Berg HA, Price DA, Sewell AK. Tricks with tetramers: how to get the most from multimeric peptide-MHC. Immunology. 2009;126(2):147-64.

69. Field AC, Vink C, Gabriel R, Al-Subki R, Schmidt M, Goulden N, et al. Comparison of lentiviral and sleeping beauty mediated alphabeta T cell receptor gene transfer. PLoS One. 2013;8(6):e68201.

70. Sommermeyer DN, J.; Weinhold,M.;. Designer T cells by T cell receptor replacement. Eur J Immunol. 2006;36: 3052–3059(2006).

71. Hadrup SR, Schumacher TN. MHC-based detection of antigen-specific CD8+ T cell responses. Cancer Immunol Immunother. 2010;59(9):1425-33.

72. Hensley-McBain T, Heit A, De Rosa SC, McElrath MJ, Andersen-Nissen E. Optimization of a whole blood phenotyping assay for enumeration of peripheral blood leukocyte populations in multicenter clinical trials. J Immunol Methods. 2014;411:23-36.

73. Izsvak Z, Ivics Z. Sleeping beauty transposition: biology and applications for molecular therapy. Mol Ther. 2004;9(2):147-56.

74. al Se. A new approach to gene therapy using Sleeping Beauty to genetically modify clinical-grade T cells to target CD19. Immunological Reviews. 2014;Volume 257(2014).

75. Singh et al. - 2014 - A new approach to gene therapy using Sleeping Beauty to genetically modify clinical-grade T cells to target CD19.pdf.

76. Wilber A, Frandsen JL, Geurts JL, Largaespada DA, Hackett PB, McIvor RS. RNA as a source of transposase for Sleeping Beauty-mediated gene insertion and expression in somatic cells and tissues. Mol Ther. 2006;13(3):625-30.

77. Deniger DC, Pasetto A, Tran E, Parkhurst MR, Cohen CJ, Robbins PF, et al. Stable, Nonviral Expression of Mutated Tumor Neoantigen-specific T-cell Receptors Using the Sleeping Beauty Transposon/Transposase System. Mol Ther. 2016;24(6):1078-89.

# Publication List

“Transfer of minimally manipulated CMV- specific T cells from stem cell or third-party donors to treat CMV infection after allogeneic hematopoietic stem cell transplantation: a prospective multicentre trial”

Neuenhahn M, Albrecht J, Odendahl M, Schlott F, Dössinger G, Schiemann M, **Lakshmipathi S**, Martin K, Bunjes D, Harsdorf S, Weissinger EM, Menzel H, Verbeek M, Uharek L, Kröger N, Wagner E, Kobbe G, Schroeder T, Schmitt M, Held G, Herr W, Germeroth L, Bonig H, Tonn T, Einsele H, Busch DH, Grigoleit GU. Leukemia. 2017 Feb 17. doi: 10.1038/leu.2017.16.

# Acknowledgement

Many people have helped me throughout the course of my PhD in one form or another, for which I am truly thankful. First and foremost among those is Professor Dirk H Busch, for his timely advice, encouraging words and tremendous support as my advisor who to me is not just a great scientist but a great supervisor and Doctor father with qualities that I hope to emulate in my own career. Similar thanks also go to Prof.Angela Krackhardt and Prof.Ulrike Protzer as my mentors.

Very large thanks also go to Dr.George Dössinger and Dr.Killian Schober, both of whom very patiently answered my silly questions and helped me find my feet within the complicated workframe of my project. The main facility around which my project was strongly dependent on was the sort facility headed by Dr.Mathias Scheimann and his team especially Lynnette Henkel, Immanuel Andrea and Hanna Ulrich who assisted and guided me throughout. I would like to express my sincere appreciation to the whole team for supporting my project even when it meant to stay beyond working hours or sharing antibodies at critical phases of my project. Thanks also go to Dr.Michael Neuenhan and his group for sequencing several of the early experiments in this thesis. Dr.Julia Albrecht who constantly helped me improve my understanding of related topics outside my project. I also would like to specially thank Isabelle Schiedwitz for all the single cell PCRs she did for me and also helped me in the project to learn from her experience.

Thanks to Anna Hochholzer who helped me generate reagents on time which would have otherwise delayed my project timelines, similar thanks to Monica Hemmel who also with her experience helped me during my time in the lab. I would like to again thank Prof.Dirk H Busch and Kilian Schober who always motivated me and helped me finish my project work. A special mention of Ms.Desislava Zlatanova who is my PhD program co-ordinator who guided me in every step since the time of my interview, I would like to thank her for her constant support.

While I am indebted to many current and past lab members for help, there are few that merit particular mention Yi Li Cho, Bianca Weissbrich, Lynette Henkel and Inge Hensel who motivated me encouraged me and brought out the best in me. I want to also thank Fabian Mohr, Fabian Schlott and other team members for helping me actually realize that I know what I was talking about. My innumerable and frantic project discussion sessions with Yi Li

Cho must also be noted. I would like to make a special mention of Annina Schmidt, Manuel Effenberger, Vlad Clateiu and Thomas Müller who as a part of their projects worked together with me to bring several improvements in techniques which we used together. They worked in improvising few methods which greatly helped me in my project.

Also, special mention of my good friends Katherine Molter, Kerstin Weiss in the lab and others in the course group who I call as crazy scientists for being there as peers and academically supported me during many downsides of PhD life. I would like to also express my gratitude towards Britta Schmidt who looked out for me as a friend and a parent in the initial phase of my move to a new country. It is the group of friends I call family in Germany today who laughed with me during my celebrations and were there to motivate me when I missed home, my special thanks goes out to every single one of you.

I must thank my family especially my father who was the main inspiration to pursue PhD, my mother who is my pillar of support and brother for providing me all the strength I needed and had pride in me no matter what I wanted to do I thank them for believing in me, my hard work and dreams, it is their faith and prayers which sustained me so far. Words cannot express how grateful I am to my husband Rohan for all the sacrifices he made on my behalf and also for his critical feedback and support through all my PhD years. Without him backing me all these years with his constant support and understanding a PhD would not have been possible. I would also like to thank his mother and family for their support and kind words.

My heartfelt gratitude to my friends Anil, Lavanya, Ramya and family back home in India for their encouraging words. You all be very pleased to know that it’s almost done so I can finally come home and see you all.